



Norwegian University of
Science and Technology

A Comparison of Railway Load Models for Geotechnical Analysis

Thea Lind Christiansen

Civil and Environmental Engineering

Submission date: June 2018

Supervisor: Gudmund Reidar Eiksund, IBM

Co-supervisor: Geir Svanø, Bane NOR

Norwegian University of Science and Technology
Department of Civil and Environmental Engineering



Report Title: A Comparison of Railway Load Models for Geotechnical Analysis	Date: 08.06.2018
	Number of pages (incl. Appendix): 126
	Master Thesis x
Name: Thea Lind Christiansen	
Professor in charge/supervisor: Gudmund Reidar Eiksund	
Other external professional contacts/supervisors: Geir Svanø	

Abstract:

Bane NOR is responsible for developing the railway network in Norway. In Norway, the Eurocodes are specifying how structural design in general should be conducted. This also applies to the railways. To guide those responsible for developing the railway network in Norway, Bane NOR has developed a set of design rules called technical regulations. These regulations aim to meet the requirements from the European standards.

The load model in the Eurocode representing vertical loading due to normal rail traffic actions on earthworks is called Load Model 71. It is described by four axle loads $Q_{vk} = 250$ kN over the length 6.4 m, and a line load $q_{vk} = 80$ kN/m outside this length. The technical regulations developed by Bane NOR describes the loads from railways as a line load $q = 110$ kN/m for most cases. In February, a rule to check for Load Model 71 when doing calculations considering sheet pile walls was included. Bane NOR is currently investigating whether their load model considering geotechnics meets the requirements specified in the standard.

Throughout this master's thesis, the results from simulations done in PLAXIS 3D will be presented. Focus will be to find the differences between these two load models. For the assessment of the problem, two different case studies will be conducted. One of them will look into slope stability and the other one investigates how the load models affects a sheet pile wall adjacent to the track.

In advance of the simulations, calculations has been done to illustrate the difference between 2D- and 3D-modelling in PLAXIS, and to figure out the best design of the models in PLAXIS 3D. Results from these calculations shows that PLAXIS 2D is a more accurate modelling program than PLAXIS 3D. Other calculations illustrates that the lower the height of the slope, the greater the differences between the load models, and that the differences will increase with the absence of a frost protection layer.

From the slope stability analyses it is found that the applied line load $q = 87$ kN/m gives the same safety level in the model as when applying Load Model 71. The simulations of the sheet pile wall adjacent to the track gives results showing that the response in the wall when Load Model 71 is applied is close to the one that occurs when applying the line load $q = 125$ kN/m.

Even though more research should be done prior to any revisions of the regulations, the results in this thesis can be used as basis. The obtained final results provides background to suggest that the line load can be reduced for slope stability analyses. For calculations considering sheet pile walls adjacent to the track, it seems that Bane NOR did right when they included the requirement to check for Load Model 71. If a line load is to be included in the regulations for this case, it seems that the value has to be higher than 110 kN/m.

Keywords:

- | |
|--|
| 1. Regulations considering railways |
| 2. Slope stability analysis |
| 3. Analysis of sheet pile wall |
| 4. Finite element modelling in PLAXIS 3D |

Thea Lind Christiansen

Preface

This master's thesis has been written as part of my Master of Science in Civil and Environmental Engineering, under the Geotechnical division at Norwegian University of Science and Technology in Trondheim. The work with the thesis was carried out during the spring semester of 2018, and the topic was proposed by the Norwegian Railway Directorate Bane NOR. My supervisors during this semester has been Professor Gudmund Reidar Eiksund and Doctor of Engineering Geir Svanø.

Trondheim, 8 June 2018

Thea Lind Christiansen

Thea Lind Christiansen

Acknowledgements

I would like to extend a very special thank you to my supervisors Gudmund Reidar Eiksund and Geir Svanø for several meetings throughout the process, and for constructive feedback on my work. Gudmund was always available when I had questions for him, and has been very patient. Geir took the time to meet me at NTNU as often as I wanted, and has been extraordinarily engaged in this project. Their guidance has been helpful for me in the process of writing this thesis.

I want to acknowledge the Norwegian Railway Infrastructure Company Bane NOR who developed the assignment for this master's thesis, and made it possible by kindly providing necessary data.

Geotechnical division at NTNU has given me inputs and priceless support. The regular "cake-Friday" has contributed to both motivation and joy. A special thanks goes to Johannes Mydland who always was there when I had trouble with LaTeX.

Finally, I would like to express my appreciation to my family and friends for personal support and for encouraging me to put on a brave face and complete the thesis at the appointed time. The last couple of weeks would have been impossible without you.

T.L.C.

Summary

Bane NOR is responsible for developing the railway network in Norway. In Norway, the Eurocodes are specifying how structural design in general should be conducted. This also applies to the railways. To guide those responsible for developing the railway network in Norway, Bane NOR has developed a set of design rules called technical regulations. These regulations aim to meet the requirements from the European standards.

The load model in the Eurocode representing vertical loading due to normal rail traffic actions on earthworks is called Load Model 71. It is described by four axle loads $Q_{vk} = 250$ kN over the length 6.4 m, and a line load $q_{vk} = 80$ kN/m outside this length. The technical regulations developed by Bane NOR describes the loads from railways as a line load $q = 110$ kN/m for most cases. In February, a rule to check for Load Model 71 when doing calculations for sheet pile walls was included. Bane NOR is currently investigating whether their load model considering geotechnics meets the requirements specified in the standard.

Throughout this master's thesis, the results from simulations done in PLAXIS 3D will be presented. The focus will be to find the differences between these two load models. For the assessment of the problem, two different case studies will be conducted. One of them will look into slope stability and the other one investigates how the load models affects a sheet pile wall adjacent to the track.

In advance of the simulations, calculations have been done to illustrate the difference between 2D- and 3D-modelling in PLAXIS, and to figure out the best design of the models in PLAXIS 3D. Results from these calculations shows that PLAXIS 2D is a more accurate modelling program than PLAXIS 3D. Other calculations illustrate that the lower the height of the slope, the greater the differences between the load models, and that the differences will increase with the absence of a frost protection layer.

From the slope stability analyses it is found that the applied line load $q = 87$ kN/m gives the same safety level in the model as when applying Load Model 71. The simulations of the sheet pile wall adjacent to the track gives results showing that the response in the wall when Load Model 71 is applied is close to the one that occurs when applying the line load $q = 125$ kN/m.

Even though more research should be done prior to any revisions of the regulations, the results in this thesis can be used as basis. The obtained final results provide background to suggest that the line load can be reduced for slope stability analyses. For calculations considering sheet pile walls adjacent to the track, it seems that Bane NOR did right when they included the requirement to check for Load Model 71. If a line load is to be included in the regulations for this case, it seems that the value has to be higher than 110 kN/m.

Sammendrag

Bane NOR er ansvarlige for utviklingen av jernbaneinfrastrukturen i Norge. I Norge står dimensjoneringsreglene for byggverk skrevet i Eurokodene. Disse gjelder også for jernbanen. For å rettlede de som dimensjonerer og bygger jernbanenettet i Norge, har Bane NOR utviklet et sett med normaler som kalles for teknisk regelverk. Dette regelverket har som mål å oppfylle kravene fra de europeiske standardene.

Lastmodellen i Eurokoden som representerer de vertikale lastene fra normal jernbanetrafikk på geotekniske løsninger kalles lastmodell 71. Denne er beskrevet av fire akselbelastninger $Q_{vk} = 250$ kN over lengden 6.4 m, og en linjelast $q_{vk} = 80$ kN/m utenfor denne lengden. I det tekniske regelverket, utviklet av Bane NOR, er lastene fra jernbanen som oftest representert med linjelasten $q = 110$ kN/m. I februar ble en regel knyttet til spuntvegger inkludert, med et krav om å utføre kontroll av slike beregningene med lastmodell 71. Bane NOR holder nå for tiden på med å undersøke hvorvidt deres lastmodell oppfyller kravene slik de er spesifisert i standarden.

I løpet av denne masteroppgaven vil resultater fra simuleringer utført i PLAXIS 3D bli presentert, der modellene har som formål å undersøke forskjellene mellom disse to lastmodellene. For å utforske problemstillingen, vil to ulike studier bli gjennomført. En av dem vil se på skråningsstabilitet og den andre vil undersøke hvordan lastmodellene påvirker en spuntvegg nær sporet.

I forkant av simuleringene er beregninger blitt utført for å illustrere forskjellen mellom 2D- og 3D-modellering i PLAXIS, og for å finne den beste utformingen av modellene i PLAXIS 3D. Resultatene fra disse beregningene viser at PLAXIS 2D er et mer presist modelleringsprogram enn PLAXIS 3D. Andre beregninger viser at jo lavere høyden på skråningen er, jo større blir forskjellene mellom lastmodellene, og at forskjellene mellom de to er størst uten frostsikringslag.

Fra analysene av skråningsstabiliteten viser det seg at en påført linjelast $q = 87$ kN/m gir samme sikkerhetsnivå i modellen som når lastmodell 71 påføres. Simuleringene av spuntveggen ved siden av sporet gir resultater som peker på at responsen i vegg når lastmodell 71 påføres likner mest på den som oppstår når linjelasten $q = 125$ kN/m påføres.

Selv om mer forskning bør gjøres i forkant av eventuelle endringer i regelverket, kan resultatene fra denne oppgaven brukes som et utgangspunkt. De oppnådde resultatene gir bakgrunn for å foreslå at linjelasten kan reduseres for analyser knyttet til skråningsstabilitet. For beregninger knyttet til spuntvegger nær sporet, ser det ut til at Bane NOR gjorde rett i å inkludere lastmodell 71 inn i regelverket. Dersom en linjelast skal inkluderes for dette tilfellet, bør verdien være høyere enn 110 kN/m.

Table of Contents

Preface	i
Acknowledgements	iii
Summary	v
Sammendrag	vii
Table of Contents	xi
List of Tables	xiii
List of Figures	xvii
Abbreviations	xviii
Symbols	xix
1 Introduction	1
1.1 Background	1
1.1.1 Problem Formulation	2
1.2 Objectives	4
1.3 Limitations	4
1.4 Methods	5
1.5 Outline of the Thesis	5
2 Literature Review concerning Loads from Railways	7
2.1 The Projects this Master's Thesis is based on	7
2.1.1 Kvisldalen Railway Bridge	8
2.1.2 The Østfold Line between Oslo S and Ski	9
2.2 European Standard applicable in Norway	10

2.2.1	EN 1991-2: Traffic Loads on Bridges	10
2.3	Bane NORs Technical Regulations	12
2.3.1	Book 520: Substructure	12
2.4	Technical Regulations in Scandinavia	14
2.4.1	Technical Regulations in Sweden	14
2.4.2	Technical Regulations in Denmark	16
2.4.3	A Comparison of the Regulations in Norway, Sweden and Denmark	17
2.5	Previous Studies	19
2.5.1	Pile supported embankment slabs under railway track line <i>Research report 28 from the Finnish Transport Agency</i>	19
2.5.2	2D Loads for Stability Calculations of Railway Embankments <i>Research report 56 from the Finnish Transport Agency</i>	21
2.6	Active, Direct and Passive Undrained Shear Strength	23
3	Finite Element Analysis in PLAXIS	25
3.1	Material Models in PLAXIS	26
3.1.1	Soil and Interfaces	26
3.1.2	Plates	32
3.1.3	Beams	34
3.1.4	Interfaces	34
3.2	Meshing	35
3.2.1	The use of PLAXIS 2D versus PLAXIS 3D	35
3.3	Calculation phases	38
3.3.1	Initial phase	38
3.3.2	The subsequent phases	39
3.3.3	Calculation process	39
4	Modelling in PLAXIS 3D	41
4.1	Geometry of the Substructure for both Examples	41
4.1.1	Superstructure	42
4.2	Slope Stability near the Railway Track	43
4.2.1	Geometry of the model	44
4.2.2	Soil settings	45
4.3	Sheet Pile Wall adjacent to the Railway	47
4.3.1	Geometry of the model	47
4.3.2	Soil settings	48
4.3.3	Structural elements	48
4.4	Vertical Surface Loads	51
4.4.1	Loading from superstructure	51
4.4.2	Equivalent vertical loading due to rail traffic actions	54

4.4.3	Load model from Bane NOR	56
5	Simulations	57
5.1	Slope Stability Analysis	57
5.1.1	Calculations of slope stability	58
5.2	Analysis of the Sheet Pile Wall adjacent to the Track	60
5.2.1	Calculations of the loads impact on the wall	60
6	Results and Discussion	65
6.1	The effect of the Height of the Slope	65
6.2	The Effect of the Frost Protection Layer	67
6.2.1	Comparison of the results from the slope stability analysis	69
6.2.2	Comparison of the results from the analysis of the sheet pile wall adjacent to the track	70
6.2.3	Summary of the comparisons	71
6.3	Results from the Slope Stability Analysis	71
6.3.1	LM71* vs. LMBN	71
6.3.2	Comparison of LM71* and different values of the distributed load	74
6.4	Results from the Analysis of the Sheet Pile Wall adjacent to the Track	77
6.4.1	LM71* vs. LMBN	78
6.4.2	Comparison of LM71* and different values of the distributed load	80
6.5	Summarising Discussion	81
7	Conclusions and Recommendations for Further Work	87
7.1	Summary and Conclusion	87
7.2	Recommendations for Further Work	89
	Bibliography	91
	Appendix	97
A	Slope Stability Example	99
A.1	Material Parameters	99
B	Sheet Pile Wall Example	101
B.1	Material Parameters	101
B.2	Calculations of Steel Details	105
B.3	Moment Diagrams of Walings	106

List of Tables

2.1	Loads for Train load 1	15
2.2	Values of Train load 2	16
2.3	Results from Finnish Transport Agency's report 56	22
3.1	Standard material models in PLAXIS	26
3.2	Input parameters Mohr-Coulomb model (Brinkgreve et al., 2017)	28
3.3	Input parameters Hardening Soil model (Nordal, 2017b)	30
3.4	Input parameters NGI-ADP model (Brinkgreve et al., 2017)	31
3.5	Input parameters for an elastic plate	33
3.6	Input parameters Beam	34
4.1	Material parameters subgrade, part 1	43
4.2	Material parameters subgrade, part 2	43
4.3	Short description of layers	48
4.4	Material parameters for the sheet pile wall	50
4.5	Material parameters for walings and struts	51
5.1	Material parameters used for the slope stability analysis	58
6.1	Effect on the struts, with and without a frost protection layer	70
6.2	Factor of safety for load models	73
6.3	Factor of safety for different load models	74
6.4	Results from analysis of sheet pile wall adjacent to the track	79
6.5	Results from analysis of sheet pile wall adjacent to the track	80
7.1	Final results from simulations in PLAXIS 3D	88

List of Figures

1.1	The railway network in Norway (Svingheim, 2011)	2
1.2	Load Models applicable in Norway	3
2.1	Map over the parcel between Venjar and Langset (FINN kart, 2018)	8
2.2	Map with the location of Oslo S and Ski (FINN kart, 2018)	9
2.3	Load Model 71 and characteristic values for vertical loads (Norsk Standard, 2017)	11
2.4	Characteristic load for a single-track line(Bane NOR, 2017b)	13
2.5	Schematic map showing maximum allowed meter weight according to the classifications of the lines (Fevang, 2016)	15
2.6	Load distribution for a bogie	16
2.7	Scandinavian regulations considering slope stability	18
2.8	Scandinavian regulations considering sheet pile walls	18
2.9	The seven load models used in simulations	20
2.10	Two of the load models used in the calculations	21
2.11	Principle of ADP and the proposed tests for evaluation of the strengths (Grimstad et al., 2011)	23
2.12	Triaxial test to measure active and passive undrained shear strength (Nordal, 2017a)	23
2.13	Active and passive shear strengths (Nordal, 2017a)	24
2.14	Direct shear strength (Norwegian Geotechnical Institute, ud)	24
3.1	Mohr-Coulomb failure criteria	27
3.2	The yield surfaces in the Hardening Soil model (Nordal, 2017a)	29
3.3	Definition of the E-modules in the Hardening Soil model	30
3.4	Failure surface under a line-load	31
3.5	Definition of positive normal forces, shear forces and bending moments for a plate based on local system of axes (Brinkgreve et al., 2017)	32
3.6	Local axes and forces for a beam (Brinkgreve et al., 2017)	34

3.7	Models in PLAXIS for the slope	36
3.8	The very fine mesh of models in PLAXIS for the slope	36
3.9	Elements used in PLAXIS 2D and PLAXIS 3D	37
3.10	Factor of safety with respect to step	37
4.1	The structure of the layers in the super- and substructure	41
4.2	Length of the model in PLAXIS	43
4.3	PLAXIS-model used when calculating slope stability	44
4.4	Characteristic strengths for different ground levels beneath Kvisldalen bridge	45
4.5	Modelling of the sheet pile wall adjacent to the track	47
4.6	Initial phase in three dimensions	48
4.7	AZ 18-700 profile with lengths	49
4.8	Local system of axes in sheet pile wall	49
4.9	Transverse distribution of actions (Norsk Standard, 2017)	52
4.10	Load Model 71 (Norsk Standard, 2017)	54
4.11	Illustration of Load Model 71	55
4.12	Bane NOR's load model (Bane NOR, 2018b)	56
5.1	Final model used for slope stability calculations	57
5.2	Distributed loads on the model in PLAXIS 3D	58
5.3	Surface mesh of the slope stability model	59
5.4	Initial model in PLAXIS 3D	60
5.5	Structural elements in PLAXIS 3D-model	61
5.6	Distributed loads on the model with sheet pile wall	61
5.7	Surface mesh of the model with sheet pile wall	62
5.8	The six phases of the calculation when Bane NORs load model is applied	63
6.1	Slope failures for the heights 5, 15 and 25 m	66
6.2	Factor of safety versus height of slope	67
6.3	Frost protection layer added to the models	68
6.4	Comparison of the case with and without a frost protection layer	69
6.5	Comparison of the case with sheet pile wall, with and without the frost protection layer	70
6.6	No load model applied, $\sigma_z = 0$ kPa	72
6.7	LM71* applied, $ \sigma_{z,LM71*} = 67.7$ kPa	72
6.8	LMBN applied, $ \sigma_{z,LMBN} = 47.7$ kPa	72
6.9	The development of the safety factor	75
6.10	The very end of the plot	75
6.11	Slope failure surfaces	76
6.12	Incremental deviatoric strains in the toe of the slope	76

6.13 Load Model 71 applied	78
6.14 Bane NOR's load model applied	79

Abbreviations

2D	=	Two-dimensional
3D	=	Three-dimensional
ADP	=	Active-direct-passive
Avg	=	Average
FEM	=	Finite element method
kN	=	Kilo newton
kPa	=	Kilo pascal
LM71	=	Load model 71
LM71*	=	Approximated distributed load model based on LM71 (Described in section 4.4.2)
LMBN	=	Load model developed by Bane NOR (Described in section 4.4.3)
NGI	=	Norwegian Geotechnical Institute
OCR	=	Over consolidation ratio
POP	=	Pre-overburden pressure

Symbols

A	=	Cross section area
a	=	Attraction
c	=	Cohesion
d	=	Thickness
E	=	Young's modulus
G	=	Shear modulus
γ	=	Unit weight
$\Delta\gamma_s$	=	Incremental deviatoric strain
I	=	Moment of inertia
K_0	=	Earth pressure coefficient at rest
k	=	Permeability
M	=	Bending moment
ΔN	=	Incremental normal force
ν	=	Poisson's ratio
ϕ	=	Friction angle
ψ	=	Dilatancy angle
Q	=	Point load
q	=	Distributed load
R_{inter}	=	Strength reduction factor
$s_{u,A}$	=	Active undrained strength
$s_{u,D}$	=	Direct undrained strength
$s_{u,P}$	=	Passive undrained strength
σ'_f	=	The effective normal stress on the failure plan
σ_t	=	Tension cut-off and tensile strength
σ_z	=	Vertical surface load in PLAXIS
τ_f	=	Shear strength on the failure plan
$ u $	=	Total displacement
z	=	Depth

Chapter 1

Introduction

1.1 Background

The railway system is transporting passengers and goods all over the world. It has good environmental effects, especially when clean electric hydro power is used, and the network is constantly evolving. In Norway, the annual number of embarking passengers was approximately 70 million between year 2012 and 2016(Statistisk sentralbyrå, 2017).

The first railway in Norway opened in 1854, and was a line from Kristiania, now Oslo, to Eidsvoll(Svingheim, 2004). In the early years, the railway lines were built within the borders of the country. Later they were extended past the border to Sweden. The railway network, as it is in Norway today, is illustrated in figure 1.1. From this figure one can see that the railway lines are connected to Sweden in four locations.

Since the railway network in Norway is linked together with Sweden, similar trains will be found both in Sweden and Norway. This means that the railway lines have to withstand the same loads in these two countries. Sweden is again connected to Finland and Denmark, which in turn is linked to other European countries. From this follows that the railway lines all over Europe should resist the same train loads.



Figure 1.1: The railway network in Norway (Svingheim, 2011)

1.1.1 Problem Formulation

Bane NOR is the government agency responsible for developing the railway network in Norway. There are many challenges related to developing the railway, such as geotechnical structures below and beside the track. To cope with these challenges Bane NOR has developed a set of design rules called *Technical regulations*. The regulations for the geotechnical field are described in the part called *Book 520* about the substructure and the part *Book 525* about bridges and constructions. Bane NOR is currently working on revising these regulations, adjusting the guidelines on geotechnics to make them easier to use. (Svanø, 2017)

The Eurocodes specify how structural design should be conducted within the European Union, and Norway have adopted these Eurocodes. Eurocode NS-EN 1991-2:2003+NA:2010 is originally intended for bridge design, but will also work as a standard for vertical loading due to rail traffic actions for new or replaced geotechnical structures(Norsk Standard, 2017). If an existing structure is renewed or upgraded, the

calculations should be done according to Eurocode NS-EN 15528:2015(Norsk Standard, 2015). In this master's thesis, the focus is on new or replaced structures, and henceforth NS-EN 1991-2:2003+NA:2010 will be used.

Loads from railways are described in Book 520(Bane NOR, 2017b) in Bane NOR's technical regulations as a distributed line load, represented with q_{BN} and shown in figure 1.2a, when calculations related to slope stability or bearing capacity are to be done. This regulation aims to meet the requirements from the European standards. For calculations related to structures adjacent to the track, it is described that the calculations have to be controlled according to the European standard.

The load model representing the static effect of vertical loading due to normal rail traffic that applies to geotechnics in Eurocode NS-EN 1991-2 is called Load Model 71. This load model is described by four axle loads over 6.4 m length, and a distributed line load beyond this, as shown in figure 1.2b.

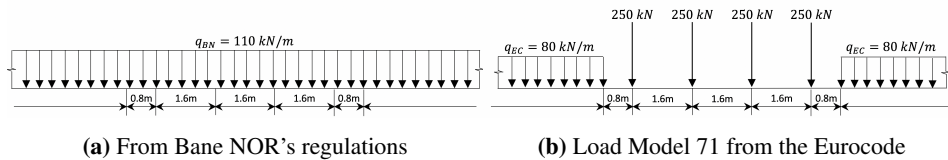


Figure 1.2: Load Models applicable in Norway

Geotechnical analysis is an important part in most of the projects considering railways, and the type of load model used can affect the economy, timeframes and further projects design.

It has been identified some problems when applying Load Model 71 on geotechnical structures, as the loads are mainly intended for bridge structures(Kalliainen and Kolisoja, 2017). In addition, this load model represents a fictive bogie and differs from actual loads from railways. However, the Eurocodes must be followed in Norway, and these days Bane NOR is investigating whether their load model meets the requirements specified in the standard. If not, they should change their technical regulations for geotechnical calculations.

The origin of the current provisions with a line load of 110 kN/m is uncertain, but geotechnicians in Bane NOR believe the background is that 110 kN/m is a mean value for the loads from railways which can be used in many cases. Thus, it is expected that the line load can both lead to oversized and undersized geotechnical structures for the railways. In some cases, Bane NOR may take unnecessary, expensive actions due to strict regulations. In other cases, current rules may even cause railway lines not to be built. Nevertheless, what matters the most is that the regulations ensures that the train passengers and goods are safe and taken care of.

The purpose of this master's thesis is to look into and compare the regulations developed by Bane NOR to the guidelines in the Eurocode by using the three dimensional finite element software program PLAXIS 3D. The focus will be held on vertical loading due to normal rail traffic. It will be investigated whether Bane NOR's regulations related to earthworks differs greatly from the regulations in the European standard, and if that is the case, how Bane NOR should revise their regulations.

1.2 Objectives

The aim of this master's thesis is to investigate the regulations used to develop the railways in Norway today. These will be compared to the European regulations, where the goal is to get an insight into whether Norway meets the European requirements.

The main objectives of this master's thesis are the following:

1. Doing a slope stability analysis with 3D FEM to compare the cases when two different load models are applied
2. Investigate the two load models' effect on a sheet pile wall adjacent to the track with the use of 3D FEM
3. Give a suggestion to Bane NOR on how they should revise their technical regulations according to the obtained results

PLAXIS 3D will be used for finite element modelling in 1. and 2.

1.3 Limitations

First of all, the thesis is limited in such a way that the load models only will be investigated for two different cases, one for slope stability and one for a sheet pile wall adjacent to the track. Two different models have been constructed in PLAXIS 3D, and the conclusions of the thesis is only based on the results obtained from these two models.

The investigated load models in this thesis are the one developed by Bane NOR and the one described in Eurocode NS-EN 1991-2:2003+NA:2010 called Load Model 71. Only the load models described for single-track lines are modelled in PLAXIS.

1.4 Methods

The response to the ground conditions from the two load models is to be calculated by the finite element method. Two material models have been prepared, and calculations have been done in the finite element program PLAXIS 3D.

The first model simulate the response from the load models on slope stability, where the strength($c-\phi$) reduction method is used as an assessment. The other model is used to investigate how a support structure near the railway is affected by the load models with the use of an elastoplastic analysis.

Some of the filtered data has been processed in Excel to develop relevant graphs.

1.5 Outline of the Thesis

This master's thesis is divided into seven chapters, where the remaining chapters are structured as follows:

Chapter 2

Contains relevant theory to give an introduction to the projects the models in this thesis is based on, and the interesting load models which later will be examined. Some relevant studies will be described, and theory for later chapters will be presented.

Chapter 3

Gives an introduction to the finite element program PLAXIS.

Chapter 4

Provides relevant information about the modelling done in PLAXIS 3D.

Chapter 5

Explains the procedure for the performed simulations in PLAXIS 3D.

Chapter 6

Presents the results from the simulations and leads a discussion of these along the way.

Chapter 7

Gives a summary and final conclusions of the work carried out in this master's thesis, as well as recommendations for further work.

Chapter 2

Literature Review concerning Loads from Railways

This chapter gives a theoretical background to this master's thesis. The chapter includes an introduction to the Kvisldalen Railway Bridge project, and to the Østfold line project. Further there are descriptions of the load models in the Eurocode and in the technical regulations developed by Bane NOR. A comparison of the technical regulations for railways in the Scandinavian countries is also provided, as well as summaries from two research projects done in Finland on similar issues as this master's thesis aims to investigate. At the end of this chapter the concept of *active, direct and passive undrained shear strengths* will be described briefly.

2.1 The Projects this Master's Thesis is based on

This master's thesis will contain two different simulations in PLAXIS 3D where the difference between load models will be investigated. The first simulation is a slope stability analysis, and the second is an analysis of a sheet pile wall adjacent to the track.

The models built up for these simulations are based on real examples which will be described in this chapter. Initially the example used for the slope stability analysis will be described, and then the example used to design the model including the sheet pile wall.

2.1.1 Kvisldalen Railway Bridge

The Gardermoen line is a high-speed railway line of 64 km length between Oslo and Eidsvoll in Norway. An expansion of the high-speed line to Hamar is underway, and will be finished by year 2024. This will reduce travel time between Oslo and Hamar with more than 15 minutes. One segment of this project is a 13.5 km long stretch, from Venjar in south to Langset in north, as shown in figure 2.1. At this path the existing single track railway will be extended to a double track railway. This was adopted in september 2016, and the double track is planned to be finished by the year of 2023. (Bane NOR, 2017d)

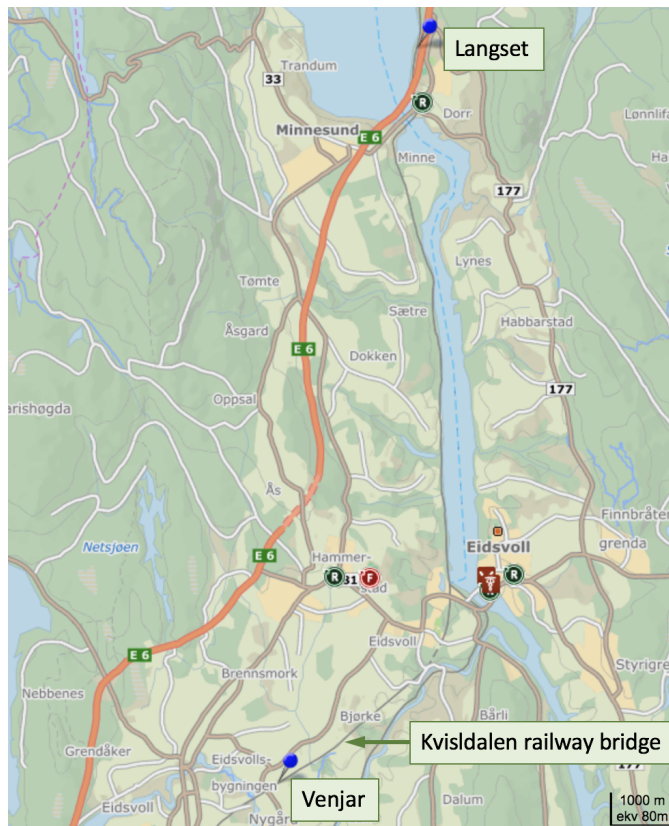


Figure 2.1: Map over the parcel between Venjar and Langset (FINN kart, 2018)

In connection with development of this double track, there has been done some calculations related to geotechnical actions near a bridge between Venjar and Eidsvoll called Kvisldalen railway bridge. These calculations are further described in the project report prepared for Bane NOR(Norwegian Geotechnical Institute, 2017). The new track for this bridge will be established south-east of the existing track.

The area between Venjar and Eidsvoll contains deep ravines. A ravine is formed by fluvial erosion of loose soils, and is a valley with steep sides. Ravines like these can present challenges related to stability of the slopes near the railroad tracks. Therefore, this project will be used as a basis when calculations considering slope stability is to be done throughout the master's thesis.

2.1.2 The Østfold Line between Oslo S and Ski

The Østfold line is a railway line between Oslo and Kornsjø in Norway. The line continues through Sweden. Between 1989 and 1996 there was an upgrade on the track where the section from Ski to Sandbukta received double track and speeds of 160 km/h. Since 2015, there has been laid down work to upgrade more sections with high speeds. This includes the Follo Line between Oslo Central station and Ski, as shown on the map in figure 2.2. (Wikipedia contributors, 2018d)

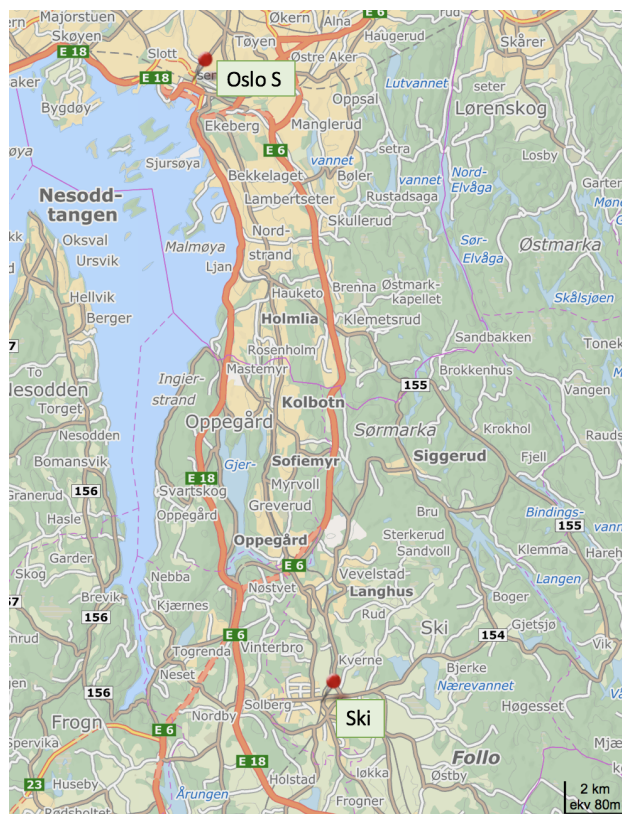


Figure 2.2: Map with the location of Oslo S and Ski (FINN kart, 2018)

The Follo Line will offer a direct route from Oslo to Ski which will reduce travel time to 11 minutes by year 2021. This project was prospected to cost over 26 billion Norwegian kroner in 2014, and will, among other things, provide increased capacity from twelve to forty trains per hour. The project will also involve an upgrade of the junction for public transport in Ski, and this part will further be emphasised in this master's thesis. (Wikipedia contributors, 2018b)

As a result of the size of the project, many site investigations have been done and several reports have been written to design different components that will be built in connection to the line. Sheet pile walls will be built near the track for parts of the Follo Line. These will be built to stabilise the soil and to minimise the vibrations in the ground from the trains. Before upgrading the station in Ski, necessary sheet pile walls have to be designed.

The design of sheet piles and other components is done by Multiconsult on behalf of Bane NOR, and it is carried out using PLAXIS 2D and Geosuite Stability. Descriptions and calculations are given in the design reports for sheet pile 12(Multiconsult, 2017b), sheet pile 13(Multiconsult, 2017c) and the report with the design basis for sheet pile 12 and 13(Multiconsult, 2017a). The simulations in this master's thesis about the sheet pile wall adjacent to the track will be based on these reports.

Since Multiconsult used PLAXIS when doing calculations in this project, the used input parameters are listed up in the reports. From the capacity check of the steel components in appendix B.2 you can see that the sheet pile of type AZ 18-700, the waling of beam type HEB400, and the strut of the same beam type, HEB400, has sufficient capacity. These steel components will hence be used in the calculations for the sheet pile wall in this master's thesis, as well as the input parameters for the materials.

2.2 European Standard applicable in Norway

2.2.1 EN 1991-2: Traffic Loads on Bridges

The ten European Standards are specifying how structural design in Europe should be conducted. Eurocode 1 describes actions on structures, where part two of this standard, EN 1991-2, defines traffic loads on bridges. This standard will, according to chapter 6.3.6.4(Norsk Standard, 2017), also work as a standard for vertical loading due to rail traffic actions for geotechnical structures. For this master's thesis normal train traffic without curves is the only thing being considered. The centrifugal forces will not be taken into account, nor will the nosing force.

Equivalent vertical loading for earthworks

Six types of load models for the railway are given in section 6.3 in this standard. Two of them represent normal rail traffic on mainline railways, LM71 and SW/0, one represent heavy loads, SW/2, another represent the loading from passenger trains at speeds exceeding 200 km/h, HSLM, and the last load model represents the effect of an unloaded train.

According to chapter 6.3.6.4 in this standard (Norsk Standard, 2017), the characteristic vertical loading due to rail traffic actions for earthworks may be taken as load model 71 or load model SW/2 for rail traffic. For earthworks under or adjacent to the track, the characteristic vertical loading should be uniformly distributed over a width of 3 m at a level 0.7 m below the surface of the track. There is no need to apply a dynamic factor to the uniformly distributed load. For design of elements close to the railway track, the maximum local vertical, longitudinal and transverse loading on the element should be taken into account.

As it throughout this master's thesis will be held focus on the vertical loading due to normal rail traffic, only Load Model 71 will be further elucidated in the sections below.

Load Model 71

The static effect of vertical loading due to normal rail traffic is represented by Load Model 71. This model was recommended by the International Railway Union in 1971, and gradually introduced by the different railway administrations after that (Calcada et al., 2008). The load arrangement for this load model is presented in figure 2.3.

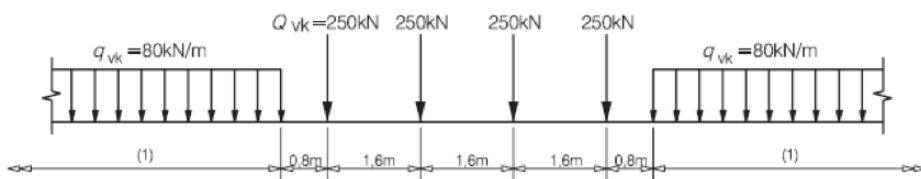


Figure 2.3: Load Model 71 and characteristic values for vertical loads (Norsk Standard, 2017)

Load Model 71 consists of four characteristic point loads $Q_{vk} = 250 \text{ kN}$ over the length of 6.4 m, and a characteristic distributed load $q_{vk} = 80 \text{ kN/m}$ outside this length. On lines carrying rail traffic which is heavier or lighter than normal rail traffic, the characteristic values given in figure 2.3 shall be multiplied by a factor α . The European Standard presents eight alpha factors, while in the national addition for Norway the only factors being used are $\alpha = 1.0$ and $\alpha = 1.33$.

In Norway, the Østfold line is the only railway line where the characteristic value has to be multiplied by $\alpha = 1.33$. For the Ofot line from Narvik to the national border there are special rules. The same location of loads as for LM71 is being used, but the axle loads has the value of 300 kN and the line load equals 120 kN/m.

2.3 Bane NORs Technical Regulations

The technical regulations developed by Bane NOR are updated regularly. These regulations have the purpose of providing essential and adequate regulations for construction of the railway. It simplifies construction, and helps Bane NOR to achieve their goals in terms of capacity, safety and cost efficiency.

There are two books considering geotechnics in these regulations, the book about the substructure, book 520, and the book about bridges and structures, book 525. Further it will be focused on the relevant part of these regulations for this master's thesis, the book about design and construction of the substructure(Bane NOR, 2017b).

2.3.1 Book 520: Substructure

The superstructure is in Bane NOR's technical regulations defined as rail pads, sleepers, ballast and the level crossings. The provisions in book 520 includes everything below the superstructure. Chapter 4 in this book is about technical requirements for the substructure. This is relevant for the issue for this master's thesis, and a summary of the chapter is described in the sections below. Chapter 6: *Ballast bed* and Chapter 8: *Stability* are also used as basis for this master's thesis, and they are referred to in later chapters.

Chapter 4: General technical requirements

This chapter provides general technical requirements when the railway substructure is to be designed and constructed. These requirements facilitates to create a safe, convenient and sustainable substructure under the railway. The chapter includes an outline of the construction properties of different materials, a description of design loads, and geotechnical conditions.

Whether a material can be used when constructing a railway depends on where in the construction it is supposed to be used. Most Norwegian rocks can be used in the subbase and the frost protection layer, while more demands are made for materials used in the ballast. Out of the soils, gravel and sand will have the best construction characteristics, but silt and clay can also be used in some cases.

From section 4 in this chapter about design loads it is referred to Eurocode 1: *Actions on structures*(Norsk Standard, 2010), where the design traffic load can be found by using equation 2.1, and Load Model 71 shall be followed when constructing new railways. The alpha factor is described in subsection 2.2.1, while the combination factor and the load factor can be found in *Eurocode 0: Basis of structural design*(Norsk Standard, 2016).

$$\begin{aligned} \text{The design traffic load} = & \text{alpha factor} \times \text{combination factor} \\ & \times \text{load factor} \times \text{line load or consentrated loads} \end{aligned} \quad (2.1)$$

When doing geotechnical calculations of the stability and the load bearing capacity of an embankment, or of a temporary track support, a line load equal to 110 kN/m should be used as the characteristic line load. The load model is shown in figure 2.4. According to book 520, this line load will usually meet the requirements described earlier in section 2.2.1 about Load Model 71. For double-track lines the calculations should be done as if both of the tracks are loaded at the same time. The tracks are loaded in the most unfavourable way when the most critical track is loaded with the line load equal to 110 kN/m, and the other with a line load equal to 90 kN/m.

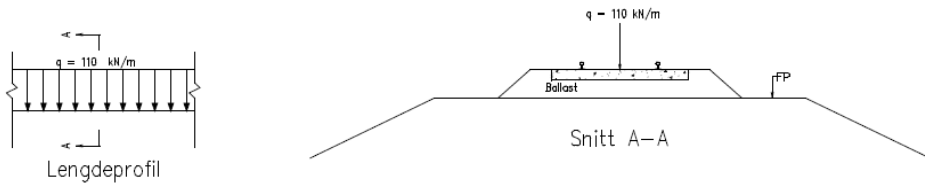


Figure 2.4: Characteristic load for a single-track line(Bane NOR, 2017b)

Previously, this load model was used in most cases when calculations related to geotechnics were done(Svanø, 2017). Probably afraid of not being conservative enough in all these cases, a new regulation was introduced into the technical regulations in February 2018. This rule determines how items or other issues close to the track, for example sheet pile walls, must be checked with Load Model 71.

2.4 Technical Regulations in Scandinavia

Scandinavia is a region consisting the three kingdoms of Sweden, Denmark and Norway. Just east of Norway you find the country Sweden, where the frontier extends over a length of 1630 km(Wikipedia contributors, 2018c). While Norway extends from about 57° to 71° north, Sweden is located a bit further south, from 55° to 69° north(Wikipedia contributors, 2018e). The southernmost of the Scandinavian nations is Denmark, which extends from 54° to 57° north(Wikipedia contributors, 2018a). As these countries are located close to each other, the ground conditions in Sweden and Denmark will be quite similar to the ones you can find in Norway, except that it does not exist quick clay in Denmark.

The rail transport system in Denmark is connected to the southern part of the railway in Sweden, and the Swedish railway system is again linked together with Norway in four different places, illustrated in figure 1.1. In each of these three countries they have their own guidelines for how to make calculations about geotechnical constructions near the railway. All three regulations are made by interpreting and simplifying the guidelines from the European standard NS-EN 1991-2.

For this master's thesis it is interesting to have a look at the differences and similarities between the technical regulations developed in Norway, Sweden and Denmark, since these countries are similar to each other. The Norwegian regulations are previously described in section 2.3, while the Swedish and Danish ones are described in the subsections below.

2.4.1 Technical Regulations in Sweden

The Swedish Transport Administration is called Trafikverket. They own and construct all state-owned roads and railways in Sweden, and they adopt the regulations and advice used in conjunction with the railway. Guidelines within geotechnics applicable in Sweden are called TK Geo 13 and TR Geo 13. TK Geo 13 is a document about the requirements, while TR Geo 13 provides guidance in connection with geotechnical constructions near the railway.

In chapter 4.3 Traffic Load in TK Geo 13, section 4.3.2 is considering loads from railways(Trafikverket, 2014). The highest expected loading from the railway throughout its lifespan is being used to design geotechnical constructions. The loading is reduced by 25 % for one of the tracks in a double track, while if there are multiple tracks, the loading for the other tracks is set to zero. The loads are placed to give the most unfavourable effect.

Loading from the railways is divided into three different types. From the technical advice *Train load 1* is the standard for most situations, for example for calculations considering stability. *Train load 2* should be followed if the spread of a landslide is limited, or when

developing constructions which can be affected by the bogie load, for example sheet pile walls close to the track. The third type of train load, *Trainload 3*, is applicable when a buffer stop is to be designed.

For the calculations in this master's thesis, the relevant train loads are Train load 1 and Train load 2, and these are hence further described.

Train Load 1

For this load type an uniformly distributed load must be distributed over a 2.5 m width, and assumed to have infinite extent in the longitudinal direction. The size of the loading can be seen in table 2.1

Table 2.1: Loads for Train load 1

Train load [maximum weight per meter]	Train load [kN/m^2]	
	Dimension with characteristic values	Dimension with partial factors
6.4	34	26
8	44	32
10	53	40
12	64	48

The case described in section 2.1.1 of The Gardermoen line has been used to develop the model for calculations considering stability in PLAXIS. Figure 2.5 shows a schematic map of maximum allowed meter weight according to the classifications of the lines. The colour of the line between Gardermoen and Oslo is mostly light yellow, which means that the meter weight is 8 tons per meter. This corresponds with the trainload of 32 kN/m^2 , which will give a distributed load over the width of 2.5 m equal to 80 kN/m .

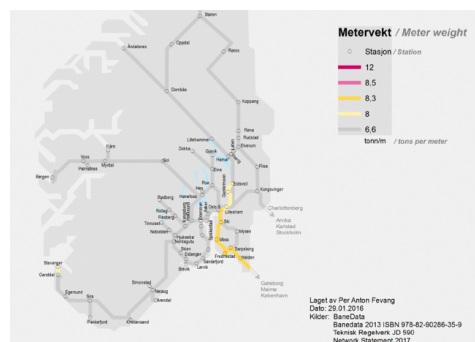


Figure 2.5: Schematic map showing maximum allowed meter weight according to the classifications of the lines (Fevang, 2016)

Train Load 2

For this load type it is described that loading from a bogie must be distributed over 2.5 m width and 6.4 m length as shown in figure 2.6. The size of the loading is entered in table 2.2.

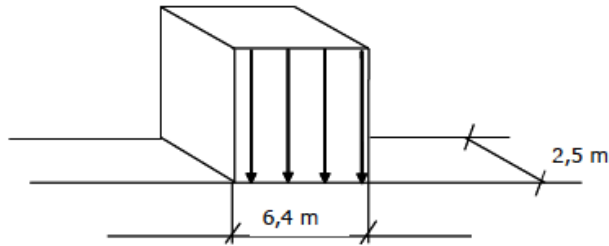


Figure 2.6: Load distribution for a bogie

Table 2.2: Values of Train load 2

Train load [maximum axle weight]	Train load [kN/m ²]	
	Dimension with characteristic values	Dimension with partial factors
22.5	74	56
25	83	62
30	99	75

Maximum axle weight is 22.5 tons in Norway, but the current standard when new tracks are built is to account for a maximum axle weight equal to 25 tons (SINTEF, 2014). The trainload will hence, from the Swedish regulations, be 62 kN/m², or have a line load of 155 kN/m distributed over the length of 6.4 m.

2.4.2 Technical Regulations in Denmark

Banedanmark is a government agency under the Danish Ministry of Transport who has the responsibility for development, maintenance and traffic control of most of the Danish railway network (Banedanmark, 2010). The technical standards and regulations developed by Banedanmark is divided into three levels. The first level, BN1, contains rules given by national og international authorities, BN2 includes technical rules, and BN3 contains technical guidance ensuring compliance of BN1 and BN2 (Banedanmark, nd).

One of the regulations developed by Banedanmark is *BN1-59-4: Regulations for bridges and earthworks under the railway* (Banedanmark, 2010). For loads on geotechnical structures it is described to use an infinite line load equal to 110 kN/m when doing a two

dimensional calculation considering stability for a single-line track. When calculations are to be done for double or multiple tracks the line load of the most critical track is set to 110 kN/m, the nearest track will have a value of 80 kN/m, and the line load for the rest of the tracks can be set to 0 kN/m.

When the calculations are to be done considering supporting walls or sheet pile walls, the regulation says that due to local increase of load from the bogie, the line load must have a value of 170 kN/m over a length of 6.4 m. Outside this length, the line load is 100 kN/m. For a double track line, the second track is described to have a line load of 80 kN/m, while for multiple tracks the other tracks will have a line load equal to 0 kN/m.

2.4.3 A Comparison of the Regulations in Norway, Sweden and Denmark

When these regulations are to be compared, the relevant regulations to look at in connection to this master's thesis are the regulations considering slope stability and those considering supporting structures near the railway. First of all, all three regulations are similar when describing that the line load acts at the level of the lower edge of the sleeper, and that the load should be distributed over a width of 2.5 m.

Regulations Considering Slope Stability

The regulations for geotechnical calculations of stability near the railway in Norway describes a characteristic distributed load equal to 110 kN/m for a single-track line. For the meter weight of the Gardermoen line, which is the relevant line in the following stability calculations of this master's thesis, the characteristic distributed load described in the Swedish regulations is equal to 80 kN/m. In the regulations developed by Banedanmark in Denmark, they use the same value of the characteristic distributed load as in Norway. The regulations for the second track in double track lines are described as a line load of 60 kN/m in Sweden, 80 kN/m in Denmark and 90 kN/m in Norway. For multiple tracks, the other tracks can be set to zero according to all three regulations.

From this comparison, which is illustrated in figure 2.7, it seems like the Norwegian regulations considering slope stability are the most conservative, while in Sweden the regulations are more liberal.

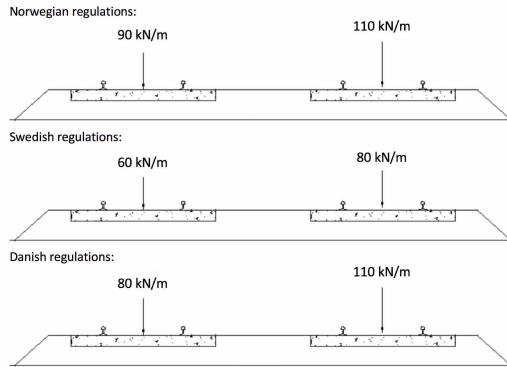


Figure 2.7: Scandinavian regulations considering slope stability

Regulations Considering Supporting Structures near the Railway

For sheet pile walls near the track in Sweden the load type Train Load 2 applies, which is a distributed load of 155 kN/m over a width of 2.5 m and a length of 6.4 m. Nothing is written about the value of the line load outside this length in the Swedish regulations.

In Denmark the loads from the bogie must be taken into account when calculations are to be done for sheet pile walls. According to their regulations the train should be modelled as a line load of 170 kN/m over the same width and length as in Sweden, and 100 kN/m beyond this length.

Due to the Norwegian regulations the same load model as for stability, where the distributed load is equal to 110 kN/m, has been used until recently. In February, new rules in the technical regulations describes that calculations of sheet piles close to the track has to be checked with Load Model 71. Load Model 71 has four axle loads of 250 kN over a width of 3 m, and a line load equal to 80 kN/m outside this length. According to the regulations developed by Bane NOR, the axle loads can be approximated to a line load equal to 156 kN/m over the length of 6.4 m.

The three different regulations are illustrated in figure 2.8.

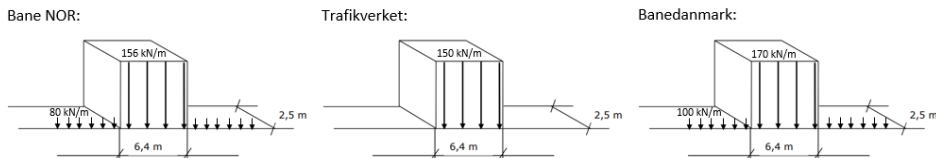


Figure 2.8: Scandinavian regulations considering sheet pile walls

Summary of the comparison

Sweden has the most liberal regulations considering slope stability, with a reduction in the line load of more than 20 percent compared to Denmark and Norway. The regulations in Sweden related to supporting structures near the railway are also describing lower design values than what can be found in the other Scandinavian countries.

As a recap of this comparison it seems like the Norwegian regulations are the most conservative in the slope stability case, where Bane NOR has the highest value for the line load when calculating slope stability. For the case with supporting structures near the railway, the Danish regulations are the most strict.

2.5 Previous Studies

In the following section two previous studies done to study the effects of different load models will be described. They are both produced for purposes of Finnish Transport Agency and their work on developing the railways in Finland.

2.5.1 Pile supported embankment slabs under railway track line *Research report 28 from the Finnish Transport Agency*

This report describes a research study which is produced for purposes of Finnish Transport Agency (Kalliainen and Kolisoja, 2017). The aim of the project was to study the effects of different load models on the vertical stress levels of pile supported embankment slabs under railway structures. The project was carried out with help from the three-dimensional finite element software PLAXIS 3D. Simulations in PLAXIS 3D included three different embankment thicknesses and seven different load models. The load models are illustrated in figure 2.9.

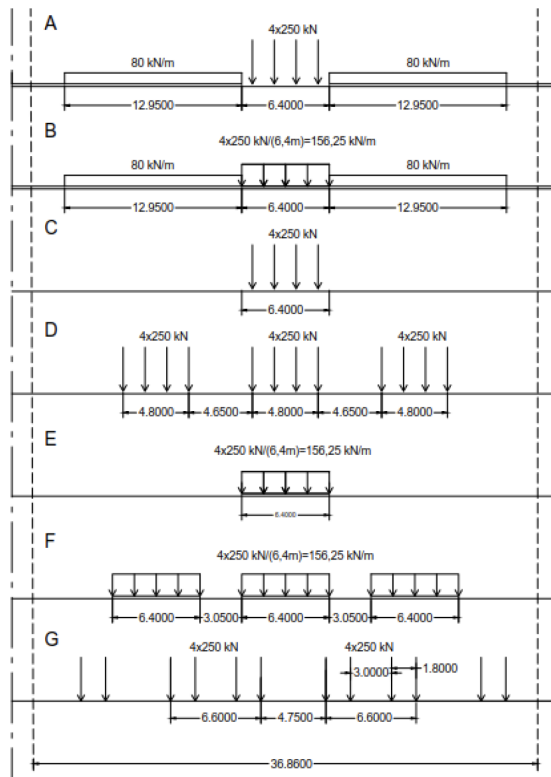


Figure 2.9: The seven load models used in simulations

Load model A is the same as Load Model 71 from the Eurocode. The results shows that load models A and F are very similar in load intensity, while load model G provides a smaller load intensity. It seems that load model A produce the highest stresses in the most intensively loaded areas when the installation depth is less than 5 m. Differences in load distribution for the different load models seems to diminish as the embankment height grows and the examined section is getting longer.

The results shows a difference in line load and point load. For the cases with point load, and especially for Load Model 71, the center area of the embankment structure will show higher levels of vertical stress. Type of load model being used has a significant impact on the load effects. The load model ruled to be applied for earthworks in Europe, Load Model 71, is originally intended for bridge design. According to this research report, this load model will lead to increasing constructions costs and uneconomical structures.

2.5.2 2D Loads for Stability Calculations of Railway Embankments

Research report 56 from the Finnish Transport Agency

This project done by the Finnish Transport Agency in 2017 had the purpose to study how the Load Model 71 from the eurocode should be applied into 2D embankment stability calculations (Savolainen et al., 2017). The loads currently defined in the Finnish guidelines for 2D stability calculations are conservative, where the equivalent loads are relatively high. According to Finnish regulations, the distributed load used for calculations in 2D is equal to 149 kN/m (trafikverket, 2016). These loads are defined by calculating the change of effective vertical stress under the bogies.

To study Load Model 71 an analyse was done of how the loads from train will have an impact beneath the railway embankment and in the subgrade. This was simulated in PLAXIS 3D, where five different load models were used. Only two of these load models will further be described, illustrated in figure 2.10, where one of them is Load Model 71 and the other is an area load with different values distributed over the width 2.6 m.

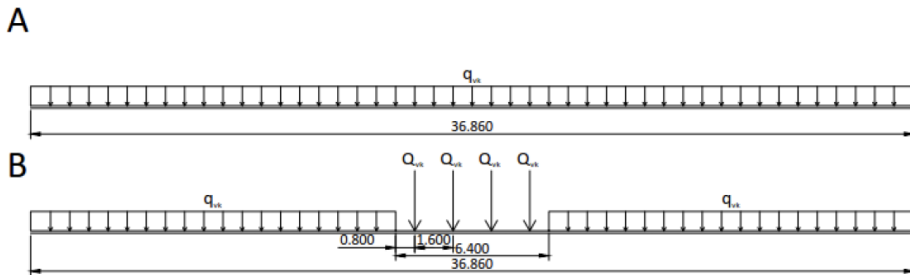


Figure 2.10: Two of the load models used in the calculations

In Norway the most commonly used alpha factor is 1.00, which will give an axle load $Q_{vk} = 250$ kN and a line load $q_{vk} = 80$ kN/m for Load Model 71. The average line load for these values are 93.24 kN/m, as shown in equation 2.2.

$$q_{avg} = \frac{4 \cdot 250 \text{ kN}}{6.4 \text{ m}} \cdot \frac{6.4 \text{ m}}{36.86 \text{ m}} + 80 \text{ kN/m} \cdot \frac{30.46 \text{ m}}{36.86 \text{ m}} = 93.24 \text{ kN/m} \quad (2.2)$$

From the results of this report one can see that the increase in effective stress under the embankment, when the loads are applied, seems to reach a peak under the embankment with the lowest height. Another interesting discovery about the height of the embankment is that the increase in the load has increasing negative impact on safety level with 1.5 m height compared to 2.5 m height.

The main purpose of the calculations was to find the 2D strip load that correspond to the Load Model 71. The final results from the stability calculations done in this study are shown in table 2.3, where the range between the minimum and the maximum 2D loads are decided by doing several different calculations. The performed calculations were done with two different types of mesh, with very soft clay, with silty subgrade, and with the NGI-ADP Soft-model.

Table 2.3: Results from Finnish Transport Agency's report 56

Load model	2D load minimum [kN/m]	2D load maximum [kN/m]
Load Model 71 ($Q_{vk} = 250 \text{ kN}$, $q_{vk} = 80 \text{ kN/m}$)	87	103

According to these results, a mean value for the 2D load is 95 kN/m, which is approximately the same as the average line load for Load Model 71 equal to 93.24 kN/m, as described in equation 2.2.

2.6 Active, Direct and Passive Undrained Shear Strength

In this section the principle of active, direct and passive shear strength will be described. The main part of the following theory is taken from the compendium of the subject "TBA4116 Geotechnical Engineering Advanced Course" (Nordal, 2017a). Figure 2.11, developed by Grimstad, Andersen and Jostad (Grimstad et al., 2011), illustrates the concept of active, direct and passive strength, and the proposed tests for assessment of the undrained strengths.

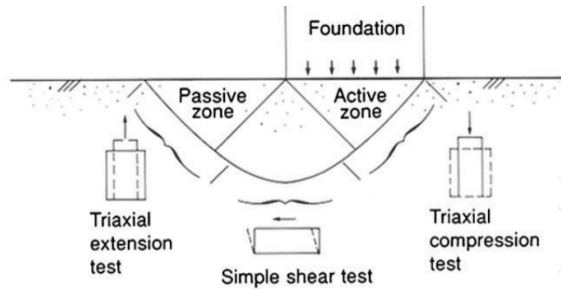


Figure 2.11: Principle of ADP and the proposed tests for evaluation of the strengths (Grimstad et al., 2011)

A known way to measure undrained strength is, as shown in the figure above, the triaxial test. This test can be done in two ways, as shown in figure 2.12. For the active triaxial test, the cell pressure is kept constant, while the piston force is increased after the consolidation is finished. The passive shear test can be done after consolidation in two ways. Either by increasing the horizontal stress while the axial stress is kept constant, or by applying a tension force in the piston, where both ways will lead to a reduction in the axial stress.



Figure 2.12: Triaxial test to measure active and passive undrained shear strength (Nordal, 2017a)

These two types of tests will give different shear strength capacities, where the active undrained strength is described with the symbol s_{uA} , while s_{uP} is used for the passive undrained strength. The difference between these strengths are illustrated in figure 2.13.

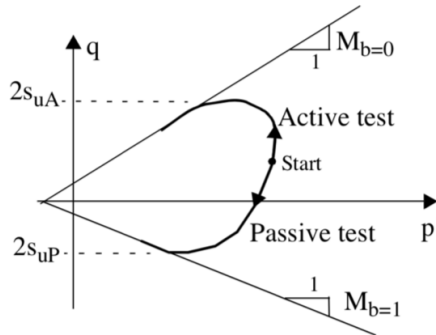


Figure 2.13: Active and passive shear strengths (Nordal, 2017a)

Another way to measure estimates of an undrained shear strength is the direct simple shear test. This test is used for the investigation of stress-strain-strength relationships for horizontal loading situations. In Norway it is common to use the NGI direct simple shear apparatus when doing this test. The concept of the test is shown in figure 2.14, where static and cyclic loading can be performed as either strain- or stress-controlled. (Norwegian Geotechnical Institute, ud)

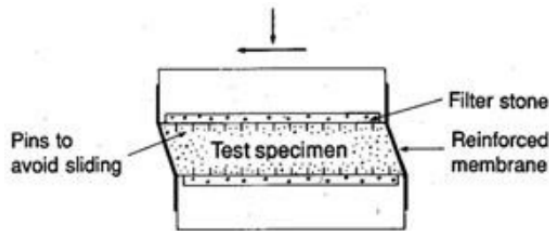


Figure 2.14: Direct shear strength (Norwegian Geotechnical Institute, ud)

The direct simple shear test uses a direct shear machine, which means that the shear strength and the normal stress are both being measured directly. The obtained undrained shear strength is thus called the undrained direct shear strength, and is described with the symbol s_{uD} . (Olson and Lai, 2004)

Chapter 3

Finite Element Analysis in PLAXIS

Geotechnical design has traditionally been carried out using simplified analyses or empirical approaches. When computer hardware and software were introduced, this resulted in considerable advances in the design and analysis of geotechnical structures. The development of the finite element program PLAXIS began at Delft University of Technology in 1987. The initial purpose of the program was to develop a finite element code for the analysis of river embankments in Holland, but PLAXIS has been extended in subsequent years, and now covers most areas of geotechnical engineering. Real situations may in this program be modelled either by a PLane strain or an AXISymmetric model, and hence the name PLAXIS. While the first PLAXIS 2D program was released for Windows in 1998, the full three-dimensional finite element program, PLAXIS 3D, was not released until 2010. (Brinkgreve et al., 2017)

The finite element method has a wide range of engineering applications, and is widely used in geotechnical engineering. One of the main steps of this method is the element discretization. This is when the geometry of the boundary value problem is replaced by a finite element mesh which is composed of small regions called finite elements. The size and the number of elements influences the final solution, where more accurate solutions can be obtained with a refined mesh of small elements. (Potts and Zdravkovic, 1999)

PLAXIS 3D is a full three-dimensional finite element program which includes static elastoplastic deformation, advanced soil models, stability analysis, consolidation, safety analysis, updated mesh analysis and steady-state groundwater flow. This chapter includes an introduction to PLAXIS 3D, a comparison of two- and three-dimensional modelling in

PLAXIS, a description of the procedure, and the available options in the program.

3.1 Material Models in PLAXIS

In the PLAXIS input program the material sets assigned to the entities in the model are listed under the button Materials. Here, the materials can be described and coloured by the user. The different types of materials available are *Soil and interfaces*, *Plates*, *Geogrids*, *Beams*, *Embedded beams* and *Anchors*. Further, the material types Soil and interfaces, Plates and Beams will be described, as these are relevant in this master’s thesis.

3.1.1 Soil and Interfaces

Both soil and rock tend to have a non-linear stress-strain behaviour under load. This behaviour can be modelled at various degrees of accuracy. PLAXIS 3D supports thirteen soil models to simulate how the soil will act when being loaded. In addition there is one option where the user can define the soil model. The standard material models in PLAXIS are listed in table 3.1 below.

Table 3.1: Standard material models in PLAXIS

Material models:	
Linear Elastic model	Mohr-Coulomb Model
Hardening Soil model	Hardening Soil model with small-strain stiffness
Soft Soil model	Soft Soil Creep model
Jointed Rock model	Modified Cam-Clay model
NGI-ADP model	Hoek-Brown model
Sekiguchi-Ohta (Viscid)	Sekiguchi-Ohta (Inviscid)
UBC3D-PLM model	User-defined model

Relevant soil models for this master’s thesis are the Mohr-Coulomb model, the Hardening Soil model and the NGI-ADP model. These are elaborated in the following sections.

Mohr-Coulomb model

The Coulomb theory was first established by Charles-Augustin de Coulomb, and later revised to a more generalised form, the Mohr-Coulomb theory, by Christian Otto Mohr at the end of the 19th century. In geotechnical engineering, the theory is used to define

shear strength of soils as well as rocks at different effective stresses. The theory contains a criterion called The Mohr-Coulomb failure criterion, which was the first criterion to account for hydrostatic stresses. It describes the linear relation between the shear strength of a material and the applied normal stress, as expressed in the general form for effective stresses in equation 3.1. (Labuz and Zang, 2012)

$$\tau_f = (\sigma'_f + a) \cdot \tan(\phi) \tag{3.1}$$

where

- τ_f = Shear stress on the failure plan,
- σ'_f = The effective normal stress on the failure plan,
- a = Attraction,
- ϕ = Friction angle.

The value of the attraction indicates whether it is possible to have tension, $\sigma' < 0$, in the soil. Angle of internal friction is a measure of the ability of a unit of soil to withstand a shear stress. Equation 3.1 describes the line representing the failure envelope in figure 3.1.

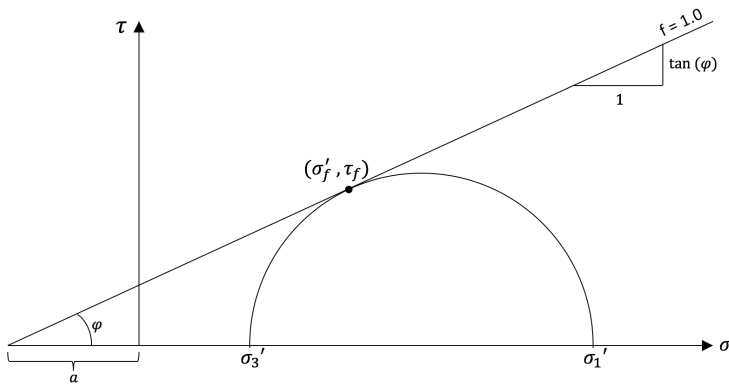


Figure 3.1: Mohr-Coulomb failure criteria

For undrained materials, the friction angle ϕ can be set to 0° and the cohesion c , where $c = a \cdot \tan(\phi)$, set to c_u which is the undrained shear strength.

This model is described in PLAXIS as a first order linear elastic perfectly-plastic model. It is a simple model with a limited number of the features soil behaviour shows in reality. The

principle of elastoplasticity is that strains and strain rates are decomposed into an elastic and a plastic part. This principle is restricted to smooth yield surfaces, while the Mohr-Coulomb model presents a multi surface yield contour. The full Mohr-Coulomb yield condition consists of the six yield functions and six plastic potential functions, where the plastic potential functions contain the dilatancy angle ψ . This parameter models positive plastic volumetric strain increments as observed for dense soils. (Brinkgreve et al., 2017)

The linear elastic perfectly-plastic Mohr-Coulomb model requires the five parameters listed below(Brinkgreve et al., 2017), which can be obtained from basic tests on soil samples. These parameters can either be effective parameters or undrained parameters, depending on the drainage type selected.

Table 3.2: Input parameters Mohr-Coulomb model (Brinkgreve et al., 2017)

Parameter	Description
Stiffness	
E	Young's modulus
ν	Poisson's ratio
Strength	
c	Cohesion
ϕ	Friction angle
ψ	Dilatancy angle
σ_t	Tension cut-off and tensile strength

Additional parameters, V_p and V_s , may be used to define stiffness based on wave velocities in the case of dynamic applications. Advanced features for this model comprise the increase of stiffness and cohesive strength, or undrained strength, with depth.

Hardening Soil model

The Hardening Soil model is an advanced model where the behaviour of different types of soils, both soft and stiff, can be simulated. It was originally proposed for sand, but is now developed to be used for other types of soils as well. This model is recommended over the simple Mohr-Coulomb model whenever soil deformations are important(Nordal, 2017a). In contrast to the Mohr-Coulomb model, the yield surface of this model is not fixed in principal stress space, but can expand due to plastic straining. This is because of the two plastic yield surfaces, the cone and the cap, as illustrated in figure 3.2.

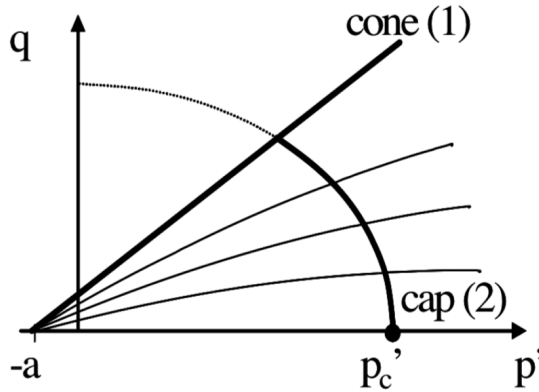


Figure 3.2: The yield surfaces in the Hardening Soil model (Nordal, 2017a)

The cone is described by the Mohr-Coulomb-criterion, where mobilized friction, $\tan(\rho)$ is used instead of $\tan(\phi)$. When loading toward failure the cone will expand and give plastic strains controlled by the increased mobilized friction. The cone will stay in its outer position when unloading, and the region beneath the cone becomes an elastic region. (Schanz et al., 1999)

In the Hardening Soil model it is also a spherical surface made by increasing plastic shear strains called a cap. The initial position of the cap is controlled by the preconsolidation stress. When loading further than the preconsolidation level, the cap will be expanded, and the soil will get plastic volumetric strains as a consequence. (Nordal, 2017a)

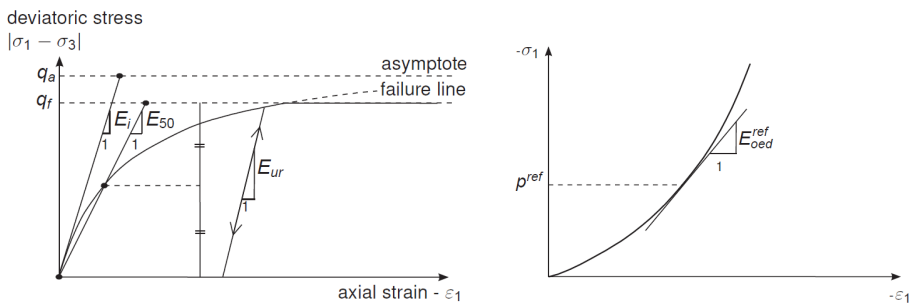
A basic feature of the Hardening Soil model is a formulation that makes the stiffness dependent on the effective stress level. The model takes into account two different types of hardening, shear hardening and compression hardening. Shear hardening is used to model irreversible plastic strains due to primary deviatoric loading, while the compression hardening is used to model irreversible plastic strains due to primary compression. (Brinkgreve et al., 2017)

Due to the complexity of the Hardening Soil model, the number of input variables in PLAXIS is high. The parameters are given in table 3.3. Even though the model has a good way of describing real life materials, it is important to have access to all of these input parameters. If these parameters are not available, a different model should be used.

Table 3.3: Input parameters Hardening Soil model (Nordal, 2017b)

Parameter	Description
Stiffness	
E_{50}^{ref}	Reference modulus for primary loading in drained triaxial test
E_{oed}^{ref}	Reference modulus for primary loading in oedometer test
E_{ur}^{ref}	Reference modulus for unloading/reloading in drained triaxial test
$power(m)$	Modulus exponent for stress dependency
ν_{ur}	Poisson's ratio for loading/unloading
Strength	
c_{ref}^f	Effective cohesion at failure
ϕ^f	Effective friction angle at failure
ψ	Dilatancy angle at failure
K0 settings	
K_0	Earth pressure coefficients at rest
OCR	Over consolidation ratio
POP	Pre-overburden pressure

How the E-modules can be found are shown in figure 3.3. The power m varies from the value 0.5 to 1.0 for Norwegian sands to soft clays, respectively. Realistic values of ν_{ur} are about 0.2, which is used as a default setting in PLAXIS. The over consolidation ratio can be found by subtracting the initial vertical stress from the initial preconsolidation stress, $OCR = \sigma_p - \sigma'_{v0}$, and the pre-overburden pressure can be found by dividing the initial preconsolidation stress by the initial vertical stress, $POP = \frac{\sigma_p}{\sigma'_{v0}}$. (Brinkgreve et al., 2017)



(a) Stress-strain relation in primary loading for a standard drained triaxial test (Nordal, 2017b) **(b)** Oedometer test results (Nordal, 2017a)

Figure 3.3: Definition of the E-modules in the Hardening Soil model

NGI-ADP model

The elastoplastic constitutive NGI-ADP model is developed from the Tresca approximation together with a modified von Mises plastic potential function. The model is based on the undrained shear strength approach, and it has the purpose of matching the design profiles of undrained shear strengths in active, direct simple shear and passive modes of loading. (Grimstad et al., 2011)

Active, direct and passive undrained shear strengths are described in section 2.6. Active and passive zone, as well as the direct simple shear strength are illustrated in figure 3.4.

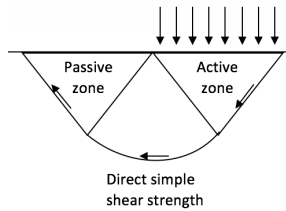


Figure 3.4: Failure surface under a line-load

Parameters for the NGI-ADP model in PLAXIS are listed in table 3.4 below.

Table 3.4: Input parameters NGI-ADP model (Brinkgreve et al., 2017)

Parameter	Description
Stiffness	
G_{ur}/s_u^A	Ratio unloading/reloading shear modulus over (plane strain) active shear strength
γ_f^C	Shear strain at failure in triaxial compression
γ_f^E	Shear strain at failure in triaxial extension
γ_f^{DSS}	Shear strain at failure in direct simple shear
Strength	
$s_{u,ref}^A$	Reference (plane strain) active shear strength
$s_u^{C,TX}/s_u^A$	Ratio triaxial compressive shear strength over (plane strain) active shear strength
z_{ref}	Reference depth at which the reference active shear strength is defined
$s_{u,inc}^A$	Increase of shear strength with depth
s_u^P/s_u^A	Ratio of (plane strain) passive shear strength over (plane strain) active shear strength
T_0/s_u^A	Initial mobilization
s_u^{DSS}/s_u^A	Ratio of direct simple shear strength over (plane strain) active shear strength
Advanced	
ν'	Poisson's ratio

Many geotechnical problems involve undrained behaviour of clay. Most models used today are effective stress based, and only indirectly obtain values for the undrained shear strength. The NGI-ADP model may be used for deformation, capacity and soil-structure interaction analyses involving undrained loading of clay. The model has direct input of shear strengths, which gives the model significant advantages for design analysis of undrained problems. (Grimstad et al., 2011)

3.1.2 Plates

The material behaviour in plate elements in PLAXIS 3D is based on the general 3D continuum mechanics theory and the assumption that the transverse stress component is negligible, $\sigma_{33} = 0$. Its behaviour is approximated by the relationship between strains and stresses as shown in the matrices in equation 3.2, assuming Poisson's ratio is small. (Jönsson, 1995)

$$\begin{bmatrix} \sigma_{11} \\ \sigma_{22} \\ \sigma_{12} \\ \sigma_{13} \\ \sigma_{23} \end{bmatrix} = \begin{bmatrix} E_1 & \nu_{12}E_2 & 0 & 0 & 0 \\ \nu_{12}E_2 & E_2 & 0 & 0 & 0 \\ 0 & 0 & G_{12} & 0 & 0 \\ 0 & 0 & 0 & kG_{13} & 0 \\ 0 & 0 & 0 & 0 & kG_{23} \end{bmatrix} \begin{bmatrix} \epsilon_{11} \\ \epsilon_{22} \\ \gamma_{12} \\ \gamma_{13} \\ \gamma_{23} \end{bmatrix} \quad (3.2)$$

In a plate element the local system of axes is such that the first and second local axis lies in the plane, while the third axis is perpendicular to the plane of the plate. Illustrations of the local axis system as well as the positive structural forces in a plate are shown in figure 3.5.

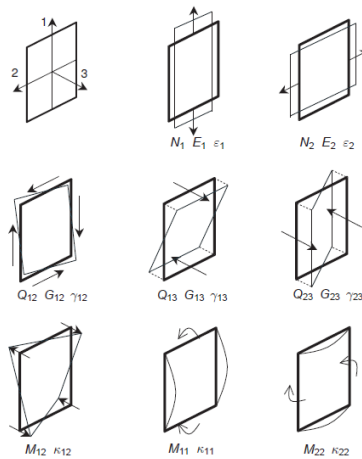


Figure 3.5: Definition of positive normal forces, shear forces and bending moments for a plate based on local system of axes (Brinkgreve et al., 2017)

The options for the material type of a plate in PLAXIS is either elastic or elastoplastic. Table 3.5 below mentions the input parameters for the elastic type of material, as the plate in this master's thesis will be modelled as an elastic plate.

Table 3.5: Input parameters for an elastic plate

Parameter	Description
d	Plate thickness
γ	Unit weight of the plate material
E_1	Young's modulus in the first direction
E_2	Young's modulus in the second direction
ν_{12}	Poisson's ratio
G_{12}	In plane shear modulus
G_{13}	Out of plane shear modulus related to shear deformation over first direction
G_{23}	Out of plane shear modulus related to shear deformation over second direction
Rayleigh α	Damping value
Rayleigh β	Damping value

All the modules from this table can be found from the following equations, where equation 3.3 describes Young's modulus and equation 3.4 describes the shear modulus (Brinkgreve et al., 2017). Poisson's ratio in these equations, $\nu = \nu_{12}$, is small and can often be assumed to be zero.

$$E_1 = \frac{12EI_1}{d^3}, \quad E_2 = \frac{12EI_2}{d^3} \quad (3.3)$$

$$G_{12} = \frac{6EI_{12}}{(1+\nu)d^3}, \quad G_{13} = \frac{EA_{13}}{2(1+\nu)d}, \quad G_{23} = \frac{EA_{23}}{2(1+\nu)d} \quad (3.4)$$

In equation 3.3 the parameter E is the actual Young's modulus of the material, and I_1 and I_2 are the moment of inertia against bending over respectively the first and second axis. The parameter I_{12} in equation 3.4 is the moment of inertia against torsion, while A_{13} and A_{23} are the effective material cross section area for shear forces Q_{13} and Q_{23} .

3.1.3 Beams

In a beam element in PLAXIS, the local first axis correspond with the axis beam direction, while the second and third axis are perpendicular to the beam axis. This, in addition to the forces in a beam, is illustrated in figure 3.6 below.

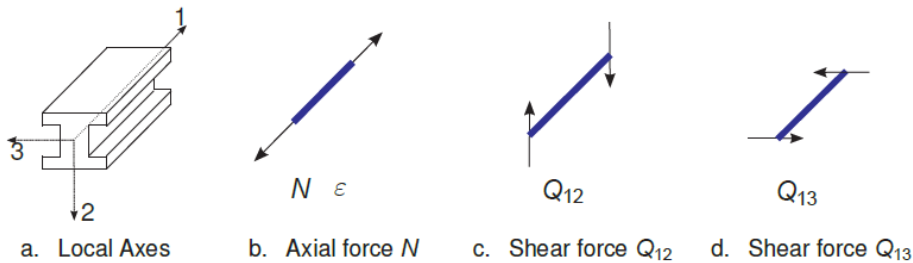


Figure 3.6: Local axes and forces for a beam (Brinkgreve et al., 2017)

The beam can either be modelled elastic or elastoplastic. As for the plates, the elastic material type will further be elaborated, as this is the relevant kind of beam for this master's thesis. Elastic behaviour of beam elements is defined in PLAXIS by the parameters described in table 3.6.

Table 3.6: Input parameters Beam

Parameter	Description
E	Young's modulus in axial direction
γ	Unit weight of the beam material
A	Beam cross section area
I_2	Moment of inertia against bending around the second axis
I_3	Moment of inertia against bending around the third axis
Rayleigh α	Damping value
Rayleigh β	Damping value

3.1.4 Interfaces

To allow for proper modelling of soil-structure interaction, joint elements called *Interfaces* should be added to the model in PLAXIS. Interfaces can be added between two soil volumes, or they can be created next to plate or geogrid elements. They are used to simulate

the contact between, for example, a plate and the surrounding soil. The term "positive" or "negative" for interfaces enables distinguishing between interfaces at each side of a surface. (Brinkgreve et al., 2017)

Interfaces has several properties, as *Material Mode*, *Permeability Condition* and *Virtual thickness factor*. The material properties available are the roughness of the interaction, described by the strength reduction factor R_{inter} . This factor is set to one by default for all materials. Another material property is the residual strength, $R_{inter,residual}$, which relates the interface strength to the soil strength. The permeability properties of the interfaces can make structural elements impermeable.

As interface elements are supposed to generate little elastic deformations, the virtual thickness of the interface should be small. The default virtual thickness factor is 0.1, which should only be reduced if the interface elements are subjected to very large normal stresses. This is because numerical ill-conditioning may occur if the virtual thickness is too small. (Brinkgreve et al., 2017)

3.2 Meshing

PLAXIS has an automated capability to generate a mesh. Our ability to model geotechnical problems has been greatly enhanced by this development. However, these advanced techniques offers a number of challenges including the effects of numerical errors and instability. The size of the mesh has to be sufficiently large so that the boundaries do not constrain the problem, and the size of the elements has to be sufficiently small to reduce discretization error. At the same time, too small elements will require excessive computer memory. (Klettke and Edgers, 2011)

The quality of the obtained results varies with the use of two- and three-dimensional modelling. In the following section a case will be presented where the stability of a slope is calculated for both two and three dimensions. The case will also give insight to what differences there are between PLAXIS 2D and PLAXIS 3D considering meshing.

3.2.1 The use of PLAXIS 2D versus PLAXIS 3D

In this section the factor of safety for slope stability obtained when using PLAXIS 2D and PLAXIS 3D will be compared. The model in this section will only be used as a tool to compare the finite element programs PLAXIS 2D and PLAXIS 3D, and how it is constructed will be further described later, in chapter 4.2. The load model used in this example is the distributed load from Bane NOR's technical regulations, as this model is easier to implement into a 2D-model than Load Model 71.

Another research project considering this is done by Anton Karlsson and Stefan Jarl Wellerhaus in their master's thesis, written in 2014. The results from this thesis indicates that calculations in two dimensions underestimates the total stability for an excavation compared to calculations in three dimensions. (Karlsson and Wellerhaus, 2014)

To illustrate the difference between calculations in two and three dimensions in this section, the models are meshed up in coarse, medium and very fine mesh for both cases. Figure 3.7a and 3.8a below illustrates the geometry and the very fine mesh of the model for the 2D case, while figure 3.7b and 3.8b gives illustrations of the 3D case in PLAXIS.

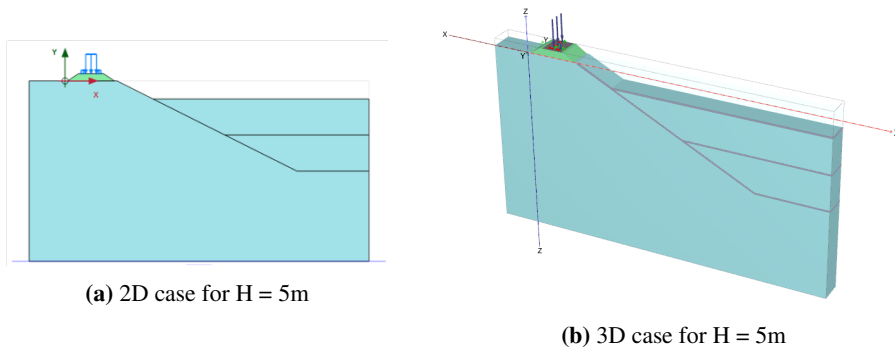


Figure 3.7: Models in PLAXIS for the slope

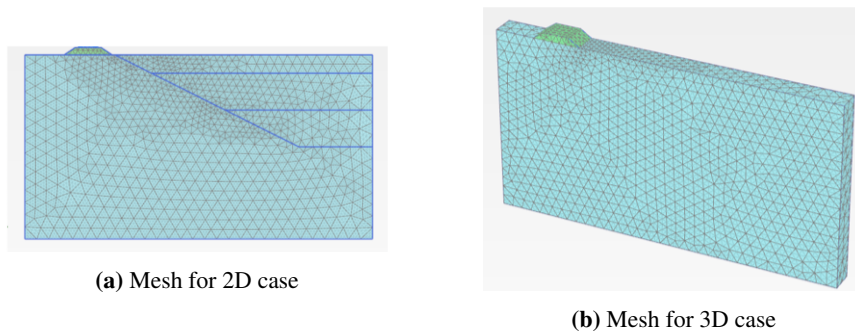


Figure 3.8: The very fine mesh of models in PLAXIS for the slope

The two dimensional figure had 1738 elements for the very fine mesh, while the model in PLAXIS 3D had 9223 elements. The default elements are 4th order 15-node triangular in PLAXIS 2D, illustrated in figure 3.9a, and quadratic tetrahedral 10-node elements in PLAXIS 3D, as shown in figure 3.9b. For PLAXIS 3D the element is simpler and requires less memory, but the element will not give as accurate results as the 15-noded elements in PLAXIS 2D. (Brinkgreve et al., 2017)

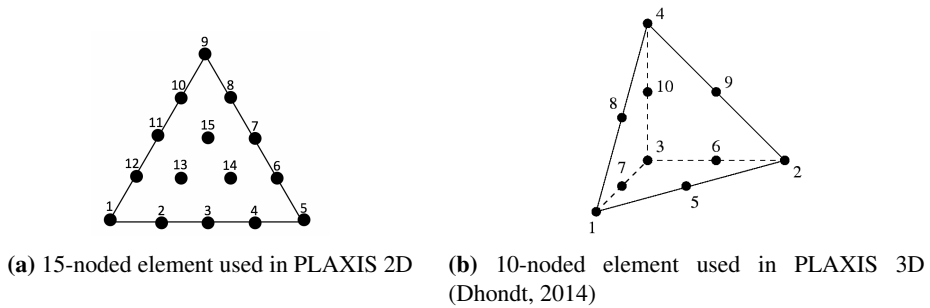


Figure 3.9: Elements used in PLAXIS 2D and PLAXIS 3D

The development of the factor of safety with respect to step is shown in figure 3.10. This graph shows that the model in PLAXIS 3D gives larger values for the factor of safety compared to the results from PLAXIS 2D.

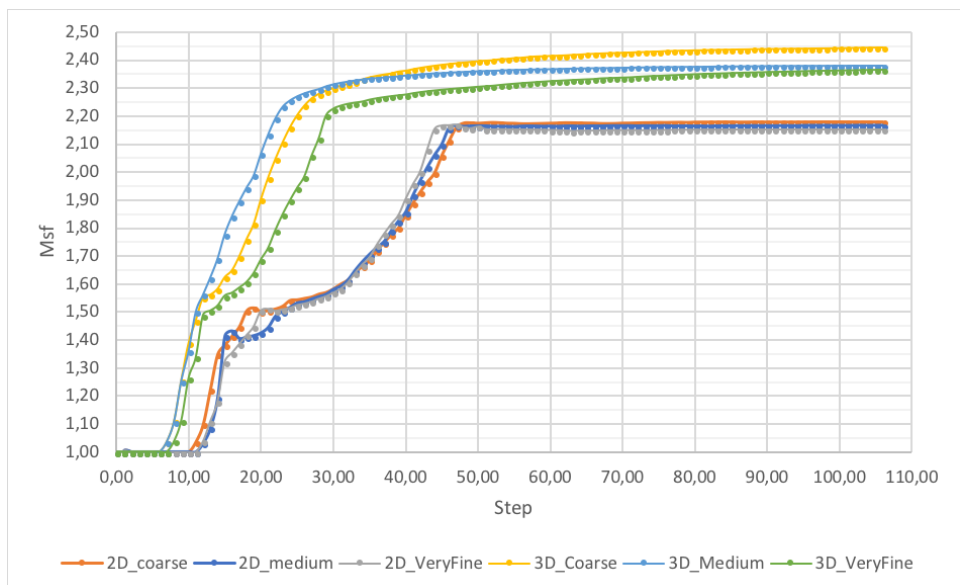


Figure 3.10: Factor of safety with respect to step

Another important issue from this plot is that all graphs seems to have a kink near where the factor of safety is equal to 1.5. From this point the three graphs from PLAXIS 2D seems to increase with approximately the same incline, before they stabilises at almost the same value, between 2.15 and 2.20. The graphs from PLAXIS 3D seems to have different slopes after this point, and they do not stabilise in the same way as the graphs

from PLAXIS 2D. Figure 3.10 visualises that PLAXIS 2D provides clearer results than PLAXIS 3D.

The results in figure 3.10 supports the findings from Karlsson and Wellerhaus' master's thesis, where they found that 2D calculations underestimates the total stability. However, as mentioned earlier in this section, the simple elements in PLAXIS 3D will not give as accurate results as the elements in PLAXIS 2D. It is clear that the finer mesh you use, the lower factor of safety you get in 3D calculations. For 2D, the difference is not significant. This makes it possibly more accurate to say that 3D calculations overestimates the total stability. It is important to keep that in mind when assessing results later in this thesis.

3.3 Calculation phases

Before the calculations in PLAXIS can be done, the sequential calculation phases has to be defined, as well as the type of calculation for each phase. The first phase is called *Initial phase*, while the following phases are named *Phase 1*, *Phase 2* and so on.

3.3.1 Initial phase

In the initial phase the initial stresses are generated. These stresses can either be generated by using Gravity loading, Field stress or the K_0 procedure. It is noted in the PLAXIS manual that the K_0 procedure is preferred in cases where the surface is horizontal and the soil layers parallel to the surface (Brinkgreve et al., 2017). The calculations in this master's thesis has these characteristics, thus only the K_0 procedure will be described further.

K_0 procedure is a calculation method where the loading history of the soil is taken into account when the initial stresses for the model are defined. The coefficient K_0 represents the lateral earth pressure at rest, where the value of K_0 , for a normally consolidated soil, is expressed by equation 3.5. The symbol ϕ is representing the friction angle in the soil. The value of K_0 is usually larger in an over-consolidated soil. (Brinkgreve et al., 2017)

$$K_0 = 1 - \sin(\phi) \tag{3.5}$$

By choosing the K_0 procedure, PLAXIS will generate vertical stresses that are in equilibrium with the self-weight of the soil throughout the initial phase.

3.3.2 The subsequent phases

In the other phases the following types of calculation can be selected; Plastic, Consolidation, Safety, Dynamic and Fully coupled flow-deformation. The relevant calculation types for this master's thesis are Plastic and Safety. These will be further explained.

Plastic

The Plastic calculation is an elastoplastic drained or undrained analysis. It is used to carry out a deformation analysis, and the calculation is performed according to the small deformation theory (Brinkgreve et al., 2017). After a plastic calculation the available results in PLAXIS output is, among other things, the deformed mesh of the model.

Safety

By choosing the type of calculation to be Safety, the strength reduction method will be used to calculate the global safety factor. In the strength reduction method the shear strength parameters $\tan(\phi)$ and the cohesion of the soil, as well as the tensile strength are reduced until failure of the structure occurs. The factor of safety is given by the total multiplier, $\sum M_{sf}$, at failure. The total multiplier is defined by the following formulas (Brinkgreve et al., 2017);

$$\sum M_{sf} = \frac{\tan(\phi_{input})}{\tan(\phi_{reduced})} = \frac{c_{input}}{c_{reduced}} \quad (3.6)$$

The development of the total multiplier should be investigated by making a curve. In this way it can be checked whether a failure mechanism has fully developed. If not, more steps must be included in the calculation to ensure a fully developed failure mechanism.

3.3.3 Calculation process

After defining the calculation phases, the calculation process can be executed. The results are presented in the Output program. There is a wide range of facilities in the Output program to display the results of a finite element analysis in PLAXIS, where the stresses and the displacements are the main output quantities. In addition, the forces in the structural elements involved in the model will be calculated and can be retrieved from the Output program.

Chapter 4

Modelling in PLAXIS 3D

In the following chapter the modelling done in PLAXIS 3D will be described. The main reason for doing the simulations in three dimensions is the design of Load Model 71, which is not described as a line load. Initially, the build up of the two models used for simulating the effect of the different load models are described, further there is a description of the applied vertical loads and their distribution.

4.1 Geometry of the Substructure for both Examples

The models' super- and substructure in PLAXIS 3D are based on one of the layering found in the textbooks of Railway engineering(Jernbaneverket, 2017). Since the projects, which these models are based on, are located close to each other in the counties Akershus and Oslo, the substructure will be modelled in the same way for both of the analyses. The structure with the different layers is illustrated in figure 4.1.

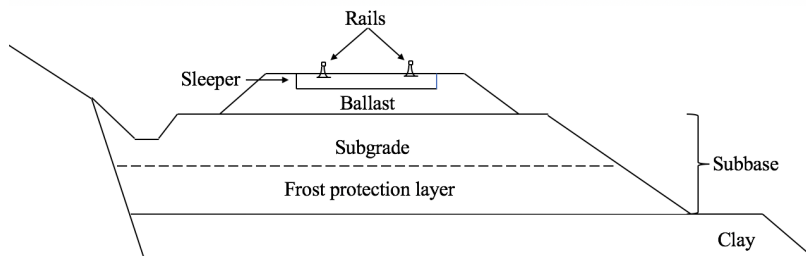


Figure 4.1: The structure of the layers in the super- and substructure

4.1.1 Superstructure

In the models in PLAXIS, the ballast, sleepers and rails are not modelled. Instead, the weight from these are calculated and included as a distributed load over a width of 5.5 m. These calculations are described in subsection 4.4.1.

It is normal to use different Norwegian rocks when constructing railways. Whether the rocks are useful depends on where in the construction it will be used. Especially for the ballast, high demands for the materials are made. In the subgrade and the frost protection layer, most of the Norwegian types of rocks can be used (Bane NOR, 2018b). The function of the subgrade is that it is a stable foundation with high bearing capacity. The subgrade shall be capable of absorbing the forces from the track, resist the long-term effects that a railway will be exposed to, and carry away water from rainfall. To prevent that frost penetrates through, it is important to have a frost protection layer. (Bane NOR, 2017c)

Due to Norwegian regulations, the thickness of the subgrade layer has to be at least 700 mm for main tracks (Bane NOR, 2017c). The most widely used material is blasted rock or gravel, both because it is easily accessible and it provides good carrying capacity. For the frost protection layer, the thickness depends on where in Norway the track is to be build.

Since the research question in this master's thesis is about the comparison of two load models, it is important that the subbase and its strength does not take up all the distributed load. The study done by the Finnish Transport Agency and described in section 2.5.1 underlines the point of having a low height of the embankment, as this will give clearer effects of load distribution. The frost protection layer will therefore not be included in the models in PLAXIS, and the subbase will only consist of subgrade. Additional background to select this delimitation is presented in section 6.2.

Subgrade

According to Norwegian regulations, the thickness of the layer of subgrade should be at least 0.7 m. The top of the subgrade has a width of 7 m for single-tracks due to the technical regulations developed by Bane NOR (Bane NOR, 2017c). From Bane NOR's technical regulations the inclination of the subgrade is stated as well, to have an inclination of 1:1.5 or flatter (Bane NOR, 2018c). As the top of the subgrade has a width of 7 m, the bottom of this layer will have a width of 9.1 m, since the inclination of 1:1.5 will be used.

For the subgrade the material model Mohr-Coulomb will be used. This is one of the simplest models in PLAXIS, and it is further described in section 3.1.1. Using figure 2.39 from the Norwegian Public Roads Administrations handbook V220 (Statens Vegvesen, 2014b), some of the material parameters of the gravel can be found. The angle of dilation controls

the amount of plastic volumetric strain developed during plastic shearing. Gravel is a non-cohesive soil, and the value of dilation angle can be estimated as $\psi = \phi - 30^\circ$ (Bartlett, 2011). The material parameters are listed up in table 4.1 below.

Table 4.1: Material parameters subgrade, part 1

Specific weight γ [kN/m ³]	Friction angle ϕ [°]	Dilation angle ψ [°]	Attraction a [kPa]
19	39	9	10

Other parameters for the gravel are found from the University of Texas at Austin’s sites (Zhu, nd). The permeability for gravel is between 0.01-1 cm/sec, the Poisson’s ratio between 0.15-1.35, and Youngs Modulus between 70-170 MPa. For this model the parameters listed up in table 4.2 will be used.

Table 4.2: Material parameters subgrade, part 2

Permeability k [m/day]	Poisson’s ratio ν [-]	Young’s modulus E [MPa]
8.64	0.25	120

4.2 Slope Stability near the Railway Track

The calculations of the slope-stability are based on the report developed for the new railway bridge in Kvisldalen, which is briefly described in section 2.1.1. Before using PLAXIS to do finite element modelling, one has to develop a realistic model. In the following sections the construction and the layering of the model will be described.

The length of the model in the y-direction will be based on two half railway carriages with 12.5 m length, as shown in figure 4.2. According to the Finnish research report described in section 2.5.1, the differences in load distribution for the different load models seems to diminish as the examined section is getting longer. There is a line of symmetry at the connection in the middle, and thus only the length of 6.25 m will be modelled in PLAXIS.

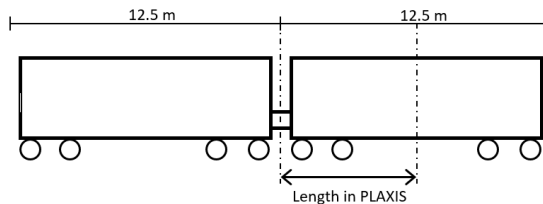


Figure 4.2: Length of the model in PLAXIS

4.2.1 Geometry of the model

From site investigations there has been documented that the area consists of dry crust above silty clay with tiny layers of sand. In the report developed by Bane NOR in conjunction with the Kvisldalen Railway bridge, the cut profiles between level 160 to 150 has inclinations where 1:2 are the steepest. Since it is desirable to have a conservative model in PLAXIS, the steepest value for the inclination will be used. The water level is set to be below the model, as this will have little or no importance for the topic in this master's thesis. From the same report it seems that the shoulder of clay beside the subbase should be approximately 0.7 m. (Norwegian Geotechnical Institute, 2017)

Final PLAXIS-model of the slope

Figure 4.3 illustrates the layers and the dimensions of the layers used in the PLAXIS model for calculating slope stability in this master's thesis. The height of the slope is set to 5 m, and the reason for this choice is substantiated and illustrated in section 6.1. The boundaries are picked such that the failure surface occurs within the model.

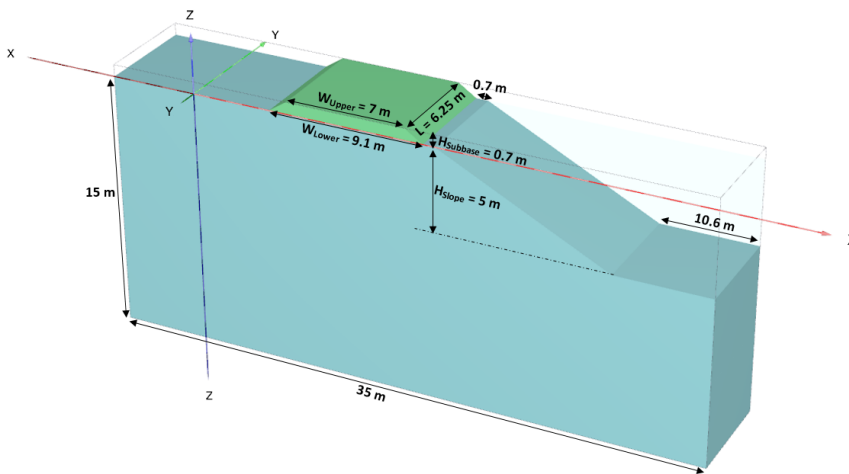


Figure 4.3: PLAXIS-model used when calculating slope stability

4.2.2 Soil settings

The soil beneath the substructure will also be modelled in PLAXIS, and the same material model as for the subgrade, Mohr-Coulomb, will be used. There has been done ground inspections in connection with preparation of the new bridge in Kvisldalen. These inspections have shown that the ground mainly consists of clay, with material unit weight equal to 20 kN/m^3 . (Norwegian Geotechnical Institute, 2017)

From CPTU-soundings a strength profile is developed as shown in figure 4.4, where active undrained strength is used to describe the strengths for the different depths(Norwegian Geotechnical Institute, 2017). The principle with active, direct and passive strength is described in section 2.6.

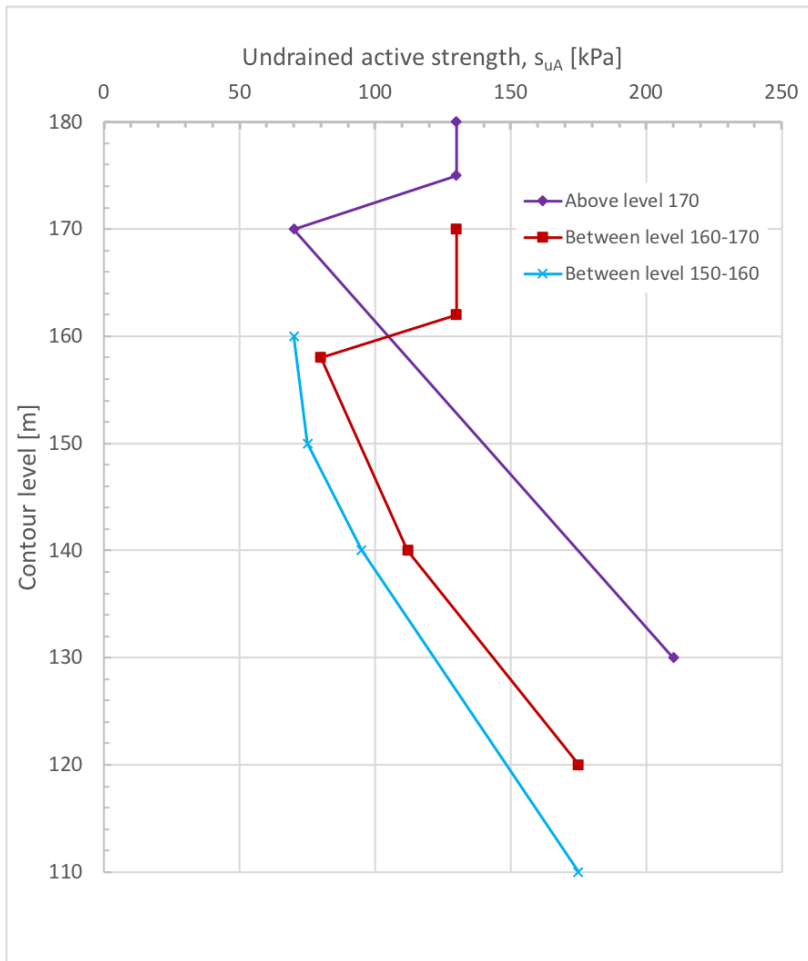


Figure 4.4: Characteristic strengths for different ground levels beneath Kvisldalen bridge

For the calculations done in the report about Kvisldalen (Norwegian Geotechnical Institute, 2017) the following anisotropy ratios has been used, see equation 4.1. The background for the selection of ADP-factors are described in the report including geotechnical parameters for the same project (Norwegian Geotechnical Institute, 2016). For the model developed in PLAXIS for this master's thesis an average value for the ratio is used, as shown in equation 4.2. Earlier experiences shows that the direct shear strength appears to be somewhere between the active and the passive shear strength, which is supported in the equations below (Nordal, 2017a).

$$\begin{aligned} s_{u,D}/s_{u,A} &= 0.68 \\ s_{u,P}/s_{u,A} &= 0.37 \end{aligned} \quad (4.1)$$

$$s_{u,avg}/s_{u,A} = \frac{\frac{s_{u,A}}{s_{u,A}} + \frac{s_{u,D}}{s_{u,A}} + \frac{s_{u,P}}{s_{u,A}}}{3} = \frac{1 + 0.68 + 0.37}{3} = 0.68 \quad (4.2)$$

The purple graph shows the design line for level 170 and above, and this will be used as a template for describing the strength parameters in the ground for the model developed in PLAXIS. Parts of the area near Kvisldalen bridge has no dry crust, and the ground in this model will thus consist of only clay. From the purple design line it seems like there is a layer of dry crust down to level 170. At level 170 the undrained active strength is 70 kPa and increases with a slope of 3.75:1 down to level 130. From this, the strength parameters for the clay can be deduced as shown in equation 4.3 below.

$$\begin{aligned} s_{u,ref} &= \text{ratio}_{avg} \cdot s_{u,A} = 0.68 \cdot 70 \text{ kPa} = 47.6 \text{ kPa} \\ s_{u,inc} &= \text{ratio}_{avg} \cdot \text{slope} = 0.68 \cdot 3.75 \text{ kPa/m} = 2.55 \text{ kPa/m} \end{aligned} \quad (4.3)$$

Summaries of all the material parameters used in connection with these simulations in PLAXIS are listed in figures A.1 and A.2 in the appendix.

4.3 Sheet Pile Wall adjacent to the Railway

The other chosen case to look at in relation to the load models for rail traffic is sheet pile walls adjacent to the track. Since the dimensions of the structural components are small compared to the overall geometry, to model them in 2D would have resulted in either a very large number of elements, or elements with unacceptable aspect ratios (Potts et al., 2002). This, in addition to Load Model 71, are the reasons for using PLAXIS 3D in this case as well. By doing calculations in PLAXIS it is desirable to get an insight in how these walls are affected by the rail traffic, and whether the simplified load model from Bane NOR gives the same effect as the load model in the Eurocode.

The model where the sheet pile wall adjacent to the track is investigated will differ from the model used for the stability-example. One of the differences is the length of the model in the y-direction. While the model used for the stability-calculations was 6.25 m long, a whole railway carriage with the length of 12.5 m, see figure 4.2, will be modelled for this example. This is done to accommodate three struts instead of two.

In this example the soil deformations are important. This makes more advanced soil models like Hardening soil model and NGI-ADP model recommended over the simple Mohr-Coulomb model (Nordal, 2017a), which was used for the example with slope stability.

4.3.1 Geometry of the model

The model in PLAXIS has been based on the PLAXIS 2D-model used in The Follo Line Project when designing the sheet piles for the Østfold line between Oslo S and Ski, shown in figure 4.5a. This project is previously described in section 2.1.2.

The geometry described in the documents developed for Bane NOR is simplified to make the 3D-model more valid for a general case. This geometry is shown in figure 4.5b. Another reason is to simplify the calculations in PLAXIS. The simplification will not have a significant influence on the results, since the interesting thing is to compare two different load models applied on the same model, and their effect on the sheet pile wall.

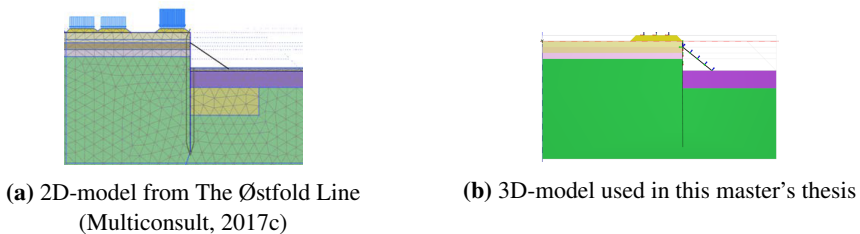


Figure 4.5: Modelling of the sheet pile wall adjacent to the track

4.3.2 Soil settings

Figure 4.6 illustrates the layering of the materials in the initial phase in three dimensions.

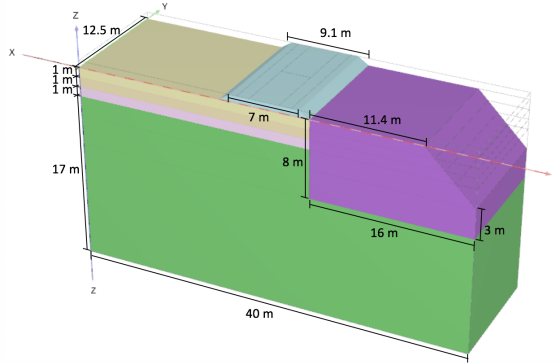


Figure 4.6: Initial phase in three dimensions

The model will consist of several different layers of soil. The subbase layer is modelled in the same way as for the slope stability model, and is described initially in section 4.1. The materials below the ground level are taken from the report for the Østfold line (Multiconsult, 2017c). Material parameters, and their numerical values from this report, are enclosed in the attachment, see Appendix B.1. The different layers and their corresponding colours and material models are listed up in table 4.3 below. Descriptions of the different material models can be found in section 3.1.

Table 4.3: Short description of layers

Colour	Material	Material model
Yellow	Dry Crust	Hardening Soil
Pink	Clay (Upper)	NGI-ADP
Light Green	Clay (Lower)	NGI-ADP
Green	Clay	NGI-ADP
Purple	Lime Cement Columns	Mohr-Coulomb

4.3.3 Structural elements

The modelling of the sheet pile wall, the walings and the struts are described in this section.

Sheet pile wall

A sheet pile wall is a screen of sheet piles forming a continuous wall by threading of the interlocks. The sheet piles can be built up by single or double piles of either Z- or

U-profiles, or single straight web profiles. The sheet piles used in the Follo Line Project was AZ 18-700 sheet piles made out of steel, as illustrated in figure 4.7. Z-type is a traditional sheet pile shape and it is used for intermediate to deep wall construction. The AZ sheet piles were introduced in 1990 by ArcelorMittal, and is described as the most advanced range of sheet piles in the world (ArcelorMittal, 2017). The number 18 behind AZ describes the elastic section modulus W_{el} per meter of the wall, while 700 describes the width of the Z-section.

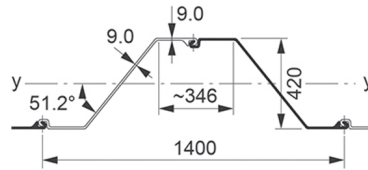
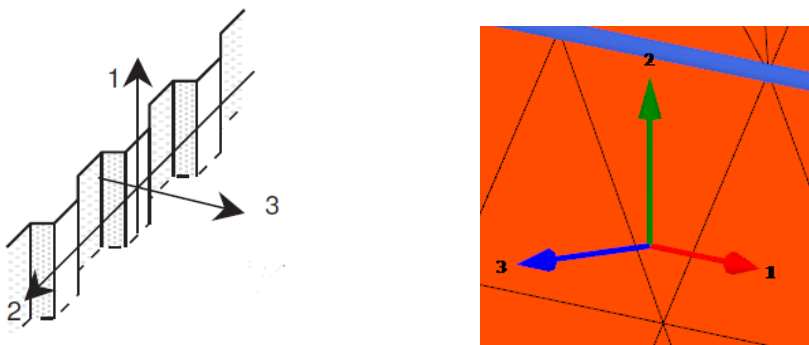


Figure 4.7: AZ 18-700 profile with lengths

For the PLAXIS 3D model, the sheet pile wall was modelled as an elastic plate with a length of 18 m, measured from figure 4-4 in the design report about sheet pile 13 (Multi-consult, 2017c). The structural behaviour of a plate is described in subsection 3.1.2. A sheet pile wall is geometrically orthotropic with different stiffness in vertical and horizontal direction, and it is known that the axial stiffness in vertical direction is larger than in the horizontal direction. The local axis, as described in the PLAXIS manual (Brinkgreve et al., 2017), are illustrated in figure 4.8a. Figure 4.8b shows the local system of axes for the plate modelled in PLAXIS for this master's thesis. The system of axes are in this model placed on the back side of the plate so that the third axis is pointing into the clay, and the first axis is the horizontal axis.



(a) Local axes for a sheet pile wall (Brinkgreve et al., 2017) **(b)** Local axes for the plate modelled in PLAXIS

Figure 4.8: Local system of axes in sheet pile wall

The local axes in the sheet pile wall modelled as a plate in PLAXIS are such that the first direction is horizontal while the second is vertical in figure 4.8b. The value of Young’s modulus in the second direction will hence be larger than in the first direction, $E_2 > E_1$. Moreover, the moment of inertia, or the flexural rigidity against bending over the vertical direction, is larger than the stiffness against bending over the horizontal direction. Thus, $I_2 > I_1$, as the second axis is the vertical axis. (Brinkgreve et al., 2017)

The material parameters are described in the PLAXIS material models manual, where the plate thickness d is defined as the height of the z-profile, see figure 4.7. Table 4.4 lists up the material parameters. The unit weight can be found by multiplying the area per m wall by the unit weight of steel, $\gamma_{\text{steel}} = 77 \text{ kN/m}^3$, and dividing it by the plate thickness. (Brinkgreve et al., 2017)

Equation 3.3 in section 3.1.2 defines the formulas for Young’s modules, where $E_{\text{steel}} = 2.1 \cdot 10^8 \text{ kPa}$. Poisson’s ratio can, according to the PLAXIS 3D manual (Brinkgreve et al., 2017), be set equal to zero. In the formulas for the shear modules in equation 3.4, the moment of inertia against torsion and the cross section area for shear forces are needed. As these values are hard to find, approximated formulas for the shear modules will be used (Brinkgreve et al., 2017), as shown in equation 4.4.

$$G_{12} = \frac{6E_{\text{steel}}I_2}{10d^3}, \quad G_{13} = \frac{E_{\text{steel}}A}{20d}, \quad G_{23} = \frac{E_{\text{steel}}A}{6d} \quad (4.4)$$

For the moment of inertia and the area in these expressions, the units are described in the product catalogue from the manufacturer as m^4/m and m^2/m , respectively.

The material parameters shown in table 4.4 are based on the ones found in one of the design reports developed for the Follo Line Project (Multiconsult, 2017c), as well as properties from the sheet-pile manufacturer (ArcelorMittal, 2015). These are the parameters used to model the sheet pile wall in PLAXIS.

Table 4.4: Material parameters for the sheet pile wall

Parameter	Name	Sheet pile wall	Unit
Thickness	d	0.420	m
Material behaviour	Type	Linear, non-isotropic	-
Young’s modulus	E_2	$1.29 \cdot 10^7$	kPa
	E_1	$6.43 \cdot 10^5$	kPa
Poisson’s ratio	ν	0.0	-
Shear modulus	G_{12}	$6.43 \cdot 10^5$	kPa
	G_{23}	$1.16 \cdot 10^6$	kPa
	G_{13}	$3.48 \cdot 10^5$	kPa

Walings and struts

A waling is a horizontal beam which is fixed to the sheet pile wall. The concept of beams in PLAXIS is further described in section 3.1.3. The waling is usually made out of steel or reinforced concrete, and it is used to transmit the force from the wall into the struts (Norsk Standard, 2010).

In appendix B.2, developed by Multiconsult for one of the design reports in The Follo Line project (Multiconsult, 2017c), it is described that both the profile of the waling and the strut are HEB400 beams. The letters HEB describes the design of the beam, while the number 400 defines the height. The material properties for a HEB400 beam are listed in table 4.5 (Manni Sipre S.p.A., 2015), and used for the modelling in PLAXIS.

Table 4.5: Material parameters for walings and struts

Parameter	Name	Waling and strut	Unit
Cross section area	A	0.01978	m ²
Material behaviour	Type	Elastic	-
Young's modulus	E	210·10 ⁶	kN/m ²
Moment of Inertia	I ₂	0.1082·10 ⁻³	m ⁴
	I ₃	0.5770·10 ⁻³	m ⁴

4.4 Vertical Surface Loads

In this section the vertical loads on the surface in the models in PLAXIS will be described. The surface of the models in PLAXIS are 0.7 m below the running surface of the track, as this is the level where the loads from Load Model 71 are described to be distributed in section 6.3.6.4 in EN 1991-2:2003+NA:2010 (Norsk Standard, 2017). Because of this, the weight of the layer of superstructure will be calculated and distributed over the surface of the models.

4.4.1 Loading from superstructure

The main parts of the superstructure are rails, sleepers and ballast. Throughout this section the weight of these components will be summarised to get an estimate of the overall weight of the superstructure.

According to both NS-EN 1991-2:2003+NA:2010 and Bane NOR's technical regulations, the transverse actions by the rails and sleepers should be distributed vertically with an inclination of 4:1, as shown in figure 4.9.

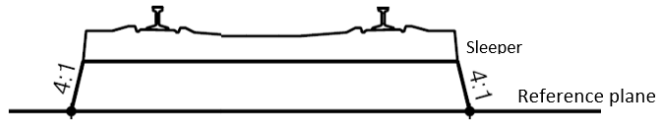


Figure 4.9: Transverse distribution of actions (Norsk Standard, 2017)

Rails

For the railway tracks in this model, the rail profile 60E1 will be used. Each profile has a distributed weight of 60.21 kg per meter, according to the technical regulations by Bane NOR about rail profiles (Bane NOR, 2014). Between the rails there is a distance of 1435 mm, and the profile has a width of 150 mm (Gjerde, 2012). This means that the load will be distributed over a width of 1735 mm. The addition to the load from these rails is calculated in equation 4.5.

Weight per meter:

$$\begin{aligned}
 W &= \text{quantity} \cdot \text{weight} \cdot \text{gravity} \\
 &= 2 \cdot 60.21 \text{ kg/m} \cdot 9.81 \text{ m/s}^2 = \underline{1.18 \text{ kN/m}}
 \end{aligned}
 \tag{4.5}$$

Uniformly distributed load:¹

$$\begin{aligned}
 \sigma_{z,\text{rails}} &= W / \text{width} \\
 &= 1.18 \text{ kN/m} / 1.7 \text{ m} = 0.69 \text{ kN/m}^2 = \underline{0.69 \text{ kPa}}
 \end{aligned}$$

Sleepers

According to Bane NOR's regulations about track structures, the sleepers should have the concrete grade C60 (Bane NOR, 2018a). For the following models it will be used sleepers with a length of 2600 mm, width of 300 mm, and a sleeper height of 234 mm. This gives a weight of 280 kg per sleeper without the fastenings (RAIL.ONE, 2014). As described in the part in the regulations about track structures, the centre-to-centre distance between the sleepers is 600 mm. The distributed load from the sleepers is calculated in equation 4.6 below.

¹An error in this equation was detected and corrected, but the wrong load, $\sigma_{z,\text{rails}} = 0.065 \text{ kPa}$, has been used for the simulations in PLAXIS. The change is considered negligible in respect to this master's thesis.

Weight:

$$\begin{aligned}
 W &= \text{weight} \cdot \text{gravity} \\
 &= 280 \text{ kg} \cdot 9.81 \text{ m/s}^2 = \underline{2.75 \text{ kN}}
 \end{aligned} \tag{4.6}$$

Uniformly distributed load:²

$$\begin{aligned}
 \sigma_{z,\text{sleepers}} &= W / \text{width} / \text{length} \\
 &= 2.75 \text{ kN} / 2.6 \text{ m} / 0.6 \text{ m} = 1.76 \text{ kN/m}^2 = \underline{1.76 \text{ kPa}}
 \end{aligned}$$

Ballast

The material in the ballast has a unit weight equal to 16 kN/m^3 , according to the book Numerical Models in Geomechanics (Pande and Pietruszczak, 2002). The model will consist of sleepers with 2600 mm length, and the ballast shoulders has to be 400 mm (Bane NOR, 2017a). Thus, the top of the ballast layer will have a width of 3400 mm. An inclination of 1:1.5, and a height of 0.7 m will give the bottom of the layer of ballast a width of 5500 mm.

According to table 1 in chapter Superstructure/Design and construction/Ballast bed in the technical regulations by Bane NOR (Bane NOR, 2017a), the necessary width of the top of the subgrade is, for the current sleepers in this model, 5150 mm, and a width of 5500 mm will satisfy this requirement. The distributed load from the layer of ballast is calculated in equation 4.7.

Volume per meter:

$$\begin{aligned}
 V &= \text{width} \cdot \text{height} \cdot \text{length} \\
 &= \frac{3.4 \text{ m} + 5.5 \text{ m}}{2} \cdot 0.7 \text{ m} \cdot 1 \text{ m/m} = \underline{3.115 \text{ m}^3/\text{m}}
 \end{aligned}$$

Weight per meter:

$$\begin{aligned}
 W &= \gamma_{\text{ballast}} \cdot V \\
 &= 16 \text{ kN/m}^3 \cdot 3.115 \text{ m}^3/\text{m} = \underline{49.84 \text{ kN/m}}
 \end{aligned} \tag{4.7}$$

Uniformly distributed load:

$$\begin{aligned}
 \sigma_{z,\text{ballast}} &= W / \text{width} \\
 &= 49.84 \text{ kN/m} / 5.5 \text{ m} = 9.1 \text{ kN/m}^2 = \underline{9.1 \text{ kPa}}
 \end{aligned}$$

²An error in this equation was detected and corrected, but the wrong load, $\sigma_{z,\text{sleepers}} = 1.06 \text{ kPa}$, has been used for the simulations in PLAXIS. The change is considered negligible in respect to this master's thesis.

Total distributed load from the superstructure

Figure 4.9 illustrates that the distribution of the weight from beneath the sleeper and down to the reference plane has a slope of 4:1. To account for this width, the values of the weight from the rails and the sleepers has to be multiplied by a magnification factor F_{dist} which is calculated in equation 4.8.

$$F_{\text{dist}} = \frac{\text{Width}_{\text{ref. plane}}}{\text{Width}_{\text{originally}}} = 1 + (0.7 \cdot 1/4 \cdot 2) = 1.35 \quad (4.8)$$

In equation 4.9 the total distributed load from the superstructure on the reference plane, 0.7 m below the track, is calculated. The total is rounded up to be on the safe side, as the fastenings among other things are not included in this approximation.

Total distributed load:³

$$\begin{aligned} \sigma_{z, \text{superstructure}} &= \sigma_{z, \text{rails}} \cdot F_{\text{dist}} + \sigma_{z, \text{sleepers}} \cdot F_{\text{dist}} + \sigma_{z, \text{ballast}} = \quad (4.9) \\ 1.35 \cdot 0.69 \text{ kPa} + 1.35 \cdot 1.76 \text{ kPa} + 9.1 \text{ kPa} &= \underline{12.41 \text{ kPa}} \end{aligned}$$

4.4.2 Equivalent vertical loading due to rail traffic actions

Load model from the European Standard

The equivalent vertical loading due to rail traffic actions for earthworks is in the European Standard EN 1991-2: *Traffic loads on bridges* described by Load Model 71 (Norsk Standard, 2017). Load Model 71 contains four point loads $Q_{\text{vk}} = 250 \text{ kN}$ over a length of 6.4 m, and a distributed load $q_{\text{vk}} = 80 \text{ kN/m}$ outside this length, see figure 4.10. This load model is described more in detail in section 2.2.1.

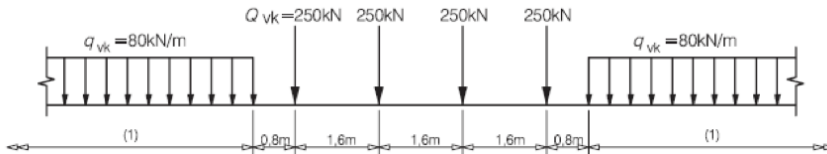


Figure 4.10: Load Model 71 (Norsk Standard, 2017)

According to section 6.3.6.4 in the standard (Norsk Standard, 2017), the vertical loading

³An error in this equation has been corrected, but the wrong total load, $\sigma_{z, \text{superstructure}} = 10.23 \text{ kPa}$, has been used for the simulations in PLAXIS. The change is considered negligible in respect to this master's thesis.

may be taken as Load Model 71 uniformly distributed over a width of 3.00 m at the level 0.70 m below the running surface of the track. The sleepers has an actual length of 2.6 m, but because of the 4:1 distribution through the ballast, as shown in figure 4.9, the reason for using 3 m as the distributed width is expressed in equation 4.10.

$$\text{Width} = 2.6 \text{ m} + 2 \cdot 0.7 \text{ m} \cdot 1/4 = 2.95 \text{ m} \approx \underline{3 \text{ m}} \quad (4.10)$$

The four axle loads in Load Model 71 corresponds to two bogies placed side by side, while the distributed load is the average over the remaining length of the train. By dividing the total load from one carriage on the average line load, the length of the train with 80 kN/m in average line load will be found. The calculation of the length is calculated in equation 4.11. Figure 4.11 illustrates the length of the carriages described in Load Model 71.

$$\text{Length} = \frac{4 \cdot Q_{vk}}{q_{vk}} = \frac{4 \cdot 250 \text{ kN}}{80 \text{ kN/m}} = \underline{12.5 \text{ m}} \quad (4.11)$$

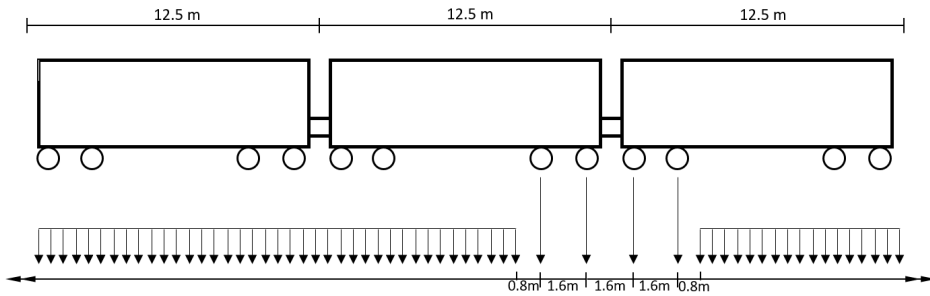


Figure 4.11: Illustration of Load Model 71

The railway carriage as described in the standard is a fictive carriage. According to table A.1 in NS-EN 15528:2015(Norsk Standard, 2015), there is no such wagon as the one described in Load Model 71. The fictive carriage in Load Model 71 is a conservative assumption, as the load in reality is placed over longer length.

According to NA.A2.4(C) in the national appendix of NS-EN 1990:2002(Norsk Standard, 2016), the load factor is 1.3 for traffic loads from railways. In this master’s thesis it will only be considered loading from one railway track, and thus the combination factor is equal to 1. The surface load used in PLAXIS is calculated as described in formula 4.12.

$$\sigma_{z,LM71} = \frac{4 \cdot Q_{LM71}}{\text{width} \cdot \text{length}} \cdot \gamma_Q = \frac{1000 \text{ kN}}{3 \text{ m} \cdot 6.4 \text{ m}} \cdot 1.3 = \underline{67.7 \text{ kPa}} \quad (4.12)$$

From now on the approximated Load Model 71, which has the value of 67.7 kPa distributed over the length 6.4 m and the width 3 m, will be expressed with the abbreviation LM71*. Load Model 71 as it appears in the eurocode will be expressed with the abbreviation LM71.

4.4.3 Load model from Bane NOR

The geotechnical load model developed by Bane NOR is described by a characteristic line load $q_{\text{BaneNOR}} = 110 \text{ kN/m}$. This load model is previously described in section 2.3.1, and visualised in figure 4.12.

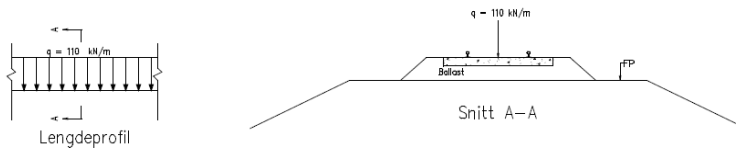


Figure 4.12: Bane NOR's load model (Bane NOR, 2018b)

According to Bane NOR's technical regulations, the line load is distributed over the width of 2.5 m. Since the load model developed by Bane NOR is to be compared with LM71, the load will be distributed at level 0.7 m below the track over the width of 3 m in PLAXIS. The load factor for traffic loads from railways is 1.3, which leads to the following expression, shown in equation 4.13, for the distributed load.

$$\sigma_{z,\text{BaneNOR}} = \frac{q_{\text{BaneNOR}}}{\text{width}} \cdot \gamma_Q = \frac{110 \text{ kN/m}}{3 \text{ m}} \cdot 1.3 = \underline{47.7 \text{ kPa}} \quad (4.13)$$

The load model developed by Bane NOR distributed over 3 m width will further in this thesis be expressed by the abbreviation LMBN.

Chapter 5

Simulations

The simulations done in PLAXIS 3D for the slope stability analysis and the sheet pile wall analysis will be described in this chapter.

5.1 Slope Stability Analysis

In this chapter a description of the simulations done in conjunction with the slope stability analysis will be presented. The description of the design and the soil settings for this model can be found in section 4.2. First of all, an explanation of the choice of model will be put forward. Further, the procedure to compare the load models of interest by doing simulations in PLAXIS 3D of slope stability will be presented.

The model used for the calculations in PLAXIS is illustrated in figure 5.1.

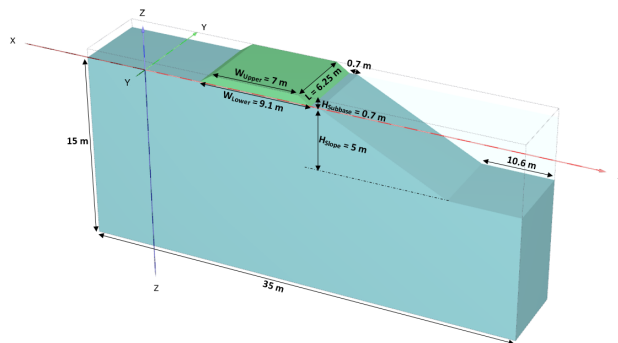


Figure 5.1: Final model used for slope stability calculations

5.1.1 Calculations of slope stability

The model, illustrated in figure 5.1 is constructed in PLAXIS 3D. The height of the slope is set to 5 m, and the thickness of the substructure is set to 0.7 m. The background for these choices are elaborated in section 6.1 and 6.2, respectively. The rest of the geometry and the parameters of the model are described in section 4.2, and listed in table 5.1 below. The material parameters as they appear in PLAXIS is attached in appendix A.

Table 5.1: Material parameters used for the slope stability analysis

Material	Material model	γ	Stiffness		Strength			
			E	ν	$s_{u,ref}$	$s_{u,inc}$	ϕ	ψ
Subbase	Mohr-Coulomb	19	120000	0.25	8.1	0	39	9
Clay	Mohr-Coulomb	20	19040	0.495	47.6	2.55	0	0

The distributed load will be placed on top of the layer of the subbase in the model. Their values and distributions are described in section 4.4. As this analysis is based on a project done at the Gardemoen line, the alpha factor in equation 2.1 under section 2.3.1 should have been set to 1.3. There has already been done many simplifications in this project, and the simplification using $\alpha = 1.0$ will be made in the following calculations. The loads are illustrated in figure 5.2 below.

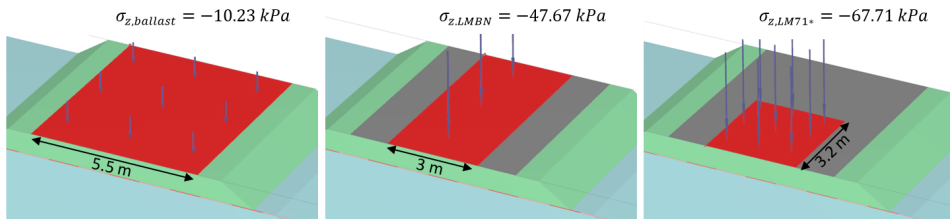


Figure 5.2: Distributed loads on the model in PLAXIS 3D

Before any calculations can be done in PLAXIS, one have to develop a mesh of the model. The concept of meshing is earlier described in chapter 3, section 3.2. Small elements are necessary to reduce the discretization errors in the model. Thus, the element distribution *fine* is used for the following calculations, with a refined mesh where the slope failure is expected to occur. Figure 5.3 illustrates the mesh of the model.

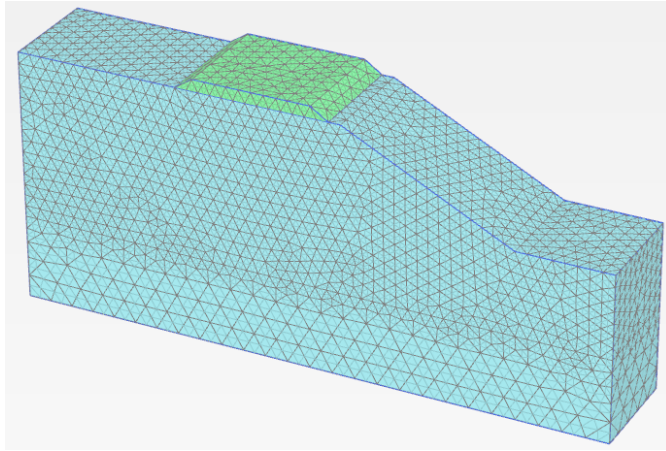


Figure 5.3: Surface mesh of the slope stability model

After the mesh has been developed, the next step in PLAXIS is to establish the flow conditions. Previously, it has been mentioned that the water level is set to be below the model, as this has little or no importance for the topic in this master's thesis. Thus the flow conditions are of little importance.

The last step to complete before calculations can be done in PLAXIS is the step where the finite element calculations are divided into several sequential calculation phases. Each of these phases corresponds to a construction stage. These are elaborated in section 3.3.

The slope stability analysis is divided into three phases, where the "Initial phase" includes the K_0 procedure for the model without the applied load model. "Phase 1" runs the Plastic type of calculation after the load model is applied, and in "Phase 2" a Safety calculation is performed for the same case. Results from the slope stability calculation are described in Chapter 6.

5.2 Analysis of the Sheet Pile Wall adjacent to the Track

Calculations done to analyse the sheet pile wall and how it is affected by the load models will be presented in this section. In section 4.3 there are descriptions of the geometry, soil settings and structure settings for this model.

5.2.1 Calculations of the loads impact on the wall

First, the model containing soil layers and substructure is defined in PLAXIS 3D. Figure 5.4 illustrates the initial structure of the model.

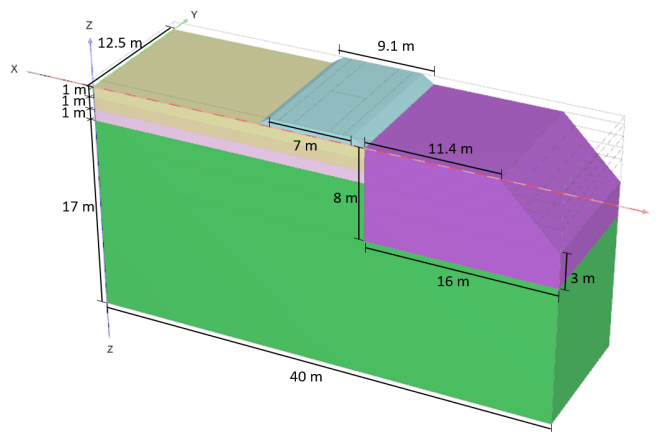


Figure 5.4: Initial model in PLAXIS 3D

When the sheet pile wall, walings and struts are to be placed, there are several things to keep in mind. First of all the interfaces have to be activated for the sheet pile wall. The importance of interfaces is described in section 3.1.4. Three struts were placed to obtain a symmetric model, and walings were located under each end of the struts.

As the model is symmetric, one have to make sure that the moment diagrams of the two walings are symmetric as well. This is true according to figure B.7 in appendix B. One of the walings, placed on the horizontal ground to the right of the wall, has the function of minimising the limitations from the element meshing under the struts. The structural elements with measurements are shown in figure 5.5.

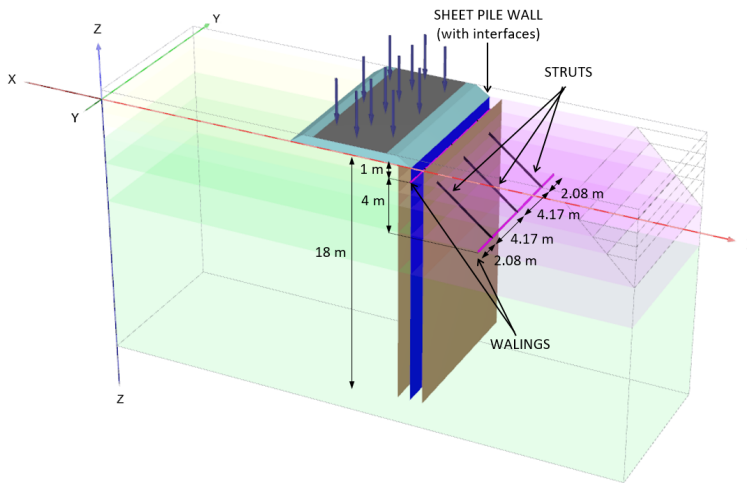


Figure 5.5: Structural elements in PLAXIS 3D-model

The layer of subbase is modelled in the same way as for the slope stability analysis, except that the layer in this model will have double length in y-direction. Figure 5.6 illustrates how the load models are distributed on top of the subbase.

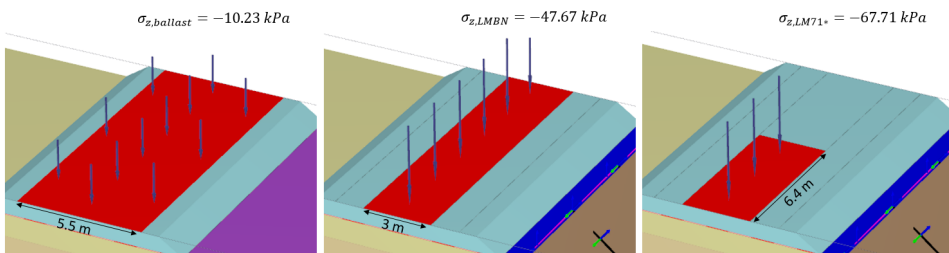


Figure 5.6: Distributed loads on the model with sheet pile wall

When this model was to be meshed, it was necessary that the areas of importance, just beneath the load, had a fine mesh. The layers deeper down will have little effect on the results, hence the mesh in these volumes was made coarser. Some of the volumes of stabilised soil on the right side of the wall will gradually be removed during the calculations, and can have a coarse mesh. Figure 5.7 illustrates the mesh of the model.

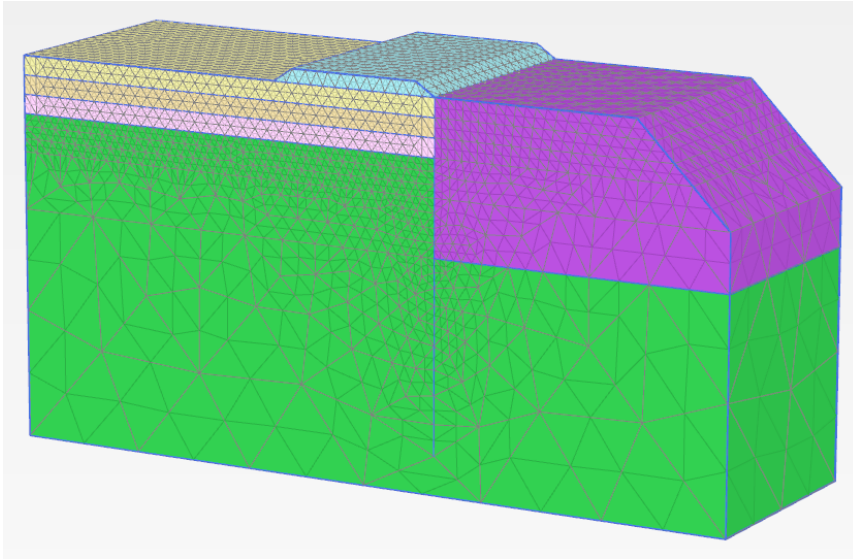


Figure 5.7: Surface mesh of the model with sheet pile wall

Finally the construction has to be divided into phases. The first phase is the "Initial phase", where the K_0 procedure will be performed to define the initial stresses for the model. For all of the subsequent phases the type of calculation will be *Plastic*. The following phase after the initial is "Phase 1", where the load from the ballast is distributed. In "Phase 2" the sheet pile wall with interfaces, three struts, and two walings are activated. When installing structural elements in the field, the procedure is different.

After the installation of the structures, the sequential excavation of the stabilised soil can start. The first excavation is 2 m deep, done in "Phase 3", before full excavation down to 5 m depth is done in "Phase 4". In the last phase, "Phase 5", the intended load model is applied. Before this phase, the displacement is set to zero to see only the effect of the load models.

Figure 5.8 illustrates these six phases, where the layer of stabilised soil is 70% transparent to visualise the structural elements.

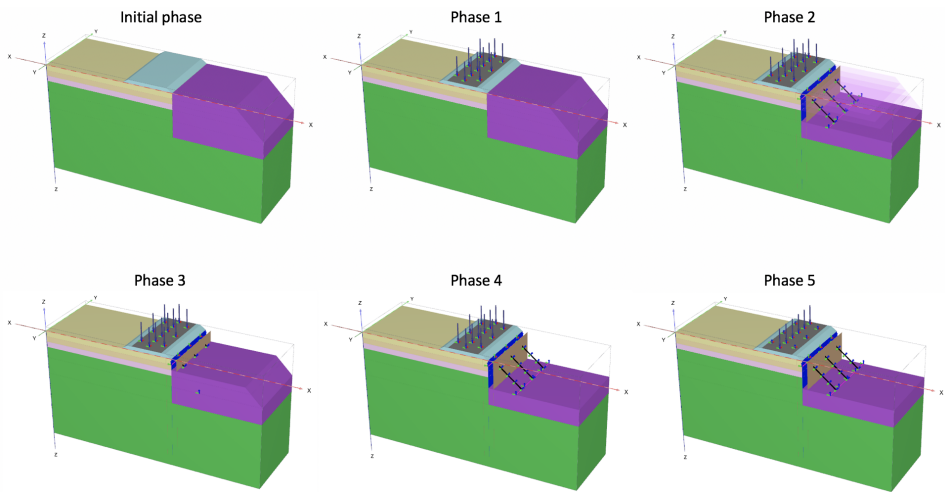


Figure 5.8: The six phases of the calculation when Bane NORs load model is applied

The results from the calculations of a sheet pile wall adjacent to the track are described in chapter 6.

Chapter 6

Results and Discussion

Bane NOR are, as described earlier, currently working on revising their technical regulations considering geotechnics. One of the issues they are investigating is whether their load model is affecting the ground in the same way as the load model from the Eurocode. The purpose of this master's thesis is to do further investigations and try to figure out whether it is appropriate for Bane NOR to change their technical regulations, and if appropriate, in what way should these be revised.

Initially in this chapter the results from simulations done to investigate the most appropriate way to design the models will be presented. In these calculations the effect of different heights of the slope has been investigated, as well as how the thickness of the substructure affects the model.

In the following sections the results from the examples with slope stability and with the sheet pile wall near the track will be presented. The results will be discussed throughout the sections, before the chapter will be completed with a summarising discussion.

6.1 The effect of the Height of the Slope

When trying to decide the best way to develop the model for the slope stability analysis, a few challenges emerged. One of them was the height of the slope.

From the research report described in section 2.5.1, the obtained results indicated that differences in load distribution for the different load models seems to diminish as the embankment height grows.

The material parameters and geometry described in section 4.2 is used for the calculations to compare the heights of the slopes. Figure 6.1a and 6.1b illustrates the slope failures for the different heights for LM71* and LMBN, respectively.

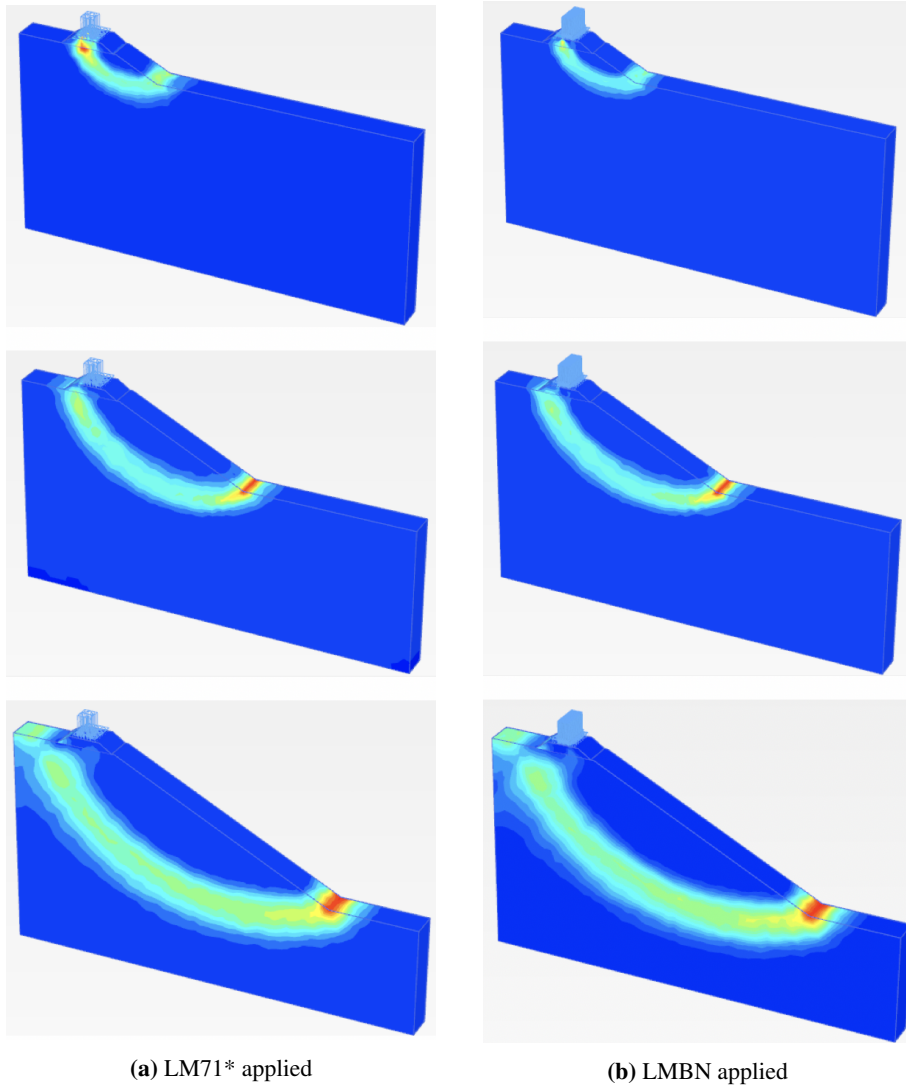


Figure 6.1: Slope failures for the heights 5, 15 and 25 m

From studying the failure slopes in figure 6.1 one can see that the failure for the 5 m high slope shows larger incremental strains near the loading for LM71* than for the load model developed by Bane NOR. For the 15 m high slope the failure slopes looks more similar,

and for the 25 m high slope it is almost impossible to detect any difference between the failure slopes.

The factors of safety found for the different heights are summarised in the plot in figure 6.2 below. This plot illustrates the same point, that the differences are greater with lower height. The factor of safety has a lower value for the slope of 25 m, but the small difference in the values for LM71* and LMBN indicate that the type of load model has small effects on the factor of safety for a slope as tall as this.

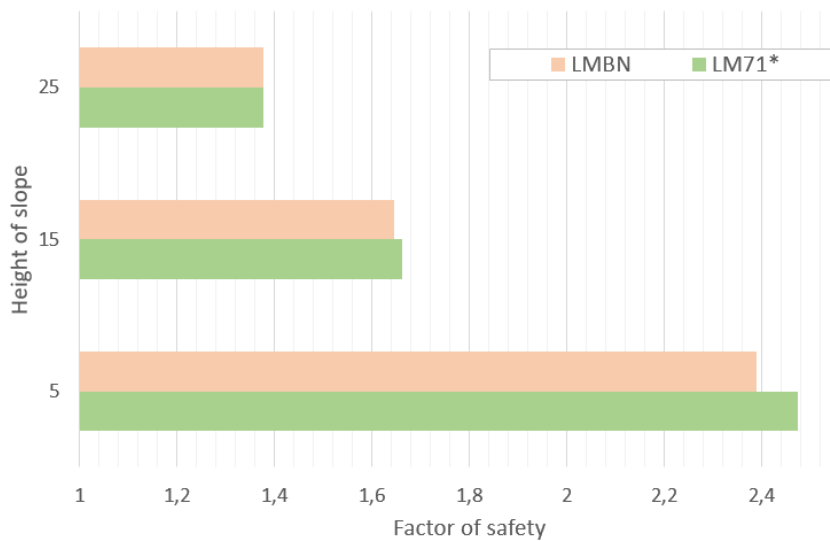


Figure 6.2: Factor of safety versus height of slope

The obtained results supports what was found in the Finnish research study, where they discovered that the increase in the load has increasing negative impact on the safety level with lower height of the embankment (Savolainen et al., 2017). In this master's thesis it is a goal to find the differences between Load Model 71 and Bane NOR's load model. It is therefore reasonable to pick the lowest height of the slope. It is desirable to get results where it is easy to distinguish between the two load models, and at the same time find the value of line load which seems to give the same response as LM71*.

6.2 The Effect of the Frost Protection Layer

In chapter 4 it is described that the frost protection layer is not included in the models used for simulations in PLAXIS for this master's thesis. To illustrate the effects of not having

a layer of frost protection in the models, the analysis will be done by including a layer of frost protection, and the results will be compared to the results without the layer.

As described previously, the thickness of the frost protection layer depends on where in Norway the track is to be built. Materials with good abilities to insulate from frost is Foamglas, expanded polystyrene and Leca among others. Gravel can also be used for this purpose, and this material will be used in the following example. The same material properties will be used for the frost protection layer as what is used for the subgrade.

The slope model in this thesis is based on the project Kvisldalen bridge, which is located in the municipality Eidsvoll in Akershus. At this location the design frost level is 23 000 h°C according to manual N200 developed by the Norwegian Public Roads Administration(Statens Vegvesen, 2014a). From figure 511.4 in the same manual, the thickness of the subgrade made out of gravel should be around 2.2 m. As the subbase layer has to be at least 0.7 m, the frost protection layer can be set to 1.5 m.

From Bane NOR's regulations, it turns out that the frost protection layer is thinner for the design level equal to 23 000 h°C. Since the following example only aims to investigate the effect of the layer, the layer thickness of 1.5 m will be used anyway.

The model for the sheet pile wall is based on the project in Ski Municipality. Here the design frost level is 14 000 h°C(Statens Vegvesen, 2014a). The thickness of the frost protection layer is thus a few centimetres less, but the layer thickness of 1.5 m will be used in this comparison as well.

In the model for the slope stability analysis the frost protection layer is placed above the ground, and beneath the layer of subbase, with the same inclination as the subbase. In the example with sheet pile wall, the frost protection layer is placed beneath the ground. This is done to prevent the location of the loads from changing. The models will have the designs shown in figure 6.3.

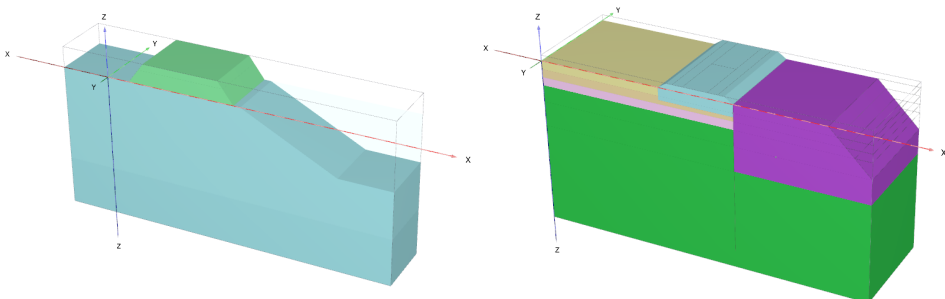


Figure 6.3: Frost protection layer added to the models

6.2.1 Comparison of the results from the slope stability analysis

The strength reduction method is used to run a safety analysis when LM71* and LMBN are applied to the model. Figure 6.4 illustrates the differences in the results with and without the frost protection layer.

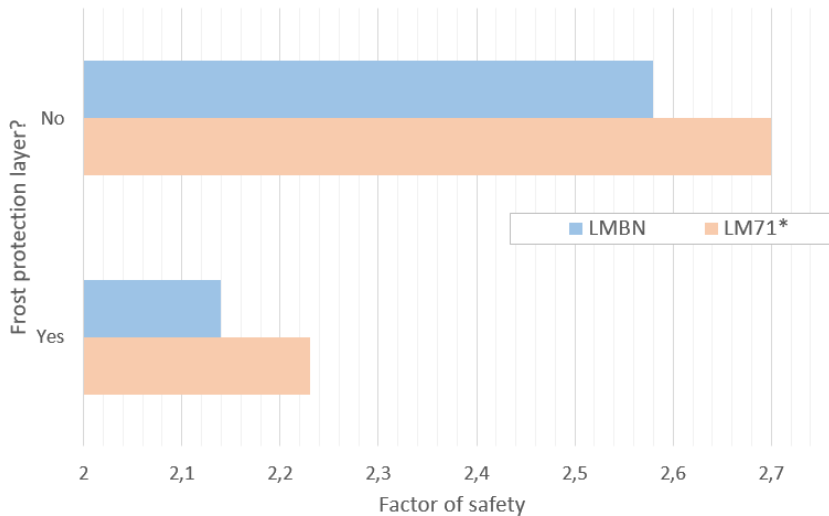


Figure 6.4: Comparison of the case with and without a frost protection layer

From figure 6.4 one can notice that the difference between the factors of safety obtained from the two load models is slightly bigger in the case with no frost protection layer. While the difference in this case has the value of 0.12, the difference when there is a layer of frost protection turns out to be 0.09. The illustration shows that the difference in factor of safety does not change significantly when a frost protection layer is applied.

The magnitude of the factor of safety decreases with a layer of frost protection. This makes sense, as the layer contributes to loads on the top of the slope. The desired aim in this example is the explicit difference between the load models. Hence, the size of the safety factor does not really matter.

The obtained results also support what has already been found in the Finnish study described in 2.5.2, that lower height of the substructure will make the differences in the effects of the load models clearer.

6.2.2 Comparison of the results from the analysis of the sheet pile wall adjacent to the track

An elastoplastic analysis is done in this example, where LM71* and LMBN is applied to the model to investigate the difference in how the sheet pile wall is affected. One way to illustrate the effect is by having a look at the incremental increase in normal forces in the struts behind the wall after the load models are applied.

Table 6.1 includes a summary of the results for both LM71* and LMBN, with and without the frost protection layer. The same results are illustrated in figure 6.5. Strut number one is the strut to the left in the model, when standing in the excavation looking at the sheet pile wall. Number two is the one in the middle, and number three is the strut to the right.

Table 6.1: Effect on the struts, with and without a frost protection layer

Frost Protection Layer?	Load Model	Increase in Normal Forces in Struts 1, 2 and 3 [kN]		
		ΔN_1	ΔN_2	ΔN_3
Yes	LM71*	83.1	46	16.5
	LMBN	68.9	69.2	68.8
No	LM71*	113.6	62	15.6
	LMBN	75	76.9	75.4

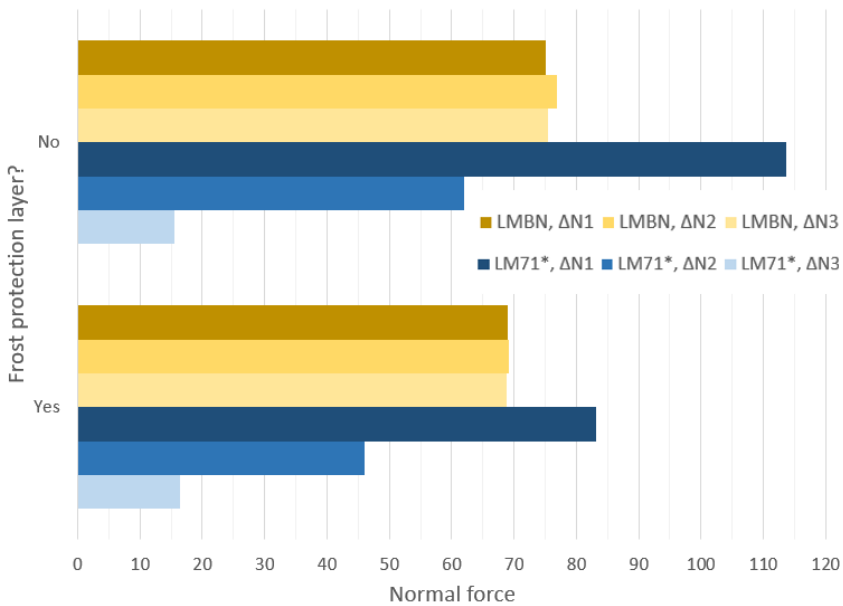


Figure 6.5: Comparison of the case with sheet pile wall, with and without the frost protection layer

The results shows that the normal forces are larger for five out of six struts in the case without the frost protection layer. For this example, the frost protection layer was placed below ground level, where it replaced dry crust and clay. The material in this layer is gravel, and it seems that the loads are more easily distributed through gravel than through dry crust and clay. This makes sense, as the gravel has high stiffness.

This example has the main purpose of investigating the effect of not including a layer of frost protection into the model. From the results it is clear that the difference between the two load models is more critical in the case with no layer of frost protection.

6.2.3 Summary of the comparisons

From these examples it has been illustrated that the differences in the two load models is most considerable in the absence of a frost protection layer. In the case analysing slope stability, the layer contributed to a lower difference between the factors of safety. In the case analysing the effect on a sheet pile wall, the layer contributed to smaller variance between the incremental normal forces in the struts behind the wall. The difference between LMBN and LM71* was most critical in the case without frost protection, regarding level of stress in struts.

6.3 Results from the Slope Stability Analysis

The results obtained from the slope stability analysis in PLAXIS 3D will be presented and discussed in this section. First, the calculations considering the case where LM71* and LMBN are applied to the model will be elaborated, then there is a discussion of the calculations considering which line load corresponds best to LM71*.

6.3.1 LM71* vs. LMBN

The results found when applying LM71* and Bane NOR's load model to the model of the slope in PLAXIS will be presented and discussed in the following part.

To illustrate the results in the best way, there are many options in the output program in PLAXIS. The following figures 6.6, 6.7 and 6.8 illustrates the deformed mesh and the slope failure in the model when "no load model is applied", when "LM71* is applied", and when "LMBN is applied", respectively.

The deformed mesh illustrates how large deformations the model will get from the different load models. Figure 6.6b, 6.7b and 6.8b are showing the effect of the total strain

increments, which indicates the most applicable failure mechanism of the slope in the final stage. The figures indicate the failure mechanisms, but the magnitude of strain increments are not relevant (Brinkgreve et al., 2017). Legend settings are the same in all figures, but the sizes of the arrows in the distributed loads are misleading.

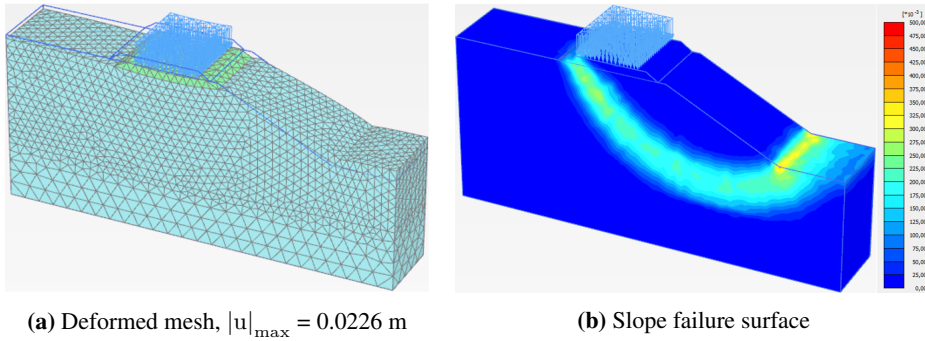


Figure 6.6: No load model applied, $\sigma_z = 0$ kPa

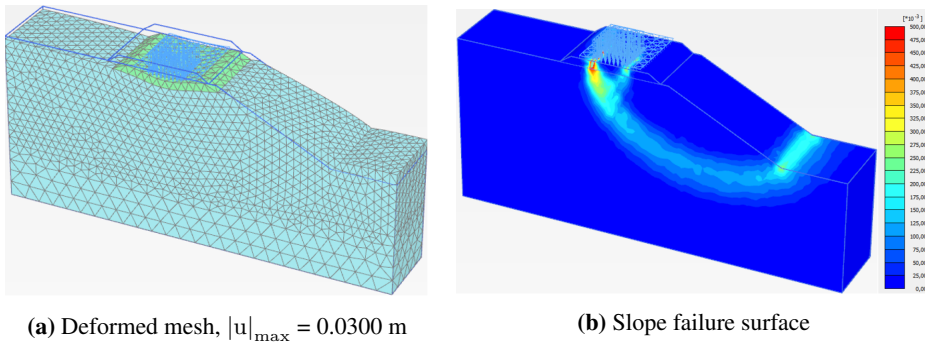


Figure 6.7: LM71* applied, $|\sigma_{z,LM71*}| = 67.7$ kPa

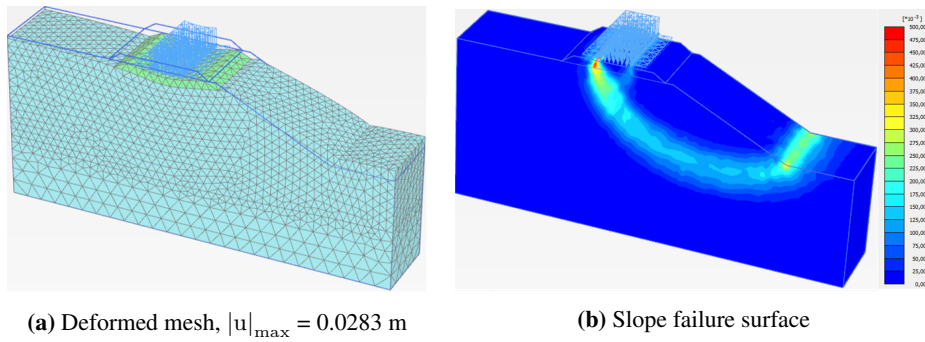


Figure 6.8: LMBN applied, $|\sigma_{z,LMBN}| = 47.7$ kPa

The deformed mesh gives an indication of how much the three applied load models affects the model in PLAXIS. No load applied will have the least effect, with the lowest deformation. The loads from LM71* and Bane NOR's regulations provides more deformed meshes, and larger values of the maximum deformations. Deformations developed from the impact of LMBN are 25% larger than the value obtained when only the weight of the superstructure accounted for the deformations. The achieved deformations from applying LM71* are again 6% larger than the ones from LMBN.

Since the figures are in three dimensions, only parts of the failure surfaces are shown. For all three cases it seems that the failure mechanism in the final stage is a toe slide. The slope failure for the case where no load model is applied seems to start right behind the layer of subbase, where the weight of the ballast and the subbase seems to be responsible for the failure. The incremental deviatoric strain seems to reach its maximum limit at the toe of the slope.

When the load models are applied to the model, the incremental strains seems to have the largest values at the left end of the distributed loads in both cases. Red colour on the figure indicates large values of strain. The area of red seems to be bigger under the distributed load when LM71* is applied, while the area of yellow in the toe of the slope seems to be bigger when LMBN is applied.

From these observations it seems that LM71* is the load model that develops the largest incremental deviatoric strains just beneath the load. The extent of this load model in the direction of the rails is small, and the load is more concentrated for this load model than for the distributed load of 110 kN/m. This can explain why the slope failure mechanism, when applying LM71*, will not spread the strains to the toe of the slope in the same way as LMBN does. The incremental strains in the toes of the slopes seems to be largest for the case with LMBN.

To illustrate the differences between the load models better, it is appropriate to look at the final factors of safety for the slope model. The factors of safety developed in PLAXIS 3D for the three different cases are listed up in table 6.2.

Table 6.2: Factor of safety for load models

Load model	Factor of safety
No model applied	3.195
LM71*	2.701
LMBN	2.581

From table 6.2 one can see that the safest case seems to be, as expected, when no load model is applied. Even though all three values are satisfactory, it turns out that Bane

NOR's load model gave the lowest factor of safety, and the factor of safety developed when applying LM71* is approximately 5% higher.

The maximum total displacement had the largest value in the model for the case when LM71* was applied. Nevertheless, the factor of safety turns out to be larger. One reason for that is the underdeveloped toe slide when applying LM71*. From the illustrations of the slope failure mechanism in figure 6.7b and 6.8b, when applying LM71* and LMBN, respectively, the toe slide is most defined for the case with the distributed load equal to 110 kN/m, LMBN.

In spite of the fact that LM71* develops larger displacements, its short extension seems to make the slope safer. More calculations will be done in the following section to figure out which value of the distributed load for Bane NOR's load model will give the same factor of safety as LM71*.

6.3.2 Comparison of LM71* and different values of the distributed load

In the previous section the results from the simulations showed that the factor of safety decreased more when Bane NOR's load model was applied compared to LM71*. This indicates that the applied load from the load model developed by Bane NOR, 110 kN/m, has a too large value, and is thus too conservative.

Different values for the distributed load has been tried out in PLAXIS to find which gives a similar response as LM71*. Table 6.3 contains an overview of the values of different distributed loads and their corresponding factor of safety. Figure 6.9 visualises a plot containing an overview of the model's way towards the failure limit for the different values of distributed loads, and figure 6.10 shows an enlargement of the end of the plot.

Table 6.3: Factor of safety for different load models

Load model	Factor of safety
LM71*	2.701
q = 110 kN/m	2.581
q = 90 kN/m	2.688
q = 87 kN/m	2.704
q = 85 kN/m	2.715
q = 80 kN/m	2.741

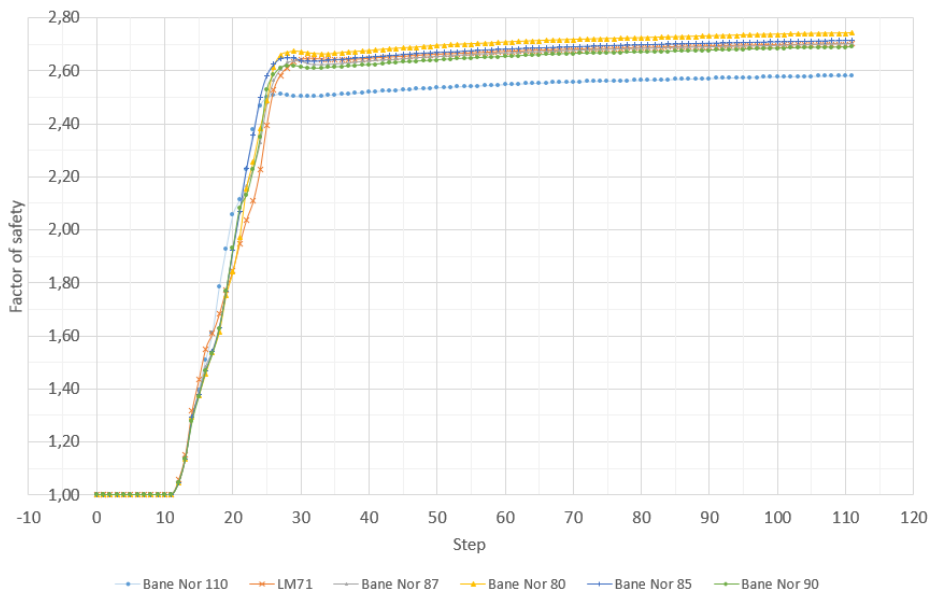


Figure 6.9: The development of the safety factor

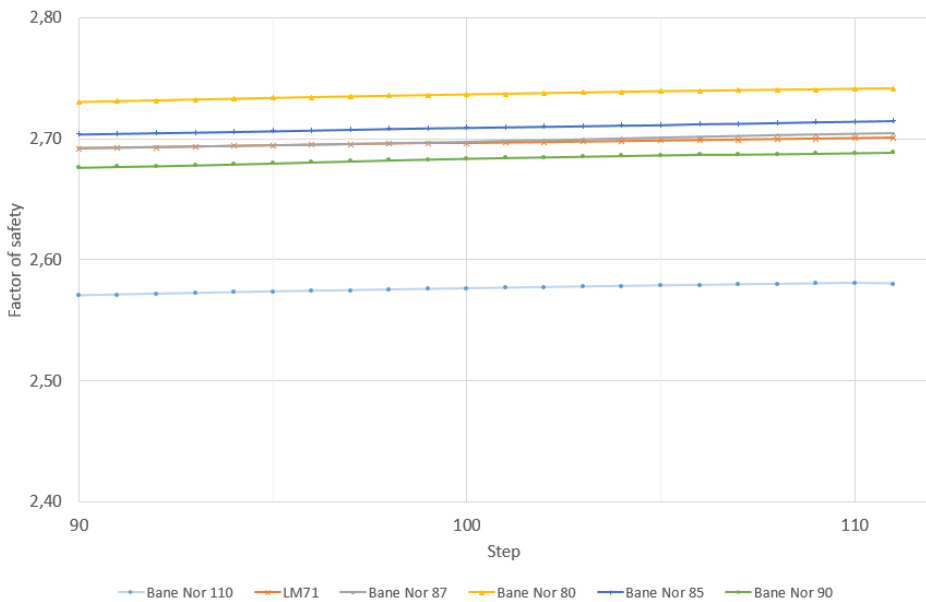


Figure 6.10: The very end of the plot

From the values in table 6.3 it is reasonable to assume that a distributed load of 87 kN/m gives a similar response as the load model from the Eurocode. By having a look at the plot in figure 6.9 and the enlargement of the end of the plot in figure 6.10 as well, it is even clearer that the distributed load with 87 kN/m gives an almost equal response in the model as when LM71* is applied.

The failure surfaces for the slope when LM71* and a distributed load of 87 kN/m are applied, are illustrated in figure 6.11 below.

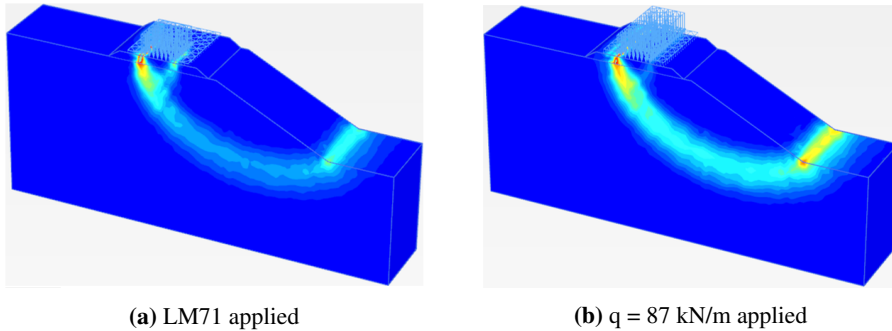


Figure 6.11: Slope failure surfaces

Even though the factor of safety turns out to be the same for these two slope failures, the failure surfaces look pretty different. The failure surface when LM71* is applied, described in section 6.3.1, seems to have largest strains just beneath the left side of the applied load. In figure 6.11b the deviatoric strains seem to obtain the largest values beneath the left side of the applied load as well. Additionally, the incremental strains developed in the toe of the model seem to be quite big.

Figure 6.8b and 6.11b for the distributed loads $q = 110 \text{ kN/m}$ and $q = 87 \text{ kN/m}$, respectively, looks quite similar at first glance. By enlarging the area of the toe of the slope, see figure 6.12, it is easier to see that the failure mechanisms actually turn out to be different.

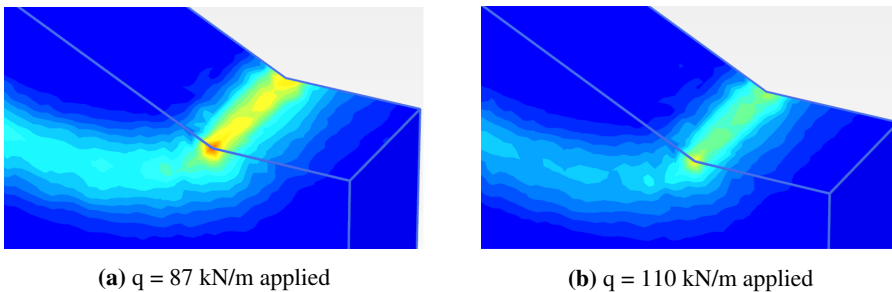


Figure 6.12: Incremental deviatoric strains in the toe of the slope

The deviatoric strains in the toe seems to be larger for the lower value of distributed load. From figure 6.6b of the failure surface when not applying any load, the strains were fairly large near the toe in that case as well. This indicates that large load values on top of the slope causes the strains not to spread as much in the slope failure surface as for the lower loads. One reason for this can be that the model goes to failure before the strains has time to spread.

Although the slope failure surfaces for LM71* and the distributed load equal to 87 kN/m are not quite the same, the simulations gave the same factor of safety. The purpose of the calculations of this analysis was to find the distributed line load giving equivalent safety level for the slope as LM71*. From these results it is reasonable to assume that Bane NOR may lower the value for the distributed load in their regulations considering slope stability.

6.4 Results from the Analysis of the Sheet Pile Wall adjacent to the Track

The results obtained from the analysis of the sheet pile wall adjacent to the track in PLAXIS 3D will be presented and discussed in this section. The calculations considering the case where the load models LM71* and LMBN are applied to the model will be elaborated first. A discussion of the calculations considering which line load corresponds best to LM71* will further be conducted.

A new regulation was written into Bane NOR's technical regulations in February, describing that items or other issues close to the track, for example sheet pile walls, must be checked with Load Model 71. It is desirable to investigate whether this regulation is necessary, and to find a value for the line load which can be used for modelling in two dimensions.

The following results are functions of the relative rigidity between the soil, substructure, sheet pile wall, struts and walings. The deformations in the wall depends on the stiffness in the struts, while the normal forces of the struts depends on the stiffness of the wall. Material parameters in the walings will also affect the results.

This study is done for one combination of these material parameters, and will hence give an equivalent line load for that case. Other combinations of material parameters may provide different results.

6.4.1 LM71* vs. LMBN

How the wall and struts were affected in different ways by LM71* and LMBN will be described and discussed in the following section. It will be focused on the deformation and bending moment of the plate, as well as the normal forces in the struts to illustrate the dissimilarities between the two load models.

Figures 6.13 and 6.14 illustrates the displacements and the bending moments of the sheet pile wall when LM71* is applied, and when LMBN is applied, respectively. The displacements are set to zero after phase 4, as described in section 5.2, and the displacements of the wall in figure 6.13a and 6.14a are therefore only results of the applied loads. The scaling is the same in all four figures.

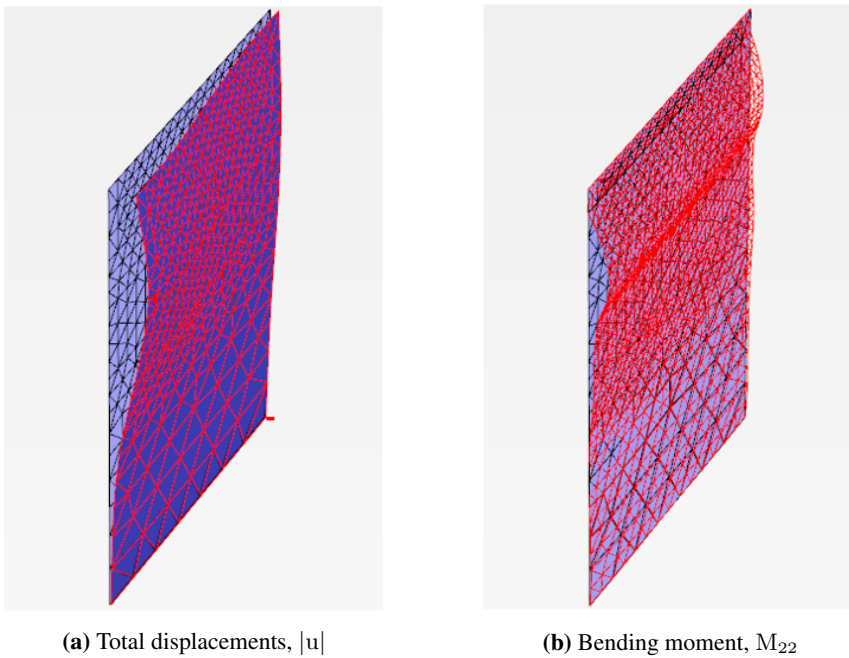


Figure 6.13: Load Model 71 applied

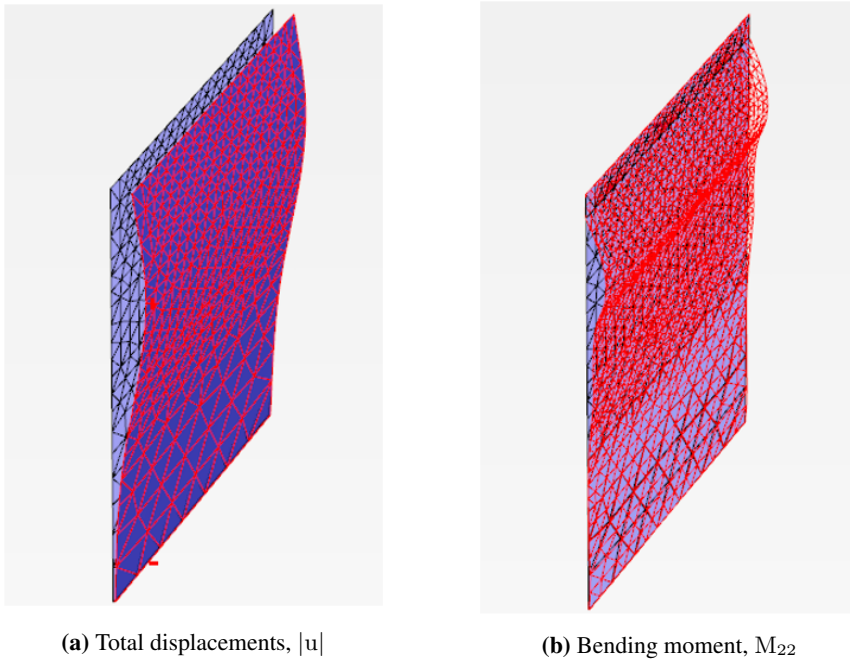


Figure 6.14: Bane NOR's load model applied

LM71* is a distributed load of 67.7 kPa on the left side of the figure, while LMBN is a distributed load of 47.7 kPa over the whole length. This causes the wall to have the biggest deformations on the left side in figure 6.13a, while in figure 6.14a the displacements are uniformly distributed over the whole length. In figure 6.13b and 6.14b, illustrating the bending moments, the differences between the load models are less visible.

In table 6.4 the incremental increases between phase 4 and phase 5, see figure 5.8, in the normal forces of the struts are listed. The values for the maximum bending moments and the maximum displacements of the wall are also listed. All values are tabulated for the three cases where no load model is applied, LM71* is applied and LMBN is applied.

Table 6.4: Results from analysis of sheet pile wall adjacent to the track

Load Model	Increase in Normal Forces in Struts 1, 2 and 3 [kN]			$ u _{\max}$ [m]	M_{\max} [kNm/m]
	ΔN_1	ΔN_2	ΔN_3		
No load model	0	0	0	$0.093 \cdot 10^{-3}$	101.6
LM71*	113.6	62	15.6	0.01524	169.2
LMBN	75	76.9	75.4	0.01345	158.9

The effect of the skewed distribution of the load in LM71* can be seen from the values for the struts in table 6.4. As the load is placed on the left side of the figure in PLAXIS, strut number one will have the largest incremental increase when the load is applied. From the table one can also see that both the maximum bending moment and the total displacement is greatest when LM71* is applied.

According to what is listed up in table 6.4 it seems like the model developed by Bane NOR is underestimating the effect of the train load on sheet pile walls and struts. The line load should have a larger value than 110 kN/m, and the most appropriate value for this line load is discussed in the next section.

6.4.2 Comparison of LM71* and different values of the distributed load

The results in table 6.4 indicate that LM71* affects both the sheet pile wall and the struts more than what the load model with line load equal to 110 kN/m does. From these results it seems that Bane NOR did right when they included the requirement to check for Load Model 71 for calculations considering sheet pile walls adjacent to the track.

However, simulations are often performed in two dimensions, which makes it difficult to make sure that Load Model 71 is complied with. Therefore it is desirable to investigate which value of the line load that will give similar response in the structural elements of this model as LM71*. This will give an indication on the value of line load that Bane NOR can put into their regulations for calculations in two dimensions related to sheet pile walls adjacent to the track.

Further in this section LM71* will be compared to different values of the line load to decide which one corresponds the best. In the following table different values of line loads are listed with associated forces and displacements.

Table 6.5: Results from analysis of sheet pile wall adjacent to the track

Load Model	Increase in Normal Forces in Struts 1, 2 and 3 [kN]			$ u _{\max}$ [m]	M_{\max} [kNm/m]
	ΔN_1	ΔN_2	ΔN_3		
LM71	113.6	62	15.6	0.01524	169.2
q = 110 kN/m	75	76.9	75.4	0.01345	158.9
q = 120 kN/m	94.8	97.3	95.3	0.01614	167.9
q = 125 kN/m	106.8	109.7	107.3	0.01765	172.4
q = 130 kN/m	119.7	123.1	120.4	0.01925	176.9

From table 6.5 it seems like the line load has to have a value of 130 kN/m for the normal forces in the struts to exceed ΔN_1 from the case where LM71* is applied. Furthermore, the value $q = 125$ kN/m will be enough to exceed the bending moment, while $q = 120$ kN/m contributes to a larger deflection than what LM71* does.

The normal forces in the struts are increasing with approximately 26% per 10 kN/m increase in the distributed load. For the displacements the values rise with 20%, while the bending moments are only increasing with 6% per 10 kN/m increase in the distributed load. This means that the struts are most affected by the increase in the distributed load.

Since it is appropriate to get only one value for the line load, $q = 125$ kN/m fulfils both the displacement and the bending moment. By rounding off to the nearest ten, ΔN is big enough in every strut for this line load. From this it follows that the recommended value for the distributed load in Bane NOR's regulations for cases like this should be no less than 125 kN/m.

6.5 Summarising Discussion

The research question for this master's thesis is to determine the correspondence between the load model described in the technical regulations used when developing railways in Norway, and the load model described in the European standard. The simulations done in PLAXIS makes it possible to give some answers to the research question and make suggestions on how Bane NOR may revise their technical regulations.

Design of the model in PLAXIS

During the construction of the models in PLAXIS, several issues came to light. First of all, it had to be determined which PLAXIS version to use. Because LM71* extends in the direction of the rails, the models had to be developed in three dimensions. The difference between two dimensional and three dimensional modelling in PLAXIS is considerable, as described in section 3.2.1. 3D calculations in PLAXIS seems to overestimate the total stability, and PLAXIS 2D provides clearer results than PLAXIS 3D. The limitations these issues results in are important to keep in mind when analysing the results from PLAXIS 3D.

Other issues were the design of the substructure, and the height of the slope in the slope stability analysis. Obtained results in this thesis for the substructure illustrates that the difference between LMBN and LM71* is most critical in the case without frost protection. It also seems that the lower height of the slope, the easier it is to distinguish between the two load models.

Results from the Slope Stability Analyses

The results described in the beginning of this chapter indicate that the current value of distributed load written in Bane NOR's technical regulations seems to be too high for slope stability analyses. The findings from the slope stability analysis in this thesis indicates that the line load of 110 kN/m should be reduced by 23 kN/m to obtain the same factor of safety for the slope as when LM71* is applied to the model.

In the Finnish report described in section 2.5.2 several variables was investigated for embankment stability. The results from this research, done in PLAXIS 3D, shows that the 2D strip load corresponding to LM71 varies between the values 87 kN/m and 103 kN/m. As the maximum line load found for 2D stability calculations in the Finnish report was 103 kN/m, this was also the value for the line load it was concluded with at the end of the report.

The line load that lead to equal safety level in the 3D stability calculation as LM71* in this thesis was 87 kN/m. In the Finnish research report it was the stability calculations conducted with a layer of very soft clay that contributed to the lowest values for the line loads. This illustrates the importance of having data from more than one example to substantiate the revision of a regional regulation.

The gap between 87 kN/m and 103 kN/m found in the Finnish report gives an indication that Bane NOR should consider to divide their regulations into different design loads for different cases. This will make the regulations more comprehensive, but it can also help avoiding unnecessary stability actions in slopes, or accidents due to low stability of the slope.

Results from the Analyses of the sheet pile wall adjacent to the track

The current rule for these kind of calculations in Norway is to check the calculations by using LM71. As the three dimensional modelling programs nowadays are limited, as demonstrated in section 3.2.1, and probably not fully incorporated for all geotechnicians yet, it is desirable to find a line load which can be used for modelling in two dimensions.

From the results obtained for the sheet pile wall adjacent to the track and the struts behind the wall, it seems like Bane NOR's load model has a value that is too low for the line load. The effects on both the wall and the struts are bigger when LM71* is applied to the model, and the line load, which seems to give more equal response in the structural elements, turns out from these results to be equal to 125 kN/m.

The case where LMBN is applied to the model in PLAXIS 3D is a symmetrical problem, as of this the load should be distributed in a symmetrical way. From table 6.5 one can see

that the normal forces in the struts are a bit different from each other. This illustrates the uncertainties of the finite element method, where the mesh refinement means a lot. The finer mesh in the model, the more similar results could be expected in the three struts.

Since the mesh in the finite element method has an impact on the results, especially when structural elements are being considered, the results from this example must be investigated further. Additionally, the results are functions of the relative rigidity between the soil, substructure, sheet pile wall, struts and walings. Other combinations of material parameters may provide different results.

However, the results illustrate well that the line load described in the technical regulations of Bane NOR is too low for calculations considering sheet pile walls close to the track. More research in this field should be done to confirm or discard the value for the line load, $q = 125 \text{ kN/m}$, suggested in this thesis.

Oversized versus Undersized Railways

When the technical regulations are to be revised, the consequences of changing values in the load model should be discussed. If the load model is described with a value for the distributed load which is larger than necessary, oversized geotechnical actions will be prepared. In the opposite case, if the distributed load in the load model is lower than what is necessary, the calculations on geotechnics will conclude with undersized structures beneath the track, or it might leave out actions in crucial areas.

The disadvantages of having a value for the line load that is too high is that the geotechnical structures below and close to the track will be oversized. Unnecessary stabilising actions, improvement of the ground in areas where it is not really needed, or oversized sheet piles. Actions like these will have negative economic consequences, and will lead to excessive time consumption.

In December 1998 there was a serious accident in Norway due to limited stability in the substructure(Valmot, 2005). Although history testifies few accidents where the geotechnical structures are to blame, these types of accidents may potentially occur if geotechnical structures are being undersized. These types of accidents could contribute to severe consequences.

According to a report written by the Institute of Transport Economics, the unit cost of serious injury caused by the railway is estimated to 2.9 million Norwegian kroner, and for deaths it is estimated to 16 million Norwegian kroner(Hagen, 1997). This report was written in 1997, and the price has probably increased significantly since then. Although economy is one of the main reasons for revising the technical regulations of Bane NOR, it is important to keep in mind that it is difficult to value a human life in terms of money.

The results put in a Scandinavian perspective

Current regulations in Sweden describes lower design values than the ones used in Norway. For the slope stability analysis in Sweden, a line load equal to 80 kN/m is described, while a distributed load of 155 kN/m over an area of 6.4 m x 2.5 m is described for calculations of sheet pile walls near the track. In Denmark the regulations are more conservative than the Norwegian ones, where a line load of 110 kN/m is described for slope stability analysis, and a distributed load of 170 kN/m over the same area as for the Swedish regulations for analysis of sheet pile walls adjacent to the track.

While the Swedish regulations are quite similar to the Norwegian ones for calculations considering sheet pile walls, with a distributed load of 155 kN/m relative to 156 kN/m, the Danish regulations are quite equal for the calculations considering stability. At the same time the Swedish regulation describing a line load of 80 kN/m for calculations considering stability is quite different from the Norwegian regulation, and the Danish one for calculations considering sheet pile walls, describing a distributed load of 170 kN/m. It would have been interesting to know the background to the provisions of the regulations in Sweden and Denmark, since they differ significantly from the regulations in Norway.

Conclusion of the discussions

An important thing to keep in mind when the results in this thesis are being considered is the importance of the design of the models in PLAXIS 3D. The design used in this thesis is fictive cases, which differs from reality in many ways. The obtained results will thus have several limitations. If the model was designed in a different way, it would probably have given other final numerical results. This means that the results have to be used with caution, but that they can give a guidance to Bane NOR on how they should proceed with their discussions on how to revise their technical regulations.

The obtained results in this thesis provides background to suggest that the line load in Bane NOR's regulations can be reduced for slope stability analysis. Even though the obtained result for the line load in this thesis, $q = 87 \text{ kN/m}$, is a reduction of 20% from the line load in the current regulations, the load is still more conservative than what is used in Sweden.

According to the results from the calculations of the sheet pile wall near the track, the wall seemed to be less affected by the line load equal to 110 kN/m than by the load from LM71*. Based on this, as well as the regulations used in Sweden and Denmark, it seems like Bane NOR was right when they changed their regulations in February and inserted the requirement to check for LM71.

The applied line load $q = 125 \text{ kN/m}$ gave the most similar response in the wall and the struts as to when LM71* was applied for the calculations in this thesis. If Bane NOR

want to include a line load in their regulations, to make it easier to perform calculations in two dimensions, the line load equal to 110 kN/m seems to be too small for calculations considering sheet pile walls adjacent to the track. The loads from the bogie have too much impact, which leads to the necessity of a greater load to take account of this.

More research on this topic should be conducted to have a broader basis for making decisions on how the technical regulations of Bane NOR should be revised. Proposals for further work on this field is described in chapter 7.

Chapter 7

Conclusions and Recommendations for Further Work

7.1 Summary and Conclusion

It is of national importance to keep the railway safe and stable. The Norwegian government agency responsible for developing the railway network is called Bane NOR. Bane NOR have developed a set of design rules, where, among other things, the regulations considering calculations in the geotechnical field is described. The European standard for vertical loading due to rail traffic actions for new or replaced geotechnical structures is called NS-EN 1991-2:2003+NA:2010, which is a standard originally intended for bridge design.

Throughout this master's thesis it has been done simulations in PLAXIS 3D to figure out the correspondence between the load model described in the technical regulations for developing railways in Norway, and the load model described in the European standard. In these simulations two specific cases have been analysed, where one of them consider the load models' effect on slope stability and the other consider their effect on a sheet pile wall adjacent to the track.

Loads from railways are described in Bane NOR's technical regulations as a distributed line load equal to 110 kN/m for calculations considering slope stability. The load model that applies to slope stability calculations in the European standard is called Load Model

71. Here the loads from railways are described by four axle loads of 250 kN over 6.4 m length, and a distributed line load equal to 80 kN/m beyond this length. To make the comparison most appropriate for the two models in PLAXIS 3D, the loads are distributed over the same width, and Load Model 71 is approximated to a distributed load of 156 kN/m over the length of 6.4 m.

In Bane NOR's regulations considering calculations of sheet pile walls adjacent to the track, it has recently been added a description saying that the calculations have to be controlled by Load Model 71 from the European standard. However, as two dimensional simulations are widely used in the geotechnical field, calculations have been done to develop a suggestion for the line load that can correspond to Load Model 71 in this case as well.

Evaluations of the technical regulations developed by Bane NOR has been made throughout the thesis by having a look at the regulations in Sweden and Denmark. From these evaluations it turns out that the Norwegian regulations has the highest value for the line load when calculating slope stability, while for the case with supporting structures near the railway, the Danish regulations are the most conservative.

PLAXIS 2D has been compared to PLAXIS 3D to illustrate the difference of the software programs. 3D calculations in PLAXIS seems to overestimate the total stability, and PLAXIS 2D provides clearer results than PLAXIS 3D.

Prior to developing the models in PLAXIS 3D, simulations were done considering the height of the slope, and whether a layer of frost protection should be included to the superstructure. It is advantageous to design a model where the differences between the two load models are the most apparent. The evaluations of these results illustrates that the differences in the two load models will be most significant with the absence of a frost protection layer, and that the differences in factors of safety between the two load models are increasing as the height of the slope decreases.

Final results from the simulations in PLAXIS 3D are represented in table 7.1. The first line in the table presents the suggested value for line load which leads to an equal safety level for slope stability in 3D stability calculations as LM71*. The second line presents the value for the line load giving similar effect to the sheet pile wall and struts as LM71*.

Table 7.1: Final results from simulations in PLAXIS 3D

Simulated case:	LM71* Distributed load (over 6.4 m) kN/m	LMBN Line load kN/m	Results from PLAXIS 3D Line load kN/m
Slope stability	156	110	87
Sheet pile wall	156	110	125

From the simulation of the slope stability case, the obtained result gave a line load equal to 87 kN/m. This result was evaluated by comparing it to the results obtained from a similar research project done in Finland. This comparison found that the Finnish research concluded on a higher line load than what was found in this thesis, but still lower than the current line load of 110 kN/m described in the regulations.

The obtained final results provides background to suggest that the line load in Bane NOR's regulations can be reduced for slope stability analysis. This is supported in the regulations used in Sweden, which describes a lower value than 110 kN/m for the line load.

According to the results from the calculations of the sheet pile wall adjacent to the track, the wall seemed to be less affected by the line load from Bane NOR's regulations than by the load from LM71*. Based on this, as well as the regulations used in Sweden and Denmark, it seems like Bane NOR was right to insert the requirement to check for Load Model 71 in February.

The suggested value for the line load from the simulations in PLAXIS 3D is estimated 15-20% larger than the current value in Bane NOR's regulations. Hence, if a line load is to be included in the regulations for this case, these results indicates that the value has to be significantly larger than 110 kN/m.

7.2 Recommendations for Further Work

Since many railway lines nowadays have two tracks, the simulations should also be done for a model with two tracks. In chapter 2 the second track in the load model developed by Bane NOR is described to have a line load equal to 90 kN/m. Further work can investigate this value to determine whether it is the right value to use when dimensioning double-track railways.

Different varieties in the PLAXIS 3D models used for the simulations in this master's thesis will provide a better basis for comparing the load models. By varying the strength parameters in the clays, varying the thickness of the substructure, trying different designs of the slope, and changing the location of the structural elements in the sheet pile wall example, among other things, the results can apply to different cases.

Several geotechnical issues remains to be explored to gain more knowledge on how Bane NOR should revise their regulations. An interesting issue is the load effect on LECA or foam glass, used as a light fill material, beneath the subbase. The load impact on culverts under a railroad is another interesting case to investigate for further work.

In the Finnish report described in section 2.5.1, the effect of seven different load models on the vertical stress levels exposed to slab structures was investigated. This is an inter-

esting study, but none of the load models in this report was similar to Bane NOR's load model. This makes it advantageous to copy the research done in the Finnish report with the inclusion of the load model with a distributed load equal to 110 kN/m.

The regulations developed in the neighbouring countries, Sweden and Denmark, differs from the technical regulations developed by Bane NOR. Contact with people from Trafikverket and Banedanmark can contribute to a better understanding of the differences between the regulations. This can provide input and ideas on how to continue the work, and it may contribute to a discussion on this topic in Sweden and Denmark as well. This could even lead to the same set of regulations covering some situations of mutual interest.

Bibliography

ArcelorMittal (2015). *The next generation of AZ sheet piles*. Production catalogue.

ArcelorMittal (2017). *Steel Foundation Solutions*. General catalogue 3.

Bane NOR (2014).

Overbygning/Prosjektering/Sporkonstruksjoner/Vedlegg/Skinneprofiler. Available from: <https://trv.banenor.no/wiki/Overbygning/Prosjektering/Sporkonstruksjoner/Vedlegg/Skinneprofiler#60E1>. [Accessed 19.02.2018].

Bane NOR (2017a). *Overbygning/Prosjektering/Ballast*. Available from: <https://trv.jbv.no/wiki/Overbygning/Prosjektering/Ballast>. [Accessed 19.02.2018].

Bane NOR (2017b). *Teknisk regelverk: Underbygning/Prosjektering og bygging*. Available from: https://trv.banenor.no/wiki/Underbygning/Prosjektering_og_bygging. [Accessed 21.03.2018].

Bane NOR (2017c). *Underbygning/Prosjektering og bygging/Banelegeme*. Available from: https://trv.banenor.no/wiki/Underbygning/Prosjektering_og_bygging/Banelegeme. [Accessed 11.04.2018].

Bane NOR (2017d). *Venjar-Langset*. Available from: <http://www.banenor.no/Prosjekter/prosjekter/venjar-langset/>. [Accessed 24.05.2018].

Bane NOR (2018a). *Overbygning/Prosjektering/Sporkonstruksjoner*. Available from: <https://trv.jbv.no/wiki/Overbygning/Prosjektering/Sporkonstruksjoner>. [Accessed 19.02.2018].

Bane NOR (2018b). *Underbygning/Prosjektering og bygging/Generelle tekniske krav*. Available from: https://trv.banenor.no/wiki/Underbygning/Prosjektering_og_bygging/Generelle_tekniske_krav. [Accessed 11.04.2018].

Bane NOR (2018c). *Underbygning/Prosjektering og bygging/Stabilitet*. Available from:

-
- https://trv.banenor.no/wiki/Underbygning/Prosjektering_og_bygging/Stabilitet. [Accessed 12.04.2018].
- Banedanmark (2010). *BN1 Banenorm: Belastnings- og beregningsforskrift for sporbrende broer og jordkonstruksjoner*. Technical report.
- Banedanmark (n.d.). *Orientering om BN-systemet*. Available from: <https://www.bane.dk/Leverandoer/Krav/Tekniske-normer-og-regler/Orientering-om-BN-systemet>. [Accessed 11.05.2018].
- Bartlett, S. F. (2011). *How does dilatancy affect the behavior of soil?* Lecture notes, University of Utah.
- Brinkgreve, R., Kumarswamy, S., Swolfs, W., and Foria, F. (2017). *PLAXIS 3D 2017*. User's manual.
- Calcada, R., Delgado, R., and e Matos, A. C. (2008). *Bridges for High-Speed Railways*. CRC Press.
- Dhondt, G. (2014). *CalculiX CrunchiX USER'S MANUAL version 2.7*. User's manual.
- Fevang, P. A. (2016). *Meter Weight*. Available from: <http://networkstatement.jbv.no/doku.php?id=vedlegg:metervekt&do=>. [Accessed 03.06.2018].
- FINN kart (2018). Map portal. Available from: <https://kart.finn.no/>.
- Gjerde, K. (2012). *Leksjon Sporgeometri*. Power Point presentation.
- Grimstad, G., Andresen, L., and Jostad, H. P. (2011). *NGI-ADP: Anisotropic shear strength model for clay*. Journal, NGI.
- Hagen, K.-E. (1997). *Ulykkeskostnader for jernbanen*. Tøi notat, TØI.
- Jernbaneverket (2017). *Underbygning/Banelegeme*. Available from: <http://www.jernbanekompetanse.no/wiki/Underbygning/Banelegeme>. [Accessed 14.03.2018].
- Jönsson, J. (1995). *Continuum Mechanics of Beam and Plate Flexure*. Aalborg University.
- Kalliainen, A. and Kolisoja, P. (2017). *28/2017: Pile supported embankment slabs under railway track line*. Research report.
- Karlsson, A. and Wellerhaus, S. J. (2014). *3D-Effects in Total Stability Evaluations*. Lund University, Sweden. Master's thesis.
- Klettke, A.-J. and Edgers, L. (2011). *A Comparison of 2D and 3D Settlement Analyses of the Tower of Pisa*. Technical report.

-
- Labuz, J. F. and Zang, A. (2012). *Mohr–Coulomb Failure Criterion. Rock Mechanics and Rock Engineering*, 45(6).
- Manni Sipre S.p.A. (2015). *Steel Rolled Beams*. Technical catalogue.
- Multiconsult (2017a). *Doc.no.: UOS-90-A-74520, Østfoldbanen VL (Oslo S) - Ski, Ski stasjon: Design Basis - SP12 & SP13*. Design report, Bane NOR.
- Multiconsult (2017b). *Doc.no.: UOS-90-A-74523, Østfoldbanen VL (Oslo S) - Ski, Ski stasjon: Design - Sheet Pile 12 west*. Design report, Bane NOR.
- Multiconsult (2017c). *Doc.no.: UOS-90-A-74530, Østfoldbanen VL (Oslo S) - Ski, Ski stasjon: Design - Sheet Pile 13*. Design report, Bane NOR.
- Nordal, S. (2017a). *TBA4116 Geotechnical Engineering Advanced Course*. NTNU. Lecture notes and background material.
- Nordal, S. (2017b). *The hardening soil model*. Power Point presentation.
- Norsk Standard (2010). *NS-EN 1991-2:2003+NA:2010, Eurokode 1: Laster påkonstruksjoner, Del 2: Trafikklast påbruer*. Standard Norge, Oslo.
- Norsk Standard (2015). *NS-EN 15528:2015, Jernbane, Linjekategorier for styring av grensesnitt mellom grenser for vogners lasteevne og infrastruktur*. Standard Norge, Oslo.
- Norsk Standard (2016). *NS-EN 1990:2002+A1:2005+NA:2016, Eurokode: Grunnlag for prosjektering av konstruksjoner*. Standard Norge, Oslo.
- Norsk Standard (2017). *NS-EN 1993-5:2007+NA:2010, Eurokode 3: Prosjektering av stålkonstruksjoner - Del 5: Peler og spunt*. Standard Norge, Oslo.
- Norwegian Geotechnical Institute (2016). *Doc.no.: UEH-00-A-55348, Gardemobanen (Gardemoen) - Eidsvoll, Geotekniske dimensjoneringsparametere, Venjar-Eidsvoll*. Design report, Bane NOR.
- Norwegian Geotechnical Institute (2017). *Doc.no.: UEH-05-A-55615, Utbygging Eidsvoll-Hamar (UEH): K53 Kvisldalen jernbanebru, Beregninger geotekniske tiltak*. Design report, Bane NOR.
- Norwegian Geotechnical Institute (u.d.). *Direct simple shear test - DSS*.
- Olson, R. E. and Lai, J. (2004). *Direct Shear Testing*.
- Pande, G. and Pietruszczak, S. (2002). *Numerical Models in Geomechanics*. CRC Press.
- Potts, D. M. and Zdravkovic, L. (1999). *Finite Element Analysis in Geotechnical Engineering*. Thomas Telford Publishing.
-

-
- RAIL.ONE (2014). *Concrete sleepers*. Production catalogue.
- Savolainen, L., Mansikkamki, J., and Kalliainen, A. (2017). *56/2017: 2D Loads for Stability Calculations of Railway Embankments*. Research report.
- Schanz, T., Vermeer, P., and Bonnier, P. (1999). *The hardening soil model: Formulation and verification. Beyond 2000 in Computational Geotechnics - 10 Years of PLAXIS*.
- SINTEF (2014). *Økt aksellast gir effektiv jernbane*.
- Statens Vegvesen (2014a). *Håndbok N200: Vegbygging*. Statens Vegvesen.
- Statens Vegvesen (2014b). *Håndbok V220 - Geoteknikk i vegbygging*. Veiledning, Statens Vegvesen.
- Statistisk sentralbyrå (2017). *SSB statistikkbank tabell 10484: Persontransport med jernbane, etter strekningstype*.
- Svanø, G. (2017). *Teknisk regelverk fra Bane NOR, "Når telen går 2017"*. Power Point presentation.
- Svingheim, N. (2004). *Jernbanen i Norge 150 år*. Available from:
<http://www.banenor.no/Nyheter/Nyhetsarkiv/Arkiv/Jernbanen-i-Norge-150-ar/>.
[Accessed 06.06.2018].
- Svingheim, N. (2011). *Jernbanekart*. Available from:
<http://www.banenor.no/Jernbanen/Jernbanekart/>. [Accessed 21.04.2018].
- Trafikverket (2014). *TK Geo 13: Trafikverkets tekniska krav för geokonstruksjoner*. Technical report.
- trafikverket, L. D. F. (2016). *RATO3 Radan Rakenne 6/2016*. Technical report.
- Valmot, O. R. (2005). *Varsler ras - stanser toget*. News article. Teknisk Ukeblad.
- Wikipedia contributors (2018a). *Danmarks geografi*. Available from:
https://no.wikipedia.org/w/index.php?title=Danmarks_geografi&oldid=18149474.
[Accessed 23.04.2018].
- Wikipedia contributors (2018b). *Follo Line*. Available from:
https://en.wikipedia.org/w/index.php?title=Follo_Line&oldid=828278870. [Accessed 05.05.2018].
- Wikipedia contributors (2018c). *Norges geografi*. Available from:
https://no.wikipedia.org/wiki/Norges_geografi. [Accessed 23.04.2018].
- Wikipedia contributors (2018d). *Østfold Line*. Available from:
https://en.wikipedia.org/w/index.php?title=%C3%98stfold_Line&oldid=834425784.
[Accessed 05.05.2018].

Wikipedia contributors (2018e). *Sveriges ytterpunkter*. Available from:
https://sv.wikipedia.org/wiki/Sveriges_ytterpunkter. [Accessed 23.04.2018].

Zhu, T. (n.d.). *Some Useful Numbers on the Engineering Properties of Materials (Geologic and Otherwise)*. The University of Texas at Austin.

Appendix

Appendix A Slope Stability Example

A.1 Material Parameters

Appendix B Sheet Pile Wall Example

B.1 Material Parameters

B.2 Calculations of Steel Details

Appendix A


Slope Stability Example

A.1 Material Parameters

Property	Unit	Value
Material set		
Identification		Clay
Material model		Mohr-Coulomb
Drainage type		Undrained (C)
Colour		RGB 161, 226, 232
Comments		
General properties		
γ_{unsat}	kN/m ³	20,00
γ_{sat}	kN/m ³	20,00
Advanced		
Void ratio		
Dilatancy cut-off		<input type="checkbox"/>
e_{init}		0,5000
e_{min}		0,000
e_{max}		999,0
Damping		
Rayleigh α		0,000
Rayleigh β		0,000

Property	Unit	Value
Stiffness		
E_u	kN/m ²	19,04E3
ν_u (ν_u)		0,4950
Alternatives		
G	kN/m ²	6368
$E_{oed,u}$	kN/m ²	643,2E3
Strength		
$s_{u,ref}$	kN/m ²	47,60
ϕ_u (ϕ)	°	0,000
ψ (ψ)	°	0,000
Velocities		
V_s	m/s	55,89
V_p	m/s	561,7
Advanced		
Set to default values		<input type="checkbox"/>
Stiffness		
$E_{u,inc}$	kN/m ² /m	0,000
z_{ref}	m	0,000
Strength		
$s_{u,inc}$	kN/m ² /m	2,550
z_{ref}	m	0,000
Tension cut-off		<input type="checkbox"/>
Tensile strength	kN/m ²	10,00E6

Figure A.1: Clay

Property	Unit	Value
Material set		
Identification		Subballast
Material model		Mohr-Coulomb
Drainage type		Drained
Colour		 RGB 134, 234, 162
Comments		
General properties		
V_{unsat}	kN/m ³	19,00
V_{sat}	kN/m ³	19,00
Advanced		
Void ratio		
Dilatancy cut-off		<input type="checkbox"/>
e_{init}		0,5000
e_{min}		0,000
e_{max}		999,0
Damping		
Rayleigh α		0,000
Rayleigh β		0,000

Property	Unit	Value
Stiffness		
E'	kN/m ²	120,0E3
ν' (ν)		0,2500
Alternatives		
G	kN/m ²	48,00E3
E_{oed}	kN/m ²	144,0E3
Strength		
c'_{ref}	kN/m ²	8,100
ϕ' (ϕ)	°	39,00
ψ (ψ)	°	9,000
Velocities		
V_s	m/s	157,4
V_p	m/s	272,7
Advanced		
Set to default values		<input checked="" type="checkbox"/>
Stiffness		
E'_{inc}	kN/m ² /m	0,000
z_{ref}	m	0,000
Strength		
c'_{inc}	kN/m ² /m	0,000
z_{ref}	m	0,000
Tension cut-off		<input checked="" type="checkbox"/>
Tensile strength	kN/m ²	<input type="text" value="0,000"/>

Figure A.2: Subballast

Appendix B

Sheet Pile Wall Example

B.1 Material Parameters

Property	Unit	Value
Material set		
Identification		LCC 13
Material model		Linear elastic
Drainage type		Drained
Colour		RGB 177, 77, 213
Comments		
General properties		
γ_{unsat}	kN/m ³	20,00
γ_{sat}	kN/m ³	20,00
Advanced		
Void ratio		
Dilatancy cut-off		<input type="checkbox"/>
e_{init}		0,5000
e_{min}		0,000
e_{max}		999,0
Damping		
Rayleigh α		0,000
Rayleigh β		0,000

Property	Unit	Value
Stiffness		
E'	kN/m ²	9090
ν' (ν_u)		0,3000
Alternatives		
G	kN/m ²	3496
E_{oed}	kN/m ²	12,24E3
Velocities		
V_s	m/s	41,41
V_p	m/s	77,47
Advanced		
Set to default values		<input checked="" type="checkbox"/>
Stiffness		
E'_{inc}	kN/m ² /m	0,000
z_{ref}	m	0,000
Undrained behaviour		
Undrained behaviour		Standard
Skempton-B		0,9783
ν_u		0,4950
$K_{w,ref} / n$	kN/m ²	340,9E3

Figure B.1: Lime/Cement column improved clay

Property	Unit	Value
Material set		
Identification		Drycrust
Material model		Hardening soil
Drainage type		Drained
Colour		 RGB 232, 230, 161
Comments		<div style="border: 1px dashed gray; height: 20px; width: 100%;"></div>
General properties		
γ_{unsat}	kN/m ³	20,00
γ_{sat}	kN/m ³	20,00
<input type="checkbox"/> Advanced		
Void ratio		
Dilatancy cut-off		<input type="checkbox"/>
e_{init}		0,5000
e_{min}		0,000
e_{max}		999,0
Damping		
Rayleigh α		0,000
Rayleigh β		0,000

Property	Unit	Value
Stiffness		
E_{50}^{ref}	kN/m ²	12,00E3
E_{oed}^{ref}	kN/m ²	12,00E3
E_{ur}^{ref}	kN/m ²	36,00E3
power (m)		1,000
Alternatives		
Use alternatives		<input type="checkbox"/>
C_c		<div style="border: 1px dashed gray; padding: 2px;">0,02875</div>
C_s		8,625E-3
e_{init}		0,5000
Strength		
c'_{ref}	kN/m ²	1,000
ϕ' (phi)	°	35,00
ψ (psi)	°	0,000
<input type="checkbox"/> Advanced		
Set to default values		<input checked="" type="checkbox"/>
Stiffness		
v'_{ur}		0,2000
p_{ref}	kN/m ²	100,0
K_0^{nc}		0,4264
Strength		
c'_{inc}	kN/m ² /m	0,000
z_{ref}	m	0,000
R_f		0,9000
Tension cut-off		<input checked="" type="checkbox"/>
Tensile strength	kN/m ²	0,000

Figure B.2: Dry crust


Property	Unit	Value	Property	Unit	Value
Material set			Stiffness		
Identification		Clay Upper 1	G_{ur}/s_u^A		200,0
Material model		NGI-ADP	γ_f^C	%	2,000
Drainage type		Undrained (C)	γ_f^E	%	5,000
Colour		 RGB 232, 214, 161	γ_f^{DSS}	%	3,960
Comments			Strength		
General properties			$s_u^A_{ref}$	kN/m ²	45,00
Y_{unsat}	kN/m ³	20,00	$s_u^{C,TX}/s_u^A$		0,9900
Y_{sat}	kN/m ³	20,00	z_{ref}	m	-1,000
Advanced			$s_u^A_{inc}$	kN/m ² /m	0,000
Void ratio			s_u^P/s_u^A		0,3500
Dilatancy cut-off		<input type="checkbox"/>	τ_0/s_u^A		0,6820
ϵ_{init}		0,5000	s_u^{DSS}/s_u^A		0,6500
ϵ_{min}		0,000	Advanced		
ϵ_{max}		999,0	v_u (nu)		0,4950
Damping					
Rayleigh α		0,000			
Rayleigh β		0,000			

Figure B.3: Clay, upper layer


Property	Unit	Value	Property	Unit	Value
Material set			Stiffness		
Identification		Clay Upper 2	G_{ur}/s_u^A		200,0
Material model		NGI-ADP	γ_f^C	%	2,000
Drainage type		Undrained (C)	γ_f^E	%	5,000
Colour		 RGB 242, 202, 241	γ_f^{DSS}	%	3,960
Comments			Strength		
General properties			$s_u^A_{ref}$	kN/m ²	23,00
Y_{unsat}	kN/m ³	20,00	$s_u^{C,TX}/s_u^A$		0,9900
Y_{sat}	kN/m ³	20,00	z_{ref}	m	-2,000
Advanced			$s_u^A_{inc}$	kN/m ² /m	0,000
Void ratio			s_u^P/s_u^A		0,3500
Dilatancy cut-off		<input type="checkbox"/>	τ_0/s_u^A		0,6820
ϵ_{init}		0,5000	s_u^{DSS}/s_u^A		0,6500
ϵ_{min}		0,000	Advanced		
ϵ_{max}		999,0	v_u (nu)		0,4950
Damping					
Rayleigh α		0,000			
Rayleigh β		0,000			

Figure B.4: Clay, lower layer

Property	Unit	Value
Material set		
Identification		Clay
Material model		NGI-ADP
Drainage type		Undrained (C)
Colour		 RGB 47, 198, 77
Comments		
General properties		
γ_{unsat}	kN/m ³	20,00
γ_{sat}	kN/m ³	20,00
Advanced		
Void ratio		
Dilatancy cut-off		<input type="checkbox"/>
e_{init}		0,5000
e_{min}		0,000
e_{max}		999,0
Damping		
Rayleigh α		0,000
Rayleigh β		0,000

Property	Unit	Value
Stiffness		
G_w/s_u^A		200,0
γ_f^C	%	2,000
γ_f^E	%	5,000
γ_f^{DSS}	%	3,960
Strength		
$s_{u,ref}^A$	kN/m ²	23,00
$s_{u,C,TX/s_u^A}$		0,9900
z_{ref}	m	-3,000
$s_{u,inc}^A$	kN/m ² /m	2,250
$s_{u,P/s_u^A}$		0,3500
T_0/s_u^A		0,6820
$s_{u,DSS/s_u^A}$		0,6500
Advanced		
ν_u (nu)		0,4950

Figure B.5: Clay, rest of the model

B.2 Calculations of Steel Details

Calculation of steel details - short strut SP13

Strut forces from PLAXIS

$$F := 1368 \text{ kN}$$

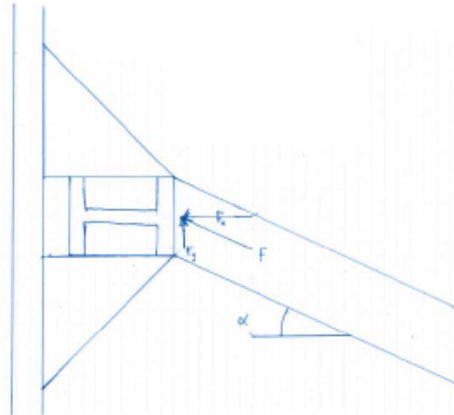
$$\alpha := 34.2 \text{ deg}$$

$$F_x := F \cdot \cos(\alpha) = 1131 \text{ kN}$$

$$F_y := F \cdot \sin(\alpha) = 769 \text{ kN}$$

Profile strut: HEB400

Profile waler: HEB400



Capacity of stut and waler is checked in a separate document.

$$f_y := 355 \text{ MPa}$$

$$\gamma_{M0} := 1.05$$

$$\nu := 0.3$$

$$\varepsilon := \sqrt{\frac{235 \text{ MPa}}{f_y}} = 0.81$$

$$E := 210000 \text{ MPa}$$

E-module steel

$$\gamma_{M0} := 1.05$$

NA.5.1.1(4) ref. /1/

$$\gamma_{M1} := 1.1$$

NA.5.1.1(4) ref. /1/

$$\gamma_{M2} := 1.25$$

NA.5.1.1(4) ref. /1/

Figure B.6: Calculation of strut and waling (Multiconsult, 2017c)

B.3 Moment Diagrams of Walings

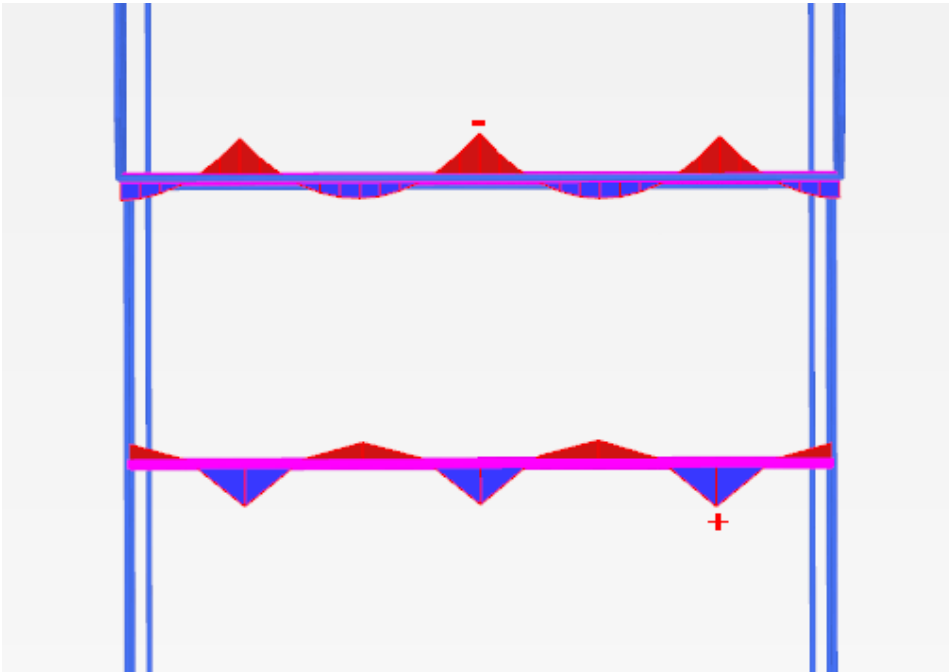


Figure B.7: Moment diagrams for the walings